PhD-FSTM-2021-071
The Faculty of Science, Technology and Medicine

DISSERTATION

Defence held on 24/09/2021 in Luxembourg

to obtain the degree of

DOCTEUR DE L'UNIVERSITÉ DU LUXEMBOURG

EN SCIENCES DE L'INGÉNIEUR

by

Raja PANDI PERUMAL

Born on 19 December 1991 in Tamil Nadu (India)

Development of a Decision Support System for Incorporating Risk Assessments during the System Design of Microsatellites

Dissertation Defence Committee:

Dr.-Ing. Holger VOOS, Dissertation Supervisor
Professor, University of Luxembourg

Dr.-Ing. Jean-Régis HADJIMINAGLOU, Chairman
Professor, University of Luxembourg

Dr. Andreas Makoto HEIN, Vice-chairman
Associate Professor, University of Luxembourg

Dr. Hubert MOSER
Director-Engineering, Flawless Photonics

Dr.-Ing. Kilian GERICKE
Professor, University of Rostock

This work was supported by FNR "Fonds national de la Recherche" (Luxembourg) through Industrial Fellowship Ph.D. grant and was carried out in collaboration with LuxSpace.

Author:

Raja PANDI PERUMAL

Dissertation Supervisors:

Dr.-Ing. Holger VOOS, Dissertation Supervisor
Professor, University of Luxembourg

Mr Florio DALLA VEDOVA, Co-supervisor
Senior Pre-Development Engineer, LuxSpace

Declaration of Authorship

I, Raja Pandi Perumal, declare that this thesis titled, 'Development of Decision Support System for Incorporating Risk Assessments during the System Design of Microsatellites' and the work presented in it are my own. I confirm that:

- This work was done wholly or mainly while in candidature for a research degree at this University.
- Where any part of this thesis has previously been submitted for a degree or any other qualification at this University or any other institution, this has been clearly stated.
- Where I have consulted the published work of others, this is always clearly attributed.
- Where I have quoted from the work of others, the source is always given. With the exception of such quotations, this thesis is entirely my own work.
- I have acknowledged all main sources of help.
- Where the thesis is based on work done by myself jointly with others, I have made clear exactly what was done by others and what I have contributed myself.

Raja Pandi Perumal

August 24, 2021, Luxembourg

Abstract

The primary purpose of this research is to develop a decision support system for the early design of an optimal and reliable satellite while making the overall conceptual design process more efficient. Generally, a satellite design process begins with a mission definition followed by the functional design of the satellite system. Beyond this, the design goes through several iterations and eventually results in a detailed satellite system design. Only then does it make sense to feed in the piece-part information to estimate the reliability of the entire satellite system. Predicted reliability from this bottom-up method may sometimes be markedly lower than the requirements. In such case, the maturity of the design is brought down, and mitigation strategies need to be implemented to meet the reliability requirements. Consequently, introducing new or redundant parts as a mitigation approach can violate the previously satisfied requirements such as mass, power and cost. Furthermore, additional design iterations are needed until all the requirements are met. Therefore, this design approach is expensive, inefficient, and can be avoided if reliability is considered from the early design phase. However, the challenge is to simultaneously perform reliability analysis and system design as they are entirely different engineering disciplines. In this research, a decision support system: DESIRA is developed to bridge the gap between these two engineering disciplines and incorporate reliability assessments during the early design phase, thus resulting in a truly optimal satellite design. With its unique features such as Reliability Allocation, Reliability Growth, Multidisciplinary Design Optimization and Reliability-Based Multidisciplinary Design Optimization, DESIRA effectively aids the system design at each maturity level.

Contents

Acknowledgments

First, I would like to thank my supervisor, Professor Holger Voos, for this incredible opportunity. The freedom he gave me to explore different research areas made me a better researcher. His visions, guidance and encouragements were essential for the successful outcome of this research.

Further, I owe my deepest gratitude to my industrial supervisor, Florio Dalla Vedova, for sharing his extensive knowledge and experience with me. This research would not have been possible without his inputs, ideas, and feedback. I wish to express my sincere appreciation to Hubert Moser for reviewing my publications.

I would also like to thank Davide Menzio, Paul Kremer, Manuel Castillo Lopez, and everyone from the SnT Automation & Research group for the insightful conversations. I would also like to express my sincere gratitude to the Luxembourg National Research Fund for financially supporting this research.

This thesis would not have been what it is without my wife, Indra Muthuvijayan. Her thoughtful perspectives, inexhaustible patience and endless wisdom, were critical in shaping my research. Last but not least, I am forever grateful to my mother, Latha Packiathai, for her unconditional love and support.

One who adapts with the change Survives

One who adapts before the change Succeeds

One who causes the change Leads.

Ray Noorda

1

Introduction

Satellite Design is a complex process that involves numerous multidisciplinary inter-related variables. The preliminary or conceptual design phase is crucial in satellite design as it elicits the requirements for the entire design. Immense effort is required during this phase, as the decisions made here massively influence the product's cost, performance, and reliability.

Over the years, reliability has become a critical aspect in satellites, especially microsatellites. At the same time, there isn't enough information available regarding the failure rate or satellite parameters in the early stages. Hence, decisions in the conceptual phase primarily rely on the limited information from past missions and tacit knowledge from domain experts. Often the design alternatives provided by the designers may seem plausible at first. However, upon detailed examination, the designs might violate some requirements or might have large safety margins and unnecessarily high redundancy levels, thus making them expensive and undesirable. This leads to an important question, How to identify "the one" best design from the array of alternatives?

In this research, a decision support system is developed to assist in identifying the best design alternative in terms of reliability, mass, power and cost. Unlike most doctoral dissertations, which are highly specialized in a particular domain, this work is intentionally kept broad enough to cover the multiple domains interlinked with satellite design. At the same time, it is also detailed enough for actual satellite design applications and implementations in the here developed DESIRA tool. Thereby, this research strives to serve as a bridge among multiple academic domains, offering a multidisciplinary approach for designing microsatellites in the early design phases.

1.1 Motivation

Global space ventures are rapidly advancing while generating a couple of disruptive waves along their way. The first wave of disruption led to the involvement of the private sector in accomplishing space-based operations for commercial applications. Earlier, due to the exorbitant cost involved, space was restricted mainly to government-based space agencies. However,

in the NewSpace era, many private companies have sent their satellites into orbits and realized substantial economic gains. The second and current wave of disruption strives to achieve more complex missions using miniature technologies without sacrificing quality and reliability. There are numerous planned missions to use Low Earth Orbit (LEO) satellite constellations to act as data relay systems, satellite-based internet providers, and perform countless other applications. The conventional satellites are massive and powerful but also sophisticated. Therefore, realizing the planned missions become extremely expensive and unrealistic with the conventional satellites, it raises a need for alternative low-cost satellites. To meet this demand, many satellite developers have turned towards small satellites/microsatellites, and the space industry is geared up to embark on a future filled with large constellations of small satellites.

Compared to the conventional equivalents, the design phase of small satellites are much shorter, and commercial-off-the-shelf components(COTS) play a significant role in cost reduction. Consequently, reliability is often a critical concern in small satellites. Reliability needs to be incorporated from the early design phase to overcome this shortcoming. *It is less expensive to design for reliability than to test for reliability*[1]. However, the status quo of the assumptions for the early stage reliability analysis is based on conventions, outdated data or expert opinions. On the other hand, implementing the on-orbit reliability knowledge in the satellite design will be more beneficial. Unfortunately, this crucial information is outdated and inadequate for the current satellite design.

Furthermore, to successfully incorporate reliability into the decision-making process early in the design, the effect of design choices on reliability must be fully understood. The satellite design can be optimized across multiple engineering disciplines by leveraging this knowledge,

and the most beneficial design can be identified. Unfortunately, the current approaches do not articulate what drives value in the design. Apart from their inherent complexity, microsatellite systems have evolving requirements and intricate interactions that further complicate the design process. Concurrent design approaches facilitate the complex design process by managing interactions between different subsystems. However, the concurrent design typically gravitates towards optimizing point designs and conducting trade studies to provide a single or a handful of design alternatives. Moreover, examining the effects on the design by changing different design variables and their concomitant effects on reliability are not intuitively possible. Therefore, additional support systems that complement the concurrent design process are required to enable informed decision-making.

1.2 Problem Statement and Research goals

This research aims to develop a decision support system in the form of the DESIRA tool to identify an optimal satellite design by incorporating reliability/risk assessments during the early design stages. The decision support system will determine the optimal design by quantifying the macro-reliability of small satellites, estimating the intrinsic reliability of design alternatives and leveraging multidisciplinary design optimization for trade-space exploration. In particular, this research strives to answer the following questions:

1. **How to estimate the reliability of satellite during the initial design phase?**
2. **How to improve the reliability of satellite while minimizing the resources?**
3. **How to identify the best satellite design during the early design stage?**
4. **How to incorporate reliability in the early satellite design?**

1.3 Thesis Structure

This thesis is structured to systematically answer the research questions presented in Section 1.2. Every chapter provides baseline arguments, methods, solutions with rationale. The thesis begins with Chapter 2 that provides a detailed literature review in satellite design, reliability analysis and multidisciplinary design optimization. Then, in Chapter 3, Statistical analysis of empirical failure data is performed. Reliability growth strategies are presented in Chapter 4. Next, in Chapter 5 Multidisciplinary Design Optimization of a Distributed Space System is presented. As a next step, in Chapter 6, Reliability-Based Multidisciplinary Design Optimization is performed. Combining the answers to the research questions, a decision support system, DESIRA developed, is presented in Chapter 7. This thesis concludes in Chapter 8 that summarizes the research.

1.4 Publications

This thesis consists of material which has been published in conference proceedings and is available under the following sources.

1. Pandi Perumal, R., Voos, H., Dalla Vedova, F., & Moser, H.: **Comparison of Multidisciplinary Design Optimization Architectures for the design of Distributed Space Systems**. – *In Proceedings of the 71st International Astronautical Congress*, (2020)

2. Pandi Perumal, R., Voos, H., Dalla Vedova, F., & Moser, H.: **Small Satellite Reliability: A Decade in Review**, Year in Review, SSC21-WKIII-02. – *Proceedings of the 35th Annual Small Satellite Conference*, (2021)

3. Pandi Perumal, R., Voos, H., Dalla Vedova, F., & Moser, H.: **Reliability-Based Multidisciplinary Design Optimization of Small Satellites**. – *AIAA Aviation forum*, (2021)

4. Pandi Perumal, R., Voos, H., Dalla Vedova, F., & Moser, H.: **Statistical Analysis of Small Satellite Reliability: 1990-2019**. – *AIAA Propulsion and Energy Forum*, (2021)

5. Pandi Perumal, R., Voos, H., Dalla Vedova, F., & Moser, H.: **DESIRA: A DEcision Support system for Incorporating Risk Assessments in early design stages**. – *In Proceedings of the 72st International Astronautical Congress*, (2021)

6. Pandi Perumal, R., Voos, H., Dalla Vedova, F., & Moser, H.: **Statistical Reliability Analysis of Large Satellites: A decade in review**. – *In Proceedings of the 72st International Astronautical Congress*, (2021)

7. Pandi Perumal, R., Voos, H., Dalla Vedova, F., & Moser, H.: **Large scale Multidisciplinary Design Optimization of a Distributed Space System**. – *In Proceedings of the 72st International Astronautical Congress*, (2021)

The developed decision support system has also been used in designing spacecrafts for deep space mission. These studies are not within the scope of this thesis but has been published as follows.

1. Pandi Perumal, R., Abbud-Madrid, A., & Voos, H.: **Atmospheric Re-entry Energy Storage (ARES)- A Novel concept for utilizing atmospheric re-entry energy**. – *In Proceedings of the Global Space Exploration Conference*, (2021)

2. Pandi Perumal, R., Menzio, D., Voos, H., Passvogel, T.: **Multidisciplinary Design Optimization of Caroline, a reusable lunar lander/ascender for on-orbit refueling of Herschel**. – *In Proceedings of the 72st International Astronautical Congress*, (2021)

3. Menzio, D., Passvogel, T., Pandi Perumal, R., Stepanova, N., Cujko, L., & Voos, H.: **Herschel Re-Supply Mission Feasibility Study**. – *In Proceedings of the 72st International Astronautical Congress*, (2021)

Know how to solve every problem that has ever been solved.

Richard Feynman

2

Literature Review

Reliability is a crucial parameter while designing a satellite. This chapter presents the reliability analysis, design methods and optimization techniques carried out hitherto for satellites design. In addition to the satellite, state of the art in other domains such as automobile and aircraft design are also examined to identify novel techniques that could

improve the satellite design process. The research gaps in the literature are identified and summarized at the end of this chapter.

2.1 Reliability Analysis

Reliability is defined as "the ability of a system or component to perform its required functions under stated conditions for a specified period of time"[2]. Since satellites' maintenance, replacement and repair work in orbit is impractical, it is important that satellites have high reliability to perform their mission successfully. Therefore, the importance of reliability is consistently recognized and emphasized by satellite developers[3]. An appropriate starting point to improve the reliability is to study the reliability trends and dominant causes of failure of the satellites launched in the past. However, a statistical analysis of on-orbit failure data is often lacking or obsolete.

Addressing the need, Castet and Saleh presented a series of papers[4–7] that investigated the satellite on-orbit reliability. It was the first study that presented the survival analysis with on-orbit satellite reliability data. The study showed that except "Control Processor", all the subsystems exhibited infant mortality. It means that the subsystems are prone to failure during the initial period in orbit. Past this period, the failure probability decreased over time and became stable. The grouping of elements in this study differed from the conventional way the satellite subsystems are grouped, thus minimizing its usefulness as literature. Nevertheless, the study confirmed that Weibull Distributions better represented the satellite reliability than Exponential Distribution that cannot model infant mortality. Dubos et al.[8] went one step further and identified the impact of satellite size on its reliability by classifying them as small, medium and large satellites. The results verified the presence of infant mortality in all

categories of satellites and identified that small satellites have the highest infant mortality. In a subsequent study, Guo et al.[9] categorized small satellites based on their mission type, developer, and design lifetime to investigate the variation in reliability for each category through statistical analysis. Since the categorization reduced the size of each dataset, it increased the uncertainty in results. However, the study's outcome provided reliability estimates for specific types of satellites, which were not available till then. On the other hand, Hamlin et al.[10] performed statistical analysis on large satellite buses and investigated the variation in reliability between the manufacturers.

The studies mentioned above provide valuable literature on the on-orbit reliability trends of satellites. However, they were carried out more than a decade ago making them outdated and inadequate for the current designs. Numerous satellites have been launched, with a sharp increase in satellites every year since these reliability studies. For example, in the last decade alone, a total of more than 1300 small satellites weighing between 1kg and 500kg were launched into orbits. Therefore it becomes crucial to investigate the current reliability trends in satellites to guide future developers. Accordingly, the first step in this research is to investigate the latest on-orbit reliability trends of small satellites and identify their vulnerable subsystems/elements. Chapter 3 presents the statistical analysis methods in detail and the latest reliability trends for various satellite categorizations using these methods.

Following the investigation on the macro reliability with statistical models, the next step in this research is to evaluate the reliability of satellites under development using these results. In general, the reliability of a system is verified by extensive testing when the system reaches a particular maturity level. However, as the system matures, it becomes difficult to implement strategies to address reliability deficiencies without fueling costs. The study published

by National Academic Press points that a small investment in reliability during the conceptual design phase would substantially reduce the life cycle costs of a system[1]. On the other hand, reliability evaluation of a system during the conceptual design phase is challenging as there is no profound information on the individual elements that constitute the satellite. The ideal workaround in this situation is to translate the reliability evaluation, a bottom-up approach, into a reliability allocation problem, a top-down approach. Reliability allocation is a process of determining the reliability of subsystems and lower level elements to reach the required system reliability. Reliability allocation methods are broadly divided into two categories: Weighting factors and Optimal reliability allocation[11]. Weighting factors use expert opinions to assign weights to subsystems, which are utilized to allocate reliability. Whereas the optimal allocation method uses numerical optimization to identify the optimum number of elements (redundancy) and element choice to optimize the system reliability or cost with respect to various resource constraints such as size, weight and power.

Researchers in the past had developed various weighting factor methods that primarily differ by the type of input required for reliability allocation. The most commonly used reliability allocation methods include Aeronautical Radio Inc. (ARINC) method[12], Advisory Group on Reliability of Electronic Equipment (AGREE) method, the Feasibility Of Objectives (FOO) method[11,13], the Integrated Factors method[14], and the Comprehensive method[15]. Recently, Li et al[16] developed a new allocation method based on fuzzy numbers. Detailed discussions on a few of these methods are presented in Chapter 4.1. Although all these methods are valuable in allocating reliability, they depend on expert opinions that may lead to biased results. A more realistic allocation can be achieved at the early design stage by combining heritage data with expert opinions.

Optimal reliability allocation methods have been an active area of research for the past few decades, with numerous methods developed to solve reliability optimization problems. Tillman et al.[17] provided a detailed literature survey of the early work in system reliability optimization and described the advantages and shortcomings of various reliability allocation methods. While all the methods presented in the study worked exceedingly well for small systems, only a few were identified as effective for large systems. These methods were successfully implemented for reliability allocation problems in diverse fields. For example, Yang et al.[18] used the Genetic Algorithm for solving the reliability allocation for nuclear power plants; Rajeevan et al.[19] applied reliability allocation techniques to enhance the availability of wind turbines; Miao et al.[20] used an improved fuzzy analytic hierarchy process to reliability allocation of chemical production systems.

Generally, with optimal reliability allocation methods, the allocation problem is classified as Redundancy Allocation Problem (RAP) and Reliability-Redundancy Allocation Problem (RRAP). As the name suggests, RAP identifies the ideal number of redundancies required to meet the system target. In addition, RRAP goes a step further and provides reliability enhancement by choosing more reliable elements. Both RAP and RRAP have been proved to be complex optimization problems to solve, thus characterized as NP-Hard optimization problems[21].

The two different redundancy strategies in reliability studies are Cold-Standby redundancy and Active redundancy[22]. A Cold-Standby redundant element is not energized and become operational only when the primary element fails, whereas an Active redundant element is always energized. Therefore, in an ideal case, a cold-standby redundant element does not fail before it is put into operation. Conversely, the failure of an active redundant element

follows a failure distribution same as its primary element and does not depend on whether the component is idle or in operation. Cold-standby is more reliable than active redundancy, but it might cause system downtime depending on the time required for failure detection and switching.

Substantial literature surveys[17,22–24] in system reliability optimization indicate that active redundancy strategy is predominantly considered in problem formulation and focused their efforts in developing novel optimization algorithms. These algorithms include Tabu search,[25], Ant colony[26], Particle swarm optimization[27] and Genetic Algorithm[28–31]. Only a very few researches investigated cold-standby redundancy. Coit et al.[32,33] determined the optimal RRAP solution for a non-repairable system using an Exponential failure rate and Erlang distributed failure rate with cold-standby redundancy. The study was further extended by treating the choice of redundancy as an additional design variable[34].

The reliability optimization problems have often been widely studied for single phased missions. However, a satellite is subject to consecutive phases such as launch, orbit transfer, on-orbit operation and disposal whose operations differ from one another. A system with more than one phase is called a multi-phased system or simply a Phased Mission System (PMS). The failure criteria of a PMS may change from phase to phase. Additionally, the system can be subjected to various set of environmental conditions, which implies that the failure rate of the same element is different in different phases[35]. Therefore the dependencies among the system elements in every phase must be included in the reliability estimation of PMS. The three conventional approaches for reliability analysis of PMS are, Combinatorial method[36,37], Markov chain method or State-space model[38], and Modular method[39]. The combinatorial method is rapid in estimating reliability, but is limited to static systems in

which the sequence of elemental failure does not affect the system reliability. Markov chain method is used for dynamic systems that have cold-standby or repairable elements. The drawback of this approach is that it grows exponentially when the number of system elements increases and suffers from the well-known state explosion problem. The modular method leverages the advantages of these two methods and is ideal for analyzing large systems, especially if only a small part of the system is dynamic. It applies the Markov chain method locally for the dynamic part of the system while applying the Combinatorial method globally. There have not been enough researches that address the reliability analysis of a large PMS such as a Satellite system. Dai et al.[40] studied structural optimization of PMS with non-repairable elements. Recently, Li et al.[41] studied the RAP of the phased mission system with a mixed redundancy strategy.

While the novel RAP and RRAP methods are employed in other domains, they are not widely used for satellite reliability analysis. Recently, Nefes et al.[42] proposed a redundancy optimization approach for designing a Satellite communication payload. Li et al.[41] solved the RAP for a simple satellite propulsion system to demonstrate their novel RAP optimization procedure. However, RAP and RRAP for an entire satellite have never been formulated so far because: for a traditional satellite, reliability is usually ensured by comprehensive testing of components and systems; the conventional satellites use space-grade components, which are highly reliable; the complexity of the satellite inhibits such formulation. However, with the recent shift in interest to small satellites, reliability continues to be more crucial than ever. The Commercial off the shelf (COTS) components used in the contemporary satellites exhibit lower reliability than space grade counterparts. Therefore the application of RAP and RRAP for small satellites is an important area for research. Chapter 4 presents the detailed

procedure and application of RAP and RRAP for small satellites.

2.2 Multidisciplinary Design Optimization

The traditional method of satellite design involves multiple design loops where every subsystem is designed in parallel and later assembled to form the complete satellite. This approach typically gravitates towards optimizing point design and trade studies to provide a few alternatives, thus often resulting in a sub-optimal satellite design. Numerous researches were carried out to optimize satellite design where numerical optimization is extensively used to optimize the individual subsystems/disciplines. For example, Boudjemai et al.[43] performed topology optimization using an enhanced Genetic Algorithm. Ravanbakhsh et al.[44] developed a structural sizing tool to minimize the total mass of the satellite. Galski et al.[45] optimized the satellite thermal subsystem for a multi-purpose satellite platform using a Generalized Extremal Optimization (GEO) algorithm. Jain and Simon[46] developed a real-time power management optimization of small satellites, and Richie et al.[47] optimized the energy storage and attitude control system of a small satellite. These optimizations produced outstandingly optimal satellite subsystems but yielded a moderately optimal satellite system due to the lack of interaction between the subsystems.

The performance of complex system is driven not only by the individual subsystem/discipline model but also their interactions. Multidisciplinary Design Optimization (MDO) is a relatively new field of engineering that simultaneously optimizes and examines the interdisciplinary coupling (interactions) to achieve better designs in a complex system such as a satellite. MDO leverages the synergism/interactions between various disciplines and incorporates them into the design calculation. The origins of MDO can be traced back to the structural

optimization community, especially to the works of Schmit et al.[48–50] and Haftka et al.[51–53]. Over the years MDO has been applied to optimize various complex systems with strong disciplinary couplings such as aircrafts[54–62], Internal Combustion Engines[63], bridges[64,65], trains[66], energy generation systems[67], wind turbines[68,69], automobiles[70–72], UAVs[73,74], Reusable Launch Vehicles[75,76] and spacecrafts[77–80].

Mosher[79,81] was the first to investigate the applicability of MDO to conceptual satellite design and developed a Spacecraft Concept Optimization and Utility Tool (SCOUT) to find the optimal satellite design. Taylor[82] advanced further by comparing MDO with traditional satellite design approaches and identified MDO as a powerful tool to improve decision-making capabilities. Jafarsalehi et al.[80] developed a distributed Collaborative Optimization (CO) framework that used Genetic Algorithm to optimize a remote sensing small satellite mission. Wu et al.[83] used a gradient-based approach to optimize a high fidelity satellite model. Hwang et al.[77] carried out a large-scale multidisciplinary optimization of a small satellite design and operation using a new mathematical framework for gradient-based MDO. Barnhart et al.[78] developed SPIDR, an automatic end-to-end design tool that addresses the entire system engineering life cycle to improve the quality of satellite. On the other hand, Fukunaga et al.[84] implemented OASIS, an adaptive problem-solver that uses machine learning to adaptively select and configure a meta-heuristic algorithm to optimize a satellite model in Multidisciplinary Integrated Design Assistant for Spacecraft (MIDAS)[85].

The main spacecraft MDO frameworks that have been developed over the years include Spacecraft System Design and Simulation Environment (SSDSE)[86], Modeling and Simulation of Satellite System (MuSSat)[87], Spacecraft Distributed Design Environment (SDIDE)[88], and Satellite Integrated Design Environment (SIDE)[89]. Also, a few efforts have been made

to optimize Distributed Space Systems (DSS) design by examining the coupling between the constellation and the satellite model. Shi et al.[90] used a surrogate assisted optimization for satellite constellation system design.

Another vital aspect of MDO is the architecture that defines the type of coupling between the models and the overall optimization process. The choice of MDO architecture has a significant impact on the optimization process and the computational costs. MDO architectures are broadly classified as hierarchical and non-hierarchical architectures. In hierarchical architecture, each child element has a parent element with which it exclusively interacts[91]. Whereas, in the non-hierarchical architectures, there are various interactions between the child elements in addition to their interaction with the parent element. Martins and Lambe[92] surveyed 14 different MDO architectures and presented a detailed insight on each of them. Due to the complex interactions among the child elements, the non-hierarchical approach is more suitable for designing and optimizing a satellite. The non-hierarchical architectures are further classified into two types based on the problem formulation. When a problem is formulated as a single optimization problem, it is called Monolithic architecture, and when it is decomposed into sub-problems to have a combined solution, it is called Distributed architecture.

A plenty of efforts have been invested to compare different MDO architectures[91,93–100]. When optimizing a complex system, Hulme and Bloebaum[95] arrived at a result favouring Multiple Design Feasible (MDF) over Individual Design Feasible (IDF) and All-At-Once (AAO). Another study by Marriage and Martins[101] concluded that Collaborative Optimization (CO) outperformed MDF when few subsystems were highly coupled while the others were not. On the contrary, benchmarking by Tedford and Martins[99] showed that IDF and

Simultaneous Analysis and Design (SAND) had the best performance over MDF and CO for their optimization problems. A recurring point made from these studies is that architecture's performance is problem-specific, and there is no one superior architecture that is suitable for all types of problems. Diverse results obtained from the above studies show that the selection of MDO architecture affects both the optimality of the solution and the computational resources required. Remarkably few researchers[90] have optimized the satellite design problem using MDO approaches, but the comparisons of MDO architectures have not yet been analyzed for the satellite design problem.

Chapter 5 presents numerical models of satellite subsystems and their interdisciplinary couplings. The developed system model is integrated into the distributed space system model, and different MDO formulations are compared for this application.

2.3 Reliability Based Multidisciplinary Design Optimization

The main challenge of designing small satellites is to reduce overall costs while satisfying performance and reliability requirements. Early inclusion of reliability analysis using reliability allocation approaches optimizes the satellite reliability while reducing the cost. Likewise, solving the satellite design problem as an MDO formulation results in a more optimized design. However, the satellite design may still be sub-optimal due to the lack of correlation between the satellite and the reliability models. Notable design improvement and cost reduction are achievable only by examining the impact of design choices on reliability. Besides, it is not intuitively possible to explore a design trade-space by varying the design variables while examining the impacts on the design and their concomitant impacts on reliability. Indeed, individual optimizations for reliability and design do not articulate what drives value in the

design, thus requiring a Reliability-Based Design Optimization (RBDO).

RBDO of an engineering system involves finding a system design such that the prescribed performance is optimized while ensuring the system reliability is above acceptable limit[102]. RBDO is widely used in industries, especially the structural design community, to integrate reliability with design optimization[103–110]. The primary focus of their studies were either to identify an effective way to formulate the problem or to develop efficient optimization procedures to solve the problem. The studies often employed deterministic models[111–113] and probabilistic models[114,115] to quantify reliability of the structural design. Multiple novel algorithms such as Genetic Algorithm(GA)[116], Particle Swarm Optimization[117,118], Directional bat algorithm[119] are exercised for RBDO to reduce the computational effort. Meng et al.[120] surveyed several RBDO researches and provided an overview of metaheuristics for RBDO problems. RBDO's success and effectiveness in solving the structural design problem have inspired other industries to utilize RBDO techniques for various high reliability demanding complex systems.

Attractive traits of RBDO and MDO can be combined as a Reliability-Based Multidisciplinary Design Optimization (RBMDO) for designing complex multidisciplinary systems. RBMDO is gradually gaining its deserved attention, particularly in the development of launch vehicles[121], aircrafts[122–126], automobiles[127,128] and turbine blades[129,130]. Similar to MDO, the computational efficiency of RBMDO also depends on the choice of MDO architecture employed. Nikbay et al.[131] optimized aircraft wings by formulating the problem as MDF architecture, resulting in the RBMDO-MDF method. Furthermore, Huang et al.[132] decoupled the system in electronic product design by formulating the problem with IDF architecture to improve the computational efficiency. On the other hand, Hui et al.[133] com-

bined Concurrent SubSpace Optimization (CSSO), which is a type of distributed MDO architecture, with the advanced first-order second-moment reliability analysis model to develop an RBMDO-CSSO method. Similarly, Ahn et al.[134] proposed an RBMDO-BLISS method in which the reliability analysis and design optimization were carried out sequentially. Despite justifying their success, RBDO and RBMDO are barely enforced in satellite design. Only a handful of studies that discuss satellite design optimization in the context of reliability have been published. Many satellite developers are yet to derive their advantages.

Combining reliability and satellite design problem results in mixed-integer nonlinear programming (MINLP) problem that is challenging to solve, mainly when involving numerous design variables. Often MINLP is divided into Nonlinear Programming (NLP) involving continuous variables and Integer Linear Programming (ILP) involving integer variables to make it computationally easier. However, the interactions between design and reliability are lost by dividing MINLP, thus producing sub-optimal design. For example, the reliability of a satellite depends on its design, and it must be modified when reliability improvement is required. In some cases, the design might not meet the reliability target within the available resources such as size, weight, power and cost (SWaP-C) when solving NLP and ILP individually.

Although, simultaneously optimizing RBMDO as MINLP is computationally expensive, it has the highest potential for optimal design. Therefore, the Surrogate model method was employed by previous researchers to reduce the complexity of the computation. A surrogate model eliminates repeated computation of complex functions by fitting the output responses with input parameters. Meng et al.[127] used a response surface model, a type of surrogate model, to reduce the computation time of coupled analysis in a hydraulic transmission

system. Roshanin et al.[121] proposed a similar approach to reduce the computational time in RBMDO of launch vehicles. Chen et al.[135], and Li et al.[136] employed the Kriging surrogate model to improve the efficiency of the RBMDO. Roy et al.[137–139] developed a Mixed Integer Efficient Global Optimization algorithm - Multiple Infill via a Multi-Objective Strategy (AMIEGO-MIMOS) to aircraft mission design which employs the Kriging surrogate model for the integer part of the problem. However, these novel approaches that include surrogate models have not been employed for the RBMDO of satellites so far.

Although, some specific ideas of RBMDO were utilized for the satellite design in previous studies. Pullen et al.[140] optimized a spacecraft design for performance uncertainty measured in terms of reliability by considering redundancy as design variables. Mosher et al.[141] considered technology choices for the spacecraft bus as design variables while optimizing the spacecraft. Mosher did not explicitly analyze reliability, but the spacecraft bus's technology choices influenced the cost, which impacted its reliability. Hassan et al.[142] carried out reliability-based design optimization by formulating both the technology choices and redundancy levels as discrete design variables in the optimization of a communication satellite.

Moreover, the reliability models in the literature formulate satellite as a single phased system instead of a Phased Mission System (PMS), resulting in disproportionate prioritization of mission-critical elements to improve the system reliability. To the best of the authors' knowledge, the RBMDO of satellites and their design in the PMS context have not been published previously, making it a unique optimization problem.

2.4 Decision Support System

Traditionally, satellite design lifecycles follow the sequential method, where conceptual design is followed by cost estimation. The traditional method calls for contributions from several teams and domain experts, thus consuming substantial time and resources. Moreover, it condemns point designs inflexible towards evolving requirements and does not account for its downstream implication. Due to these pitfalls of the traditional method, contemporary concurrent design is extensively used nowadays[143,144].

The Concurrent Design method employed in the early design phases cutbacks the time needed to produce the initial design[145]. Concurrent Design methodologies enable the simultaneous design of individual subsystems while managing their interdisciplinary interactions to improve efficiency and productivity. Over the years, several system engineering tools and support systems are developed to advance the concurrent design. GAJAT[146] was one of the earliest tools developed at NASA-JPL to replicate the mission design out of Team-X, formally called the Advanced Products Development Team. GAJAT supports the design process by providing estimates for consumable resources required for the mission, minimum required launch vehicle capability, ground segment requirements, and total mission cost. Aguilar et al.[147] developed a spreadsheet-based tool, explicitly for ease of use, at the Concurrent Design Center in The Aerospace Corporation. It assisted them in the design process by connecting all subsystems through a local server, thus allowing continual contribution from domain experts. Also, real-time discussions at the design center identified subsystem interactions that were not captured by the tool.

Although these system engineering tools enhanced the design process, they identify point

design and abstain when top-level requirements evolve. To deal with this problem, Chase et al.[148] developed a tool that connected discipline models with system-level trade models and explored the trade space of the design. Girerd et al.[149] followed a similar approach and developed the Project Trades Model (PTM) that captured the interactions between system and subsystems to enable trade studies such as system performances, costs and risks. Further adding to the contribution, Min et al.[150] performed a broader trade analysis by developing a pre-study tool called Space Architecture Development and Analysis Tool (SADAT) that generated hundreds of design options. Morse et al.[151] developed detailed engineering models to complement the point designs with a range of design alternatives. Interestingly, Lewis et al.[152] developed a modular concurrent engineering model that offered convenience in using models developed for previous missions, thus shortening the design time.

On the other hand, McInnes et al.[153] identified that these tools were biased towards large satellite designs and lacked the capabilities needed for designing small satellites. Therefore, McInnes developed the SmallSatCEM tool to support small satellite design studies. SmallSatCEM was developed in Microsoft Excel with Visual Basic in the backend for computation. Furthermore, the tool was also linked to small satellite component databases, engineering models and analysis tools related to small satellites.

Similar to SmallSatCEM, Ridolfi et al.[154] developed the System Engineering Module (SEM) to enhance the quality of the design by utilizing a multidisciplinary design process, and Chang et al.[155] developed System Engineering Design Tool (SEDT) to minimize the labour involved in the conceptual design of small satellites. Additionally, SEDT was linked to a database that contained detailed designs of 200 small satellites. Leveraging this data, SEDT could verify design parameters, provide design references and estimate a rough development

cost based on the requirements. SEDT is also considered as a statistical design analyzer owing to a large amount of data. Additionally, SEDT has a graphic user interface to provide convenience to the users. While most of the tools discussed here invested in implementing a user-friendly interface to promote its usage, identifying an optimal was not prioritized. Moreover, reliability models were not considered in these tools. SADAT is the only exception, that implemented a simple reliability model and supported numerical optimization.

2.5 Research Gap Summary

In summary, a collection of research gaps in the published literature that relate to the overarching goals of this research are given below.

- The statistical analyses of on-orbit data were carried out more than a decade ago, making them outdated and primarily inadequate for the current designs.
- Development of allocation strategy combining heritage data and expert opinions are rarely explored.
- The optimal reliability allocation strategies used for satellite designs are not formulated as RAP and RRAP problems.
- The satellite designs have not been modelled as a Phased Mission System, thus overlooking mission-critical systems in reliability analysis.
- The MDO for satellite designs is seldom employed, and a suitable MDO architecture for this application is not identified.
- RBMDO of small satellites in the context of PMS has not been studied so far.

- Design approaches that combine reliability with satellite models in the initial design phase lacks detailed research.
- The Decision support systems developed to complement the concurrent design do not leverage the latest developments in MDO and reliability analysis.

Without data you are just another person with opinion.

W.Edwards Deming

3

Statistical Reliability Analysis

The reliability of a system is an indicator that conveys how well the system performs during a given operational period without any failure or a need for repair work. Given the increasing levels of sophistication in today's engineering systems, one of the critical requirements is to design a highly reliable system within the available size, weight, power, cost

and other resources. Inadequate reliability considerations in the initial design stages can result in incompetent designs that are expensive to improve later. Hence, there is an increasing concern among satellite designers and engineers to pay particular attention to reliability from the beginning of the design.

Due to the insufficient failure data of satellites and their components, reliability analysis during the conceptual design phase becomes a complicated process. Alternatively, statistical analysis of on-orbit satellite failure data identifies a macro-reliability figure based on the satellite mass category, mission and orbit inclination. This chapter presents a methodical approach describing the steps involved in the reliability analysis of satellites.

3.1 Analysis Approach

A broad understanding of satellite reliability trends can help understand the common cause of failure and identify design choices to lower the likelihood of failure. In this chapter, the reliability trends of small satellites launched over the last three decades are investigated and compared. The dataset containing on-orbit failure data of satellites are mainly categorized based on their mass as shown in Table 3.1. However, this research strongly emphasizes on on-orbit failures of small satellites ($40 - 500$ kg).

Table 3.1: Satellite Mass Categories

Category	Mass Range [kg]
Picosatellite	$0 - 1$
Nanosatellite	$1 - 10$
Microsatellite	$10 - 100$
Minisatellite	$100 - 500$
Large satellite	$500 - 5000$

First, the non-parametric reliability functions of the satellites are calculated with the widely used Kaplan-Meier estimator. Next, the obtained reliability results are represented using suitable parametric models such as Weibull distribution and Exponential distribution. The dataset is further classified based on satellite mission, developer type, launch date, design life-time and orbit inclination to analyze their specific reliability trends. Finally, the contribution to satellite failure by the satellite subsystems is quantified for each category of the dataset, and the subsystems with high(er) propensity for failure are identified. The subsystems at risk are then subject to improvement by incorporating reliability/redundancy allocation.

3.2 Data Collection

The dataset containing on-orbit failure data of satellites is gathered from the Seradata SpaceTrak database[156]. This database is considered the most authoritative and is used by leading launch providers, satellite insurers and manufacturers. Additionally, the publicly available Satellite Missions Database[157] is also utilised to cross-verify the previously obtained dataset and append any missing information. The consolidated dataset consists of 31 picosatellites weighing from $0.1-1$ kg, 1900 small satellites weighing from $1-500$ kg, and 1702 large satellites weighing from $500-5000$ kg launched between $1990-2020$. The dataset is restricted to satellites that were successfully launched into Earth-orbits. Interplanetary missions and satellites that failed due to launcher failures are also excluded from the dataset.

For each satellite, the following data are collected: 1) launch date 2) failure date, in case of failure 3) censor date, in case of no failure 4) mission group 5) orbit inclination 6) equipment at fault 7) capability lost. Censoring occurs when a satellite is in operation by the end of the

observation window or if it is turned off before it failed. As a result, the dataset also includes right-censored data. Survival analysis of censored dataset is not trivial and has to be carefully analysed to obtain unbiased results. Kaplan-Meier estimator[158] is best suited to handle the dataset containing complete and right-censored data points.

3.3 Nonparametric Analysis of Satellite Failure Data

Nonparametric methods are distribution-free and do not rely on the assumption that the data is drawn from any parametric family of probability distributions. Kaplan-Meier is one of the nonparametric estimators used to estimate the survival function from failure data. The survival function of the Kaplan-Meier estimator is a right continuous step function with steps at failure times[158]. The Kaplan-Meier estimate of the survival function, also called the reliability function, is defined as

$$R(t) = \prod_{t_i<t} \frac{n_i - d_i}{n_i} \tag{3.1}$$

where d_i is the number of failed satellites at time t and n_i is the number of satellites operational just before the time t. The dispersion of the Kaplan-Meier estimate is captured using the 95% confidence interval. It shows the 95% likelihood that the actual reliability will fall between the upper and lower bounds, while the calculated reliability is the most likely estimate. The upper and lower bounds are calculated from the variance or standard deviation of the estimator. The variance of the Kaplan-Meier estimator is given by Greenwood's formula[159] as given below.

$$\hat{var}[R(t_i)] \equiv \sigma^2(t_i) = [\hat{R}(t_i)]^2 \sum \frac{d_i}{n_i(n_i - d_i)} \tag{3.2}$$

$$R_{95\%}(t_i) = \hat{R}(t_i) \pm 1.96\,\sigma(t_i) \tag{3.3}$$

3.4 Parametric Analysis of Satellite Failure Data

Even though nonparametric analysis is flexible, the results are difficult to interpret. Therefore a parametric model and a probability distribution function are needed to model the reliability of satellites. Weibull distribution is used to model the data whose distribution parameters are determined using the Graphical method (GM) and the Maximum Likelihood Estimate (MLE). The goodness of fit indicators such as the Coefficient of determination (R^2) for GM and Akaike Information Criterion (AIC) for MLE are used to verify the fit and compare with other distributions.

3.4.1 Weibull Distribution

One of the general practices is to model the satellite reliability using Exponential Distribution. However, the constant failure rates in Exponential Distribution inappropriately model the reliability of satellite components. Therefore the reliability bathtub curve is used to provide better models. The reliability bathtub curve consists of three key periods: infant mortality, where failure rates decrease as a function of time, normal life or useful life, where failure rates remain low and constant over time, and end of life wear-out, where the failure rates increase over time. Commercial satellites employ space-grade components, which are "burned-in" to eliminate infant moralities. The mission lifetime would be less than the normal lifetime of the weakest component and does not encounter the third key period. Therefore, it is sufficient in this case to estimate reliability in the second key period. However,

COTS components used in the small satellites are not burned-in, and the duration of the normal life is insignificant. Hence, it is crucial to consider all three periods during the design of small satellites. Weibull Distribution is generally preferred in such cases as it can model all three periods. The probability density function of Weibull Distribution is given by,

$$f(t) = \begin{cases} \left(\frac{\beta}{\alpha}\right)\left(\frac{t}{\alpha}\right)^{(\beta-1)} e^{-\left(\frac{t}{\alpha}\right)^{\beta}} \text{for } t \geq 0 \\ 0 \qquad\qquad\qquad\qquad \text{for } t < 0 \end{cases} \tag{3.4}$$

where α is the scale parameter and is expressed in units of time, t. It represents the time when 63.2% of the population has died. β is the shape parameter and is dimensionless. The failure rate or hazard rate of Weibull Distribution is written as follows.

$$\lambda(t) = \frac{\beta}{\alpha}\left(\frac{t}{\alpha}\right)^{\beta-1}, \beta > 0, \alpha > 0, t \geq 0 \tag{3.5}$$

For $0 < \beta < 1$, the failure rate is decreasing that models the infant mortality. For $\beta = 1$, the failure rate is constant and this is equivalent to Exponential Distribution. For $\beta > 1$, the failure rate is increasing that models the wear-out period. The reliability function of Weibull Distribution is

$$R(t) = e^{-\left(\frac{t}{\alpha}\right)^{\beta}} \tag{3.6}$$

3.4.2 Graphical Method

One of the simplest ways to estimate the shape and scale parameter of the Weibull Distribution is linear regression, also called the Graphical Method. The reliability function of the Weibull Distribution can be expressed as a linear equation by taking natural logarithm twice

and rearranging the equation (3.6) as follows:

$$ln[R(t)] = -\left(\frac{t}{\alpha}\right)^{\beta} \tag{3.7}$$

$$ln[-ln[R(t)] = \beta\, ln\, t - \beta\, ln\, \alpha \tag{3.8}$$

This can be rewritten as a linear equation,

$$y = mx + c \tag{3.9}$$

where $y = ln[-ln[R(t)]$, $x = ln\, t$, slope $m = \beta$ the shape parameter and intercept $c = -\beta\, ln\, \alpha$. With equation (3.9) and the reliability estimates calculated from the Nonparameteric analysis, the shape and scale parameter of the Weibull Distribution can be estimated. The coefficient of determination denoted by R^2, pronounced as "R-squared" is the indication of how well the observed on-orbit failure behaviour is replicated by the regression model. R^2 ranges between 0 to 1 where 1 indicates that the regression model perfectly fits the data.

3.4.3 Maximum Likelihood Estimation

Another way of estimating the Weibull parameters is using a Maximum Likelihood Estimator. The accuracy of the Weibull model is better using MLE compared to GM. The likelihood function is defined as a function that expresses the joint density of all observations in the dataset. The Weibull parameters that maximize this likelihood function are the most likely or the maximum likelihood values for the shape and scale parameter. The main reason for investigating this approach is its asymptotic unbiasedness and minimal variance. The

likelihood function for a censored dataset[160] is given as,

$$P(t|\alpha,\beta) = \prod_{i=1}^{n} f(t_i|\alpha,\beta)^{c_i}\, R(t_i|\alpha,\beta)^{1-c_i} \tag{3.10}$$

where c_i is the censor indicator and is equal to 0 if the datapoint is censored and 1 if failure has occurred. The function f represents the Weibull probability density function and R the reliability function. Substituting equation (3.4) and (3.6) in equation (3.10),

$$P(t_f, t_c|\alpha,\beta) = \prod_{i=1}^{n} \left(\frac{\beta}{\alpha}\right) \left(\frac{t_{f_i}}{\alpha}\right)^{(\beta-1)} e^{-\left(\frac{t_{f_i}}{\alpha}\right)^{\beta}} \prod_{i=1}^{n} e^{-\left(\frac{t_{c_i}}{\alpha}\right)^{\beta}} \tag{3.11}$$

where t_f, t_c represent the failure time and censor time respectively. The shape and scale parameter can be estimated by maximizing equation (3.11). Similar to the coefficient of determination, for MLE, Akaike Information Criterion (AIC) represents the prediction error and quality of model fit for the given data. Generally, AIC is used to compare different models, and it estimates the relative amount of information lost by the model. Lower AIC values indicate a better-fit model.

3.5 Small Satellites

The consolidated dataset consists of various classes of satellites operating in different environments. The design philosophies for each satellite is distinct from each other. Therefore, the dataset is fragmented into three subsets to get meaningful results. The reliabilities of small satellites ($40-500$ kg) are discussed in detail in the following sections. Following that, a brief discussion of the reliabilities of small satellites ($0.1-40$ kg) and large satellites (>500 kg) are presented. There are more than 1000 satellites weighing less than 40 kg in the dataset, and

they have comparatively low reliabilities. Therefore, the small satellites are separated into two groups, $0.1 - 40$ kg and $40 - 500$ kg, to eliminate the bias in results.

The analysis of the small satellite dataset is performed in two separate approaches. The first approach examines the collective reliability of small satellites by taking advantage of a large sample to gain a precise result within a narrow confidence interval. However, the results corresponding to the collective reliability conceal the reliability of an individual subset. The second approach categorises the data further based on mission type, developer type, launch date, design lifetime and orbit inclination. This approach provides the reliability of individual subsets, but the sampling size is significantly small, which gives uncertain results.

3.5.1 Collective Reliability

The dataset for collective reliability analysis consists of on-orbit data of 866 small satellites launched between January 1990 to January 2020 of which 318 satellites failed and 548 satellites were censored. Figure 3.1 shows the nonparametric model and the Weibull Distributions. Table 3.2 shows the corresponding Weibull parameters using MLE and GM. The R^2 value calculated from GM is 0.911, which strongly suggests that the Weibull Distribution is a good fit. The AIC of Weibull Distribution estimated from MLE is 2140, and the AIC of Exponential Distribution is 2278. The lower AIC value confirms that the Weibull Distribution is indeed better than the Exponential Distribution.

Table 3.2: Estimated Weibull parameters for small satellites

	Graphical - Method		MLE	
	α [years]	β	α [years]	β
Small Satellites	21.7553	0.5894	19.4949	0.6060

Here, the shape parameter is less than 1 and it clearly indicates the propensity for infant mor-

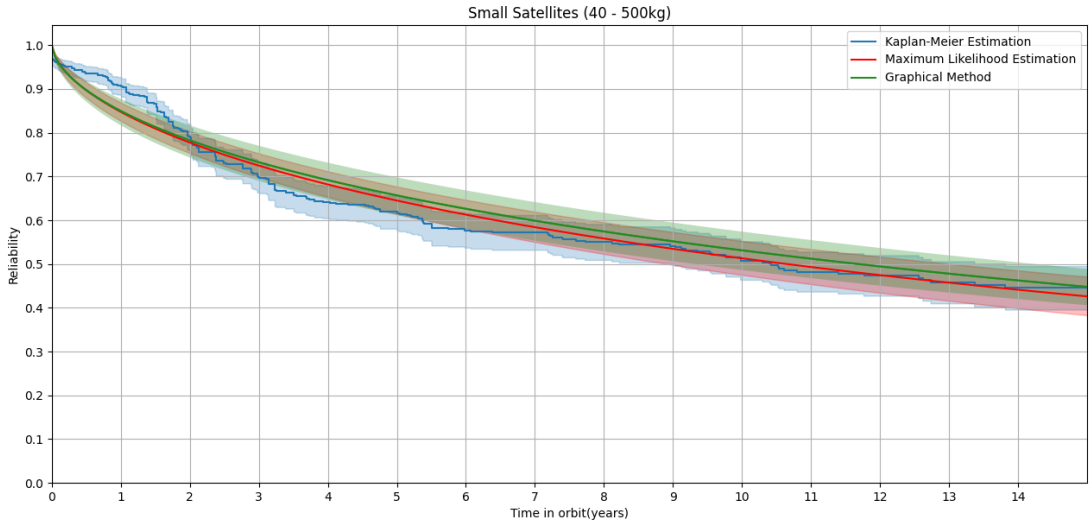

Figure 3.1: Collective reliability of small satellites launched between 1990-2020

tality. Since the Exponential Distribution can only have constant failure rate, it cannot effectively represent the actual on-orbit behaviour of satellite.

3.5.2 Reliability at different decades

The dataset is categorized into two groups to investigate the reliability of small satellite launched in the last three decades. The groups comprise satellites launched before and after 2010. Table 3.3 shows the summary of each category. The number of small satellites launched after 2010 has significantly increased. Figure 3.2 illustrates the non-parametric and Weibull models for the two groups. Table 3.4 lists the associated parameters. 7% of the small satellites launched before 2010 failed or retired within the first year, while this percentage raised to 20% for satellites launched after 2010. The decreasing shape parameter outlines the increased infant mortality of satellites launched after 2010. The surge in first-time satellite developers and comprehensive utilization of COTS components may explain this increase in infant mortal-

ity. However, at five years after launch the reliability of small satellites after 2010 has increased to 0.80 compared to 0.52 for the satellites launched before 2010. The inference here is that if new satellites outlast an initial threshold, they tend to remain functional and outperform the satellites launched before 2010 in terms of survivability.

Table 3.3: Small Satellites categorization based on launch year

Launch year	Launched	Failed	Censored
1990-2009	441	228	213
2010-2019	425	56	369

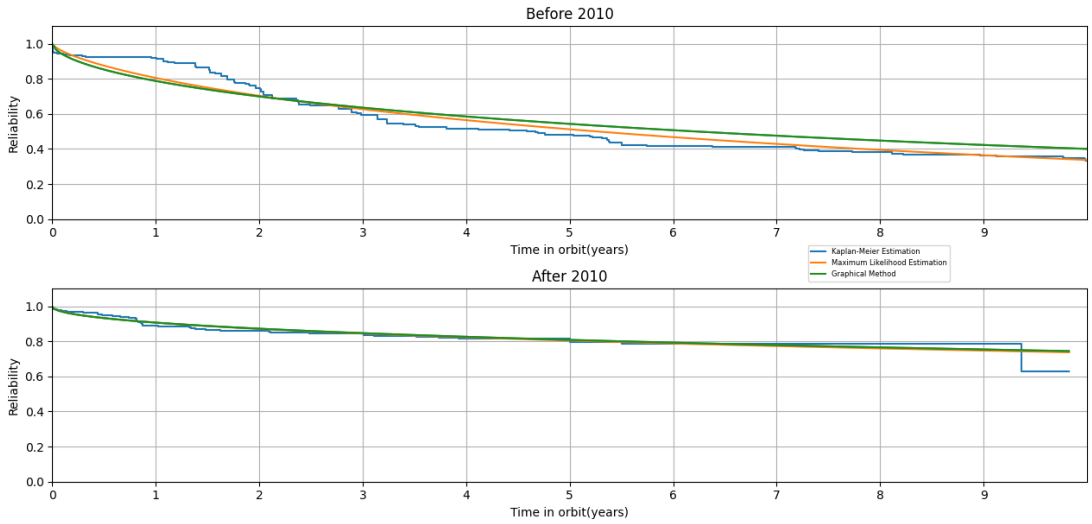

Figure 3.2: Reliability of small satellites launched at different decades

Table 3.4: Estimated Weibull parameters for small satellites categorized based on launch year

Year	Graphical - Method		MLE	
	α [years]	β	α [years]	β
1990-2009	11.6442	0.5842	8.8792	0.7009
2010-2019	122.7151	0.4840	107.9955	0.4964

3.5.3 Reliability for different mission types

This category investigates the effect of mission types on reliability. The same dataset (containing 866 satellites) is subdivided based on four major mission types: Technology Demonstration, Communication, Earth Observation, and Science Mission. Table 3.5 shows the summary of each category. The results obtained in this analysis is analogous to the results from Guo et al.[9]. The dependency of failure behaviour on the mission type barely exhibits any variation in the last decade. Figure 3.3 shows the non-parametric model and Weibull Distributions while their respective parameters are shown in Table 3.6. The shape parameters of Communication and Earth Observation satellites are relatively higher than Technology Demonstration and Science Mission satellites. Among the dataset, 53% of Earth Observation and Communication satellites were developed by private companies to offer commercial services. This foster well-designed and well-tested satellites which exhibit relatively high shape parameter. On the other hand, Technology Demonstrators are profoundly prone to failure due to their accredited purpose. Some private companies offer highly reliable satellite platform for technology demonstration. But the experimental nature of the payload, in this case, affects the overall reliability of the satellite. Science Mission satellites operate in sparsely identified or challenging environments to perform experiments. As a result, they have a higher chance of failing within the first few days of the mission. In contrast, at the end of 10 years, Communication satellites have similar reliability as that of Technology Demonstration satellites. The plummets in reliability are because the technology onboard the communication satellites becomes outdated rather quickly. Therefore, these satellites are either designed for a short life or replaced by the operators to upgrade their services. The inference here is that Communication satellites have the lowest probability to fail during the first year of opera-

tion. At the same time, Earth observation satellites have the lowest probability to fail after ten years in orbit. Science Mission and Technology demonstration satellites have higher infant mortality rates. While Technology demonstration satellites are more prone to failures than Science Mission satellites after five years in orbit.

Table 3.5: Small Satellite categorization based on Mission type

Mission	Launched	Failed	Censored
Technology	129	53	76
Communication	443	200	243
Earth Observation	183	23	160
Science	111	42	69

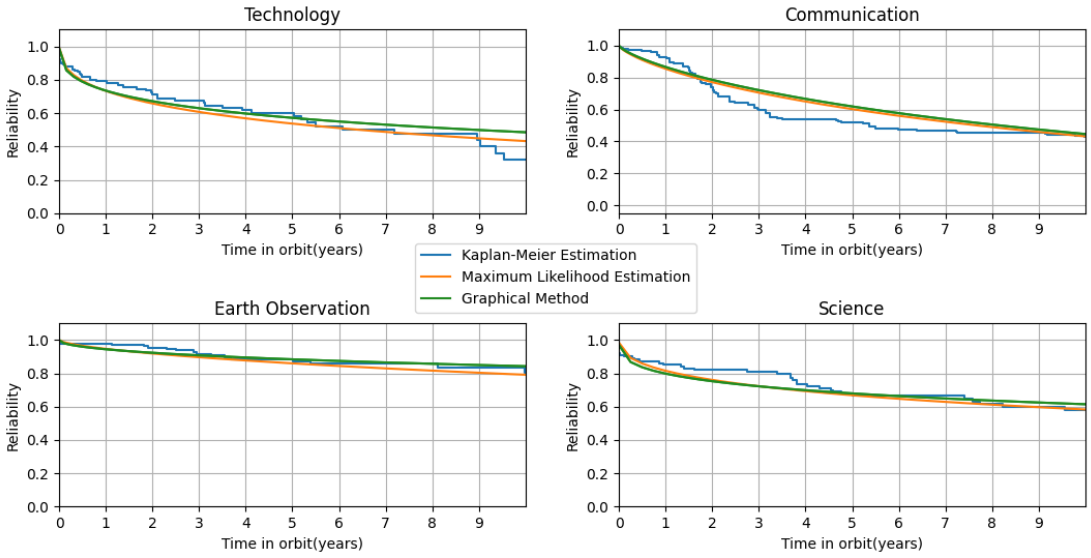

Figure 3.3: Reliability of small satellites for different mission types

3.5.4 Reliability of different satellite developer categories

In this section, the dataset is split into three groups: Government, Private, and University to investigate reliability variation among these satellite developers. Table 3.7 shows the small

Table 3.6: Estimated Weibull parameters for small satellites categorized based on mission type

Mission	Graphical - Method		MLE	
	α [years]	β	α [years]	β
Technology	23.9288	0.3706	15.0166	0.4316
Communication	13.2987	0.7507	12.6880	0.7294
Earth Observation	412.6474	0.4739	99.7970	0.6310
Science	86.1004	0.3343	43.2374	0.4217

satellites based on developers. The satellites developed by national and international space agencies are listed under the Government group, the satellites developed by commercial entities are listed under the Private group, and the satellites developed by schools, colleges and universities are listed under the University group. As expected, the University class satellites suffer significant infant mortality. Satellites under the Government group demonstrate considerably higher reliability than the University satellites. However, their reliability fades over time. In the tenth year, the reliability of University and Government satellites are indistinguishable. The complexity of Government satellites can explain the reason behind this outcome. Moreover, mere housekeeping data might qualify University satellites as operational, but that is not the case for Government satellites. Satellites developed by Private commercial entities have lower shape parameter than Government satellites but demonstrate higher reliability in the tenth year. Nevertheless, it must be taken with a grain of salt as the commercial entities are not as forth-coming as other developers about failures. Around 79% of Private satellites are censored, indicating either the satellites never failed or the satellites assumed to have retired with unreported failure information. Therefore, the reliability of Private satellite may be lower than the result presented here. Figure 3.4 shows the non-parametric and parametric while the Table 3.8 shows the associated parameters for this dataset. It is inferred that Government satellites have the lowest probability to fail during the first year of operation

while Private satellites have the lowest probability to fail after ten years in orbit.

Table 3.7: Small Satellite categorization based on Developer

Mission	Launched	Failed	Censored
Government	437	215	222
Private	374	80	294
University	55	23	32

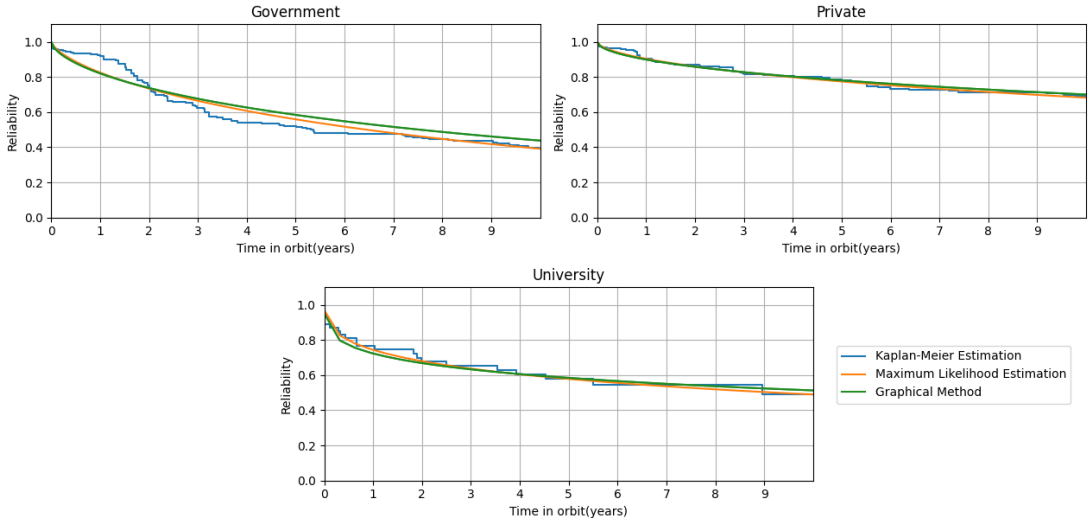

Figure 3.4: Reliability of small satellites for different satellite developers

Table 3.8: Estimated Weibull parameters for small satellites categorized based on Developer

Mission	Graphical - Method		MLE	
	α [years]	β	α [years]	β
Government	13.6189	0.6205	10.9829	0.6894
Private	71.1911	0.5256	52.9258	0.5777
University	36.3287	0.3138	24.2146	0.3818

3.5.5 Reliability for different design lifetime

The dataset is subdivided into three groups based on their design lifetime: less than or equal to five years, greater than five years, and unknown to investigate their reliabilities. Table 3.9 lists the number of satellites launched, failed and censored in each group. Figure 3.5 and Table 3.10 illustrate the non-parametric plus parametric model of the satellite groups and their associated parameters respectively. Unlike in the previous section, there is a notable difference in the shape parameters estimated by MLE and GM. Since MLE better represent the dataset than GM, it is used as a baseline for comparing the subdivided groups. As expected, the satellites with lifetime greater than 5 years have better reliability than the other two groups. The satellites with a long lifetime requirement normally comprise space-grade components, which successfully reduces the infant mortality rate. The satellites whose design life was not known, did not exhibit infant mortality. But their chances of survival faded rather quickly. They had the lowest reliability after 2 years in orbit. The inference here is that the satellites with more than five years of design life have the highest reliability.

Table 3.9: Small Satellite categorization based on Design lifetime

Mission	Launched	Failed	Censored
≤ 5	555	180	375
> 5	151	31	120
Unknown	160	107	53

3.5.6 Reliability for different inclination

Finally, to investigate the effect of the operating environment on reliability, the data is categorized into Polar and Non-Polar orbit groups. The Polar group contains the satellites

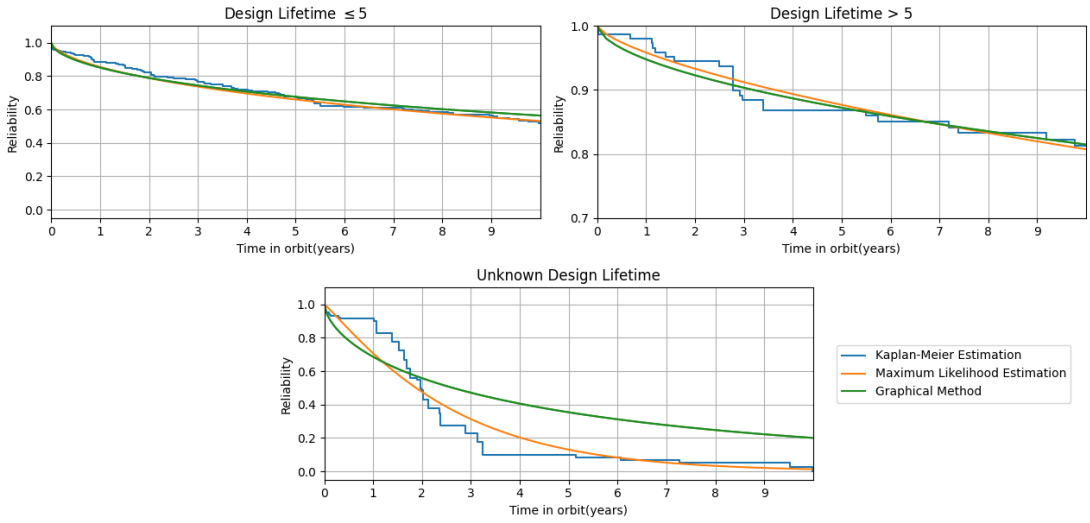

Figure 3.5: Reliability of small satellites for different design lifetimes

Table 3.10: Estimated Weibull parameters for small satellites categorized based on design lifetime

Mission	Graphical - Method		MLE	
	α [years]	β	α [years]	β
≤ 5	27.4768	0.5494	21.2312	0.6063
> 5	151.9503	0.5828	89.7667	0.7025
Unknown	4.7005	0.6302	2.6167	1.1012

operating at orbit inclined between 80° and 110° from the equatorial plane, while the Non-Polar group contains the remaining satellites as shown in Table 3.11. Interestingly, satellites in polar orbits, that are subjected to harsh environments have lower infant mortality than Non-Polar satellites. However, it is coherent that Government agencies and Private entities developed 91% of polar satellites, and most of them are experienced developers. Furthermore, stricter reliability standards are adopted for polar satellites, which contributes to this trend. Understandably over time, the polar satellites deteriorate quicker than the Non-Polar counterparts. Therefore, the reliability of Non-Polar satellites in the fifth year and tenth year is

higher than Polar satellites. Figure 3.6 captures this reliability trends whose parameters are presented in Table 3.12. The inference here is that Polar satellites have the lowest probability to fail during the first year of operation while Non-Polar satellites have the lowest probability to fail after five years.

Table 3.11: Small Satellite categorization based on Operating Environment

Mission	Launched	Failed	Censored
Polar	484	197	287
Non-Polar	382	121	261

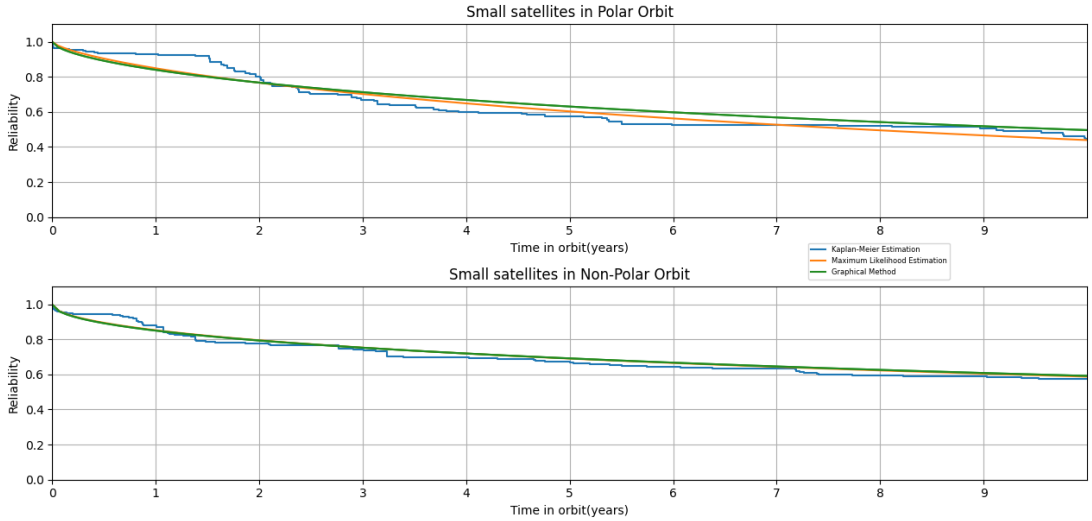

Figure 3.6: Reliability of small satellites with different orbit inclination

Table 3.12: Estimated Weibull parameters for small satellites categorized based on orbit Inclination

Mission	Graphical - Method		MLE	
	α [years]	β	α [years]	β
Polar	18.0388	0.6034	13.2237	0.7008
Non-Polar	35.6253	0.5082	33.5043	0.5220

3.5.7 Relative contribution of each subsystem to failure

As a next step further, subsystems with a high propensity to failure are identified by applying a comparative reliability analysis. The relative contribution of each subsystem to satellite failure is calculated using the model presented by Castet et al.[5]. In this model, for each subsystem j, the probability of subsystem failure, $\hat{P}_{subsystem}$ with its reliability, $\hat{R}_{subsystem}$ is given by equation 3.12. Similarly, the probability of satellite failure is calculated using equation 3.13. Here the reliability of satellite, $\hat{R}_{satellite}$ and reliability of subsystem, $\hat{R}_{subsystem}$ are non-parametric reliability obtained from Kaplan-Meier analysis. Then, the relative contribution of each subsystem is calculated using the equation 3.14.

$$\hat{P}_{subsystem} = 1 - \hat{R}_{subsystem} \tag{3.12}$$

$$\hat{P}_{satellite} = 1 - \hat{R}_{satellite} \tag{3.13}$$

$$r_j = \frac{\hat{P}_{subsystem_j}}{P_{satellite}} \tag{3.14}$$

The Table 3.13 lists the failure of each subsystem that lead to satellite failure at various points in time. Satellite failures that occurred due to collisions or debris strikes are grouped as Others. Likewise, Unknown is another category listed here representing the satellites whose failure reasons are unknown or unreported. Although Unknown represents a dominant part of satellite failure, it is omitted due to its unspecificity and to improve the interpretation of results. The remaining categories are normalized and presented as shown in Figure 3.7.

The overall trend here is that the probability of failure of each subsystem is high at the beginning and steadily reduces in the first two years. Later, the values gradually decrease and

fluctuate around a nominal value. Finally, they wear out at their end of life. The pie-chart in Figure 3.7 shows that Power is the most vulnerable subsystem among others, followed by AOCS and TTC. After 30 days in orbit, the significant failure contribution of AOCS (31.7%) and the Power (31.5%) subsystems indicate that these two systems largely drive infant mortality, followed by TTC (16%) and Mechanism (15.5%). The four major subsystems contributing to satellite failure remain the same after one year in orbit. However, here the Power (29.5%) subsystem contributes more than the AOCS (26%). A similar trend is seen between Mechanism (16.4%) and TTC (13.2%). The contribution of the power subsystem surges to 37.2% at the end of five years. Correspondingly, a sudden climb in the contributions of TTC (20.6%) and Propulsion (6.63%) are observed, whereas the contributions of AOCS (18.8%) and Mechanism (7.53%) have declined. After ten years in orbit, the Power subsystem (44.1%) remains the most probable cause of satellite failure. Meanwhile, an increase in contribution of AOCS (19.1%) and decrease in contribution of TTC (17.4%) are observed. Interestingly, the contribution from Thermal subsystem increases from 1.89% at 5 years to 5.04% at 10 years.

No satellite failed due to Payload and Structural subsystems in ten years in the examined dataset. However, this is an unlikely condition and does not represent the actual case. Payload failure directly associates with mission failure. Due to the non-transparency, it is common to expect payload failure within the unknown category. On the other hand, the structural failure of satellites occurs mainly due to the launch environment, resulting in infant mortality. This complete and immediate loss of satellite may not provide enough failure information and could be included under the Unknown category.

Despite having a high propensity of failure associated with moving parts, the Mechanism subsystem contributes less to the satellite failure than Power, AOCS and TTC subsystems.

Table 3.13: Percentage contribution to satellite failure

Failure	Percentage Contribution (%)			
	30 days	1 year	5 years	10 years
AOCS	17.75	10.41	3.76	4.32
Mechanism	8.68	6.57	1.50	1.13
OBC	2.89	2.84	0.65	0.49
Payload	0.0	0.0	0.0	0.0
Power	17.63	11.78	7.42	9.97
Propulsion	0.0	0.0	1.32	0.99
Structure	0.0	0.0	0.0	0.0
Thermal	0.0	1.65	0.38	1.14
TTC	8.95	5.26	4.12	3.94
Unknown	44.09	60.01	80.04	77.41
Other	0.0	1.47	0.80	0.60

Spacecraft design often avoids complex mechanism and employ highly reliable mechanism. Moreover, most of the mechanism, such as Solar panel Deployment and Hold Down and Release Mechanisms, are single-use mechanisms that only contribute to infant mortality.

3.6 Large Satellites

While small satellites continue to make headlines in the space industry, conventional (medium and large) satellites are still extensively used. The 640 satellites weighing between 500kg - 5000kg launched in the last decade justify this statement. High reliability is recognized as a superior trait of conventional satellites. In this section, the reliability of conventional satellites is analyzed to investigate whether they are better than small satellites to justify their exorbitant cost.

For this analysis, the reliabilities of large satellites launched between January 1990 - Jan-

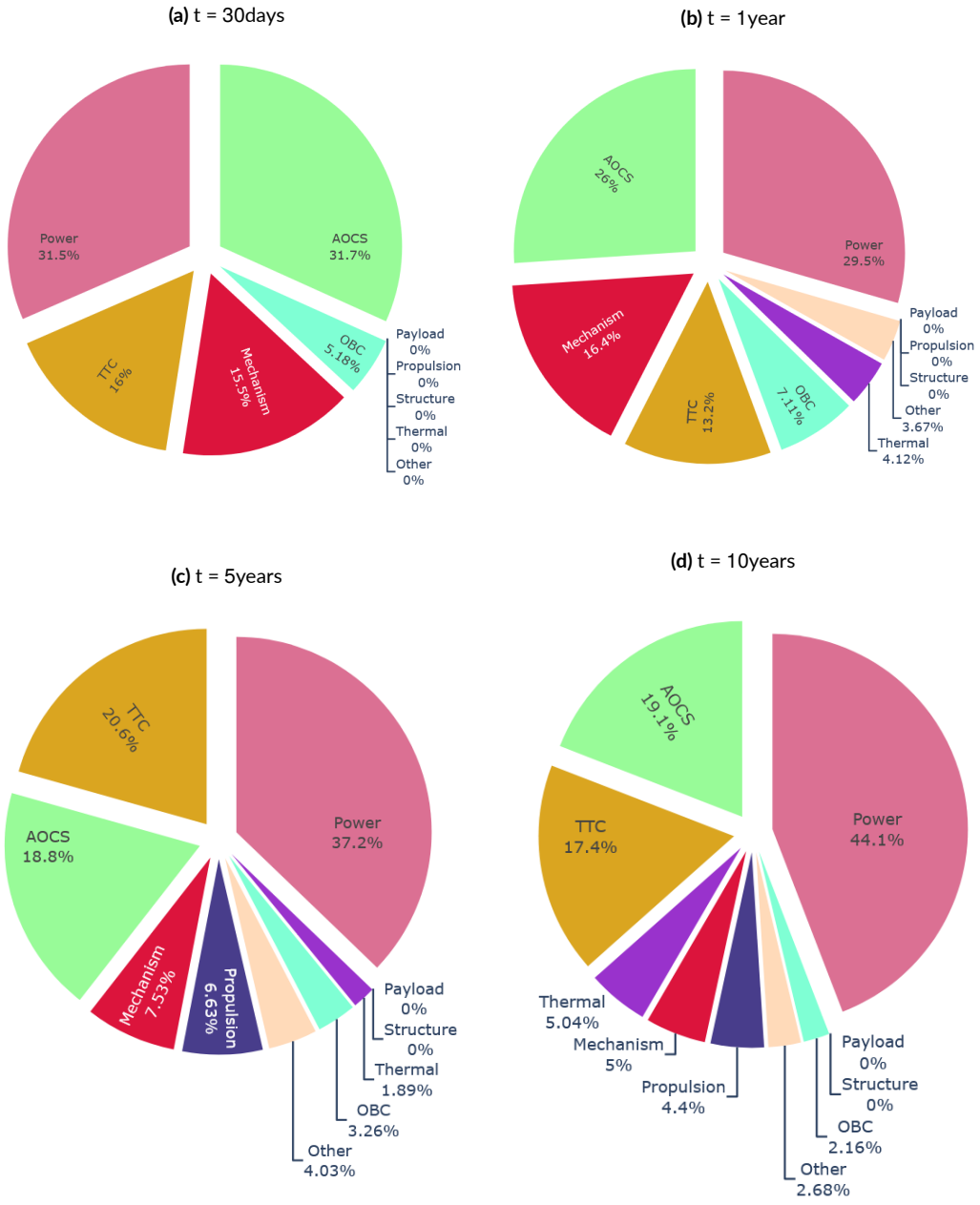

Figure 3.7: Relative contribution to satellite failure after 30days, 1year, 5years and 10 years (without unknown cause)

uary 2020 are examined. The obtained dataset consists of 1702 satellites, of which 1275 satellites are censored. Figure 3.8 shows the collective reliability of large satellites. The shape parameter less than one, as shown in Table 3.14 indicates that infant mortality is prevalent in large satellites as well. The R^2 value of 0.920, calculated from GM, shows that the Weibull Distribution is a good fit for large satellites. The corresponding AIC values of Weibull Distribution further verify its fit. Figure 3.9 shows the comparison of small satellite and large satellite reliability. It is evident that large satellites have soaring reliability than small satellites and encounter fewer causalities during the initial phases. Figure 3.10 - 3.13 show the reliability of large satellites with different categorization and Table 3.14 shows the associated parameters. Although communication satellites have more serious infant mortality than Earth Observation satellites, they have the highest reliability in the tenth year, followed by Earth Observation and Navigation satellites. Technology Demonstration satellites show the worst reliability as envisioned. Large satellites designed by Government agencies have lower infant moralities, whereas the satellites designed by Private entities have higher reliability after ten years in orbit. However, the reliability of Private satellites could be lower than the estimation as the majority of private entities are not transparent about satellite failures. Large satellites with more than ten years of design lifetime have higher infant moralities than satellites with less than ten years of design lifetime. Still, they have higher reliability after 15 years in orbit. Similarly, large satellites launched before 2010 have lower infant mortality rates, while the satellites launched after 2010 have higher reliability after ten years in orbit.

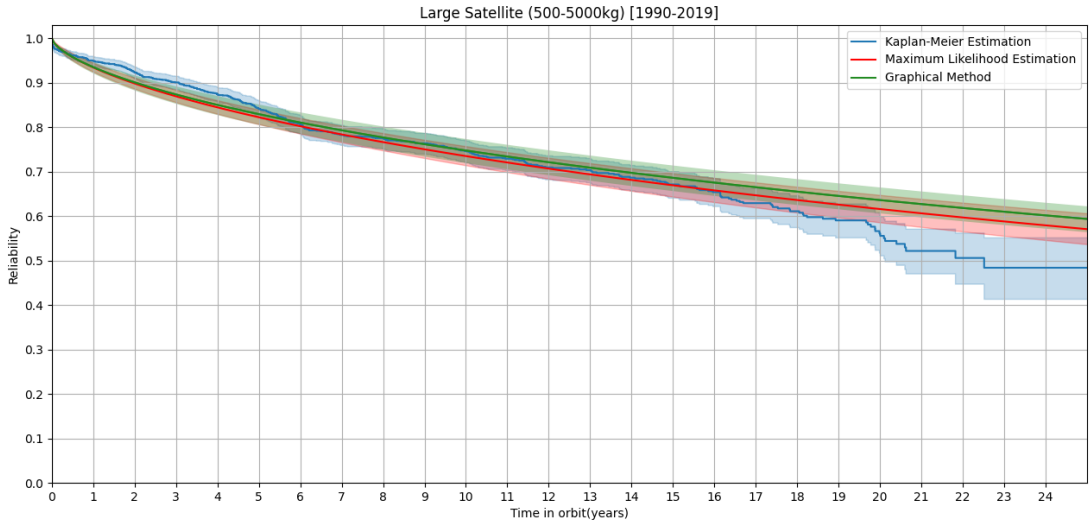

Figure 3.8: Collective reliability of large satellites launched between 1990-2019

Table 3.14: Estimated Weibull parameters for different large satellite categorization

Category	Groups	Graphical - Method		MLE	
		α [years]	β	α [years]	β
Collective		69.46	0.6363	60.45	0.6541
Mission	Technology	32.97	0.4084	15.72	0.5516
	Communication	127.45	0.5564	95.88	0.6038
	Earth Observation	56.13	0.6946	37.38	0.8193
	Science	33.18	0.5991	22.60	0.7261
	Navigation	49.26	0.6927	30.74	0.8141
Developer	Government	39.86	0.6882	33.30	0.7205
	Private	368.63	0.5007	190.70	0.5957
Design Life	$\leq$ 10 years	56.64	0.6499	44.86	0.7107
	$>$ 10 years	378.02	0.5571	393.79	0.5168
Launch Year	$<$ 2010	65.48	0.6462	54.53	0.6817
	$\geq$ 2010	1486.30	0.3816	1130.87	0.3901

3.7 Small Satellites < 40 kg

The statistical reliabilities of 1043 small satellites weighing less than 40 kg were investigated using on-orbit failure data. The shape parameter from the collective analysis, shown in

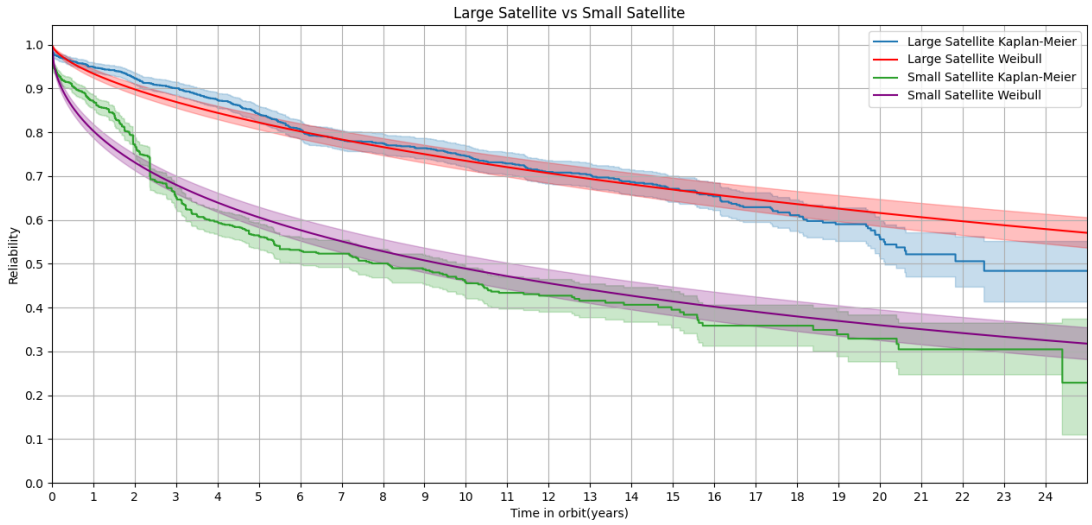

Figure 3.9: Comparison of large satellite and small satellite reliability

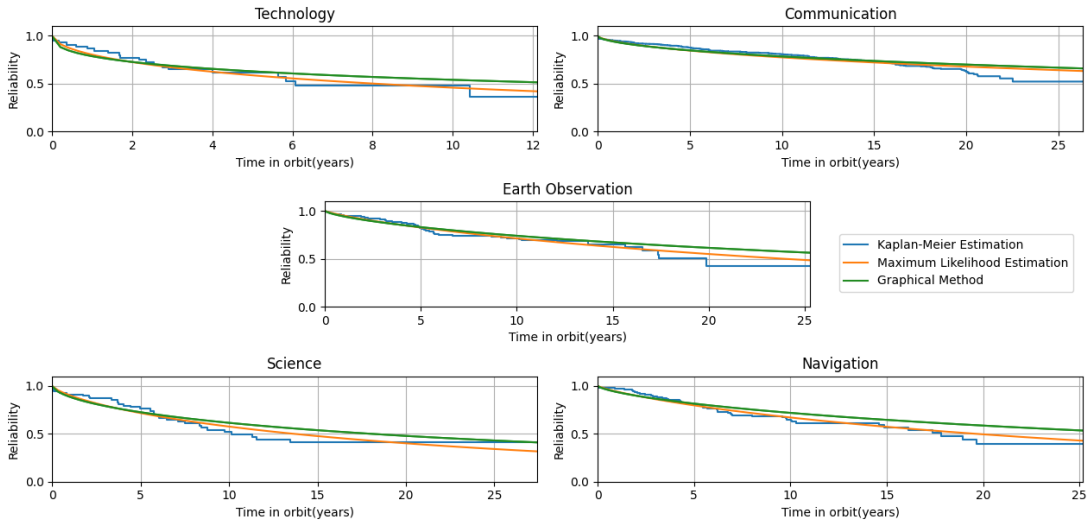

Figure 3.10: Reliability of large satellites based on Mission type

Figure 3.14 is less than one and confirms the presence of infant mortality. Figure 3.15 - 3.18 show the reliability of small satellites (< 40 kg) with different categorization. From the categorization based on launch year, it is identified that the infant mortality rates have decreased

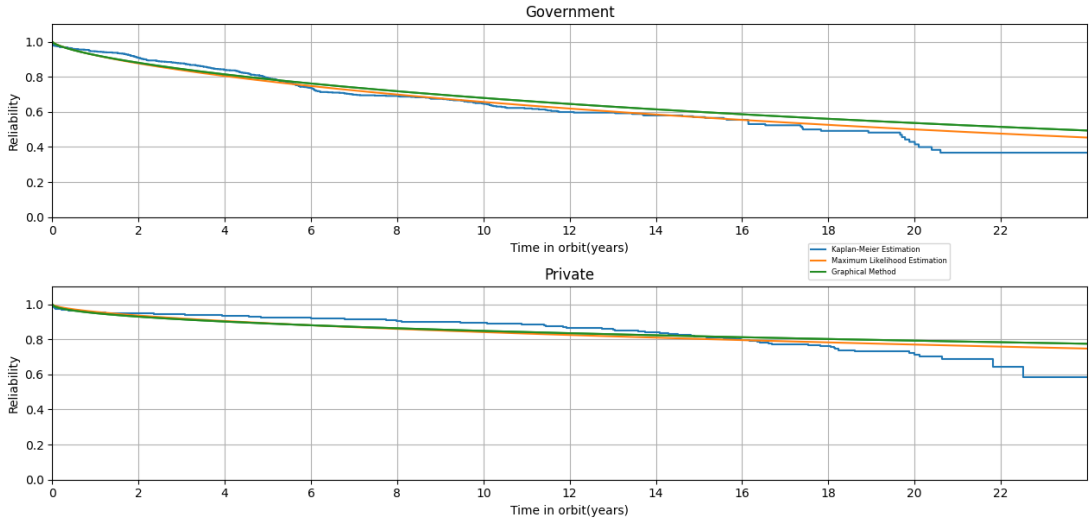

Figure 3.11: Reliability of large satellites for different developer group

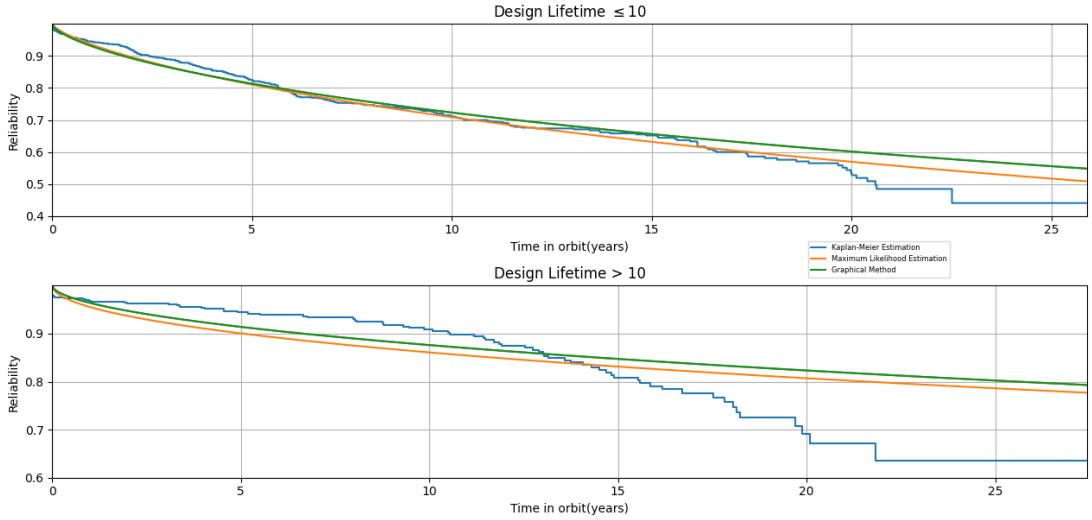

Figure 3.12: Reliability of large satellites with different design life

over the years. Communication satellites have the lowest probability of failure in terms of mission types, while the Science Mission satellites suffered from high infant mortality rates. Satellites developed by Government agencies tend to have high reliability if they survived the

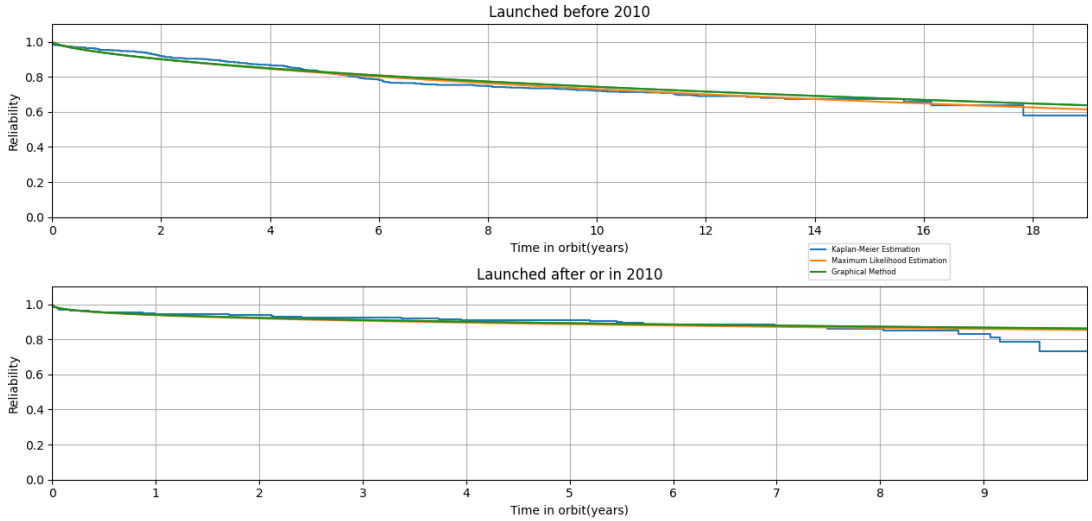

Figure 3.13: Reliability of large satellites launched in different decade

first few days in orbit. Unexpectedly, the reliability of this satellite class did not vary significantly for Polar and Non-Polar orbits. The cause of failure for 86% of the failed satellites in the dataset was Unknown. Consequently, it was not possible to identify the subsystems with a high(er) propensity for failure.

3.8 Summary

In this Chapter, the statistical reliability of 866 small satellites ($40 - 500$ kg), 1043 small satellites (< 40 kg) and 1702 large satellite (> 500 kg) were investigated using empirical failure data. As this research focuses on microsatellites that fall under the small satellite category weighing between 40-500 kg, their results are summarized below. The calculated shape parameter value for the collective reliability analysis is less than one, indicating the prevalence of infant mortality in small satellites. Small satellites launched before 2010 conferred lower infant mortality rates, while the satellites launched after 2010 were identified to have higher

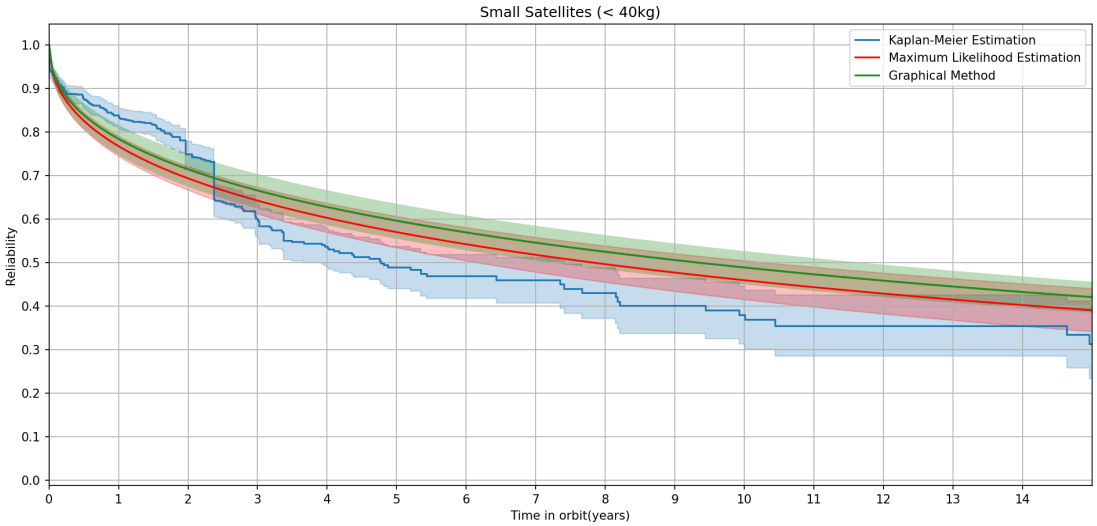

Figure 3.14: Collective reliability of small satellites < 40kg launched between 1990-2020

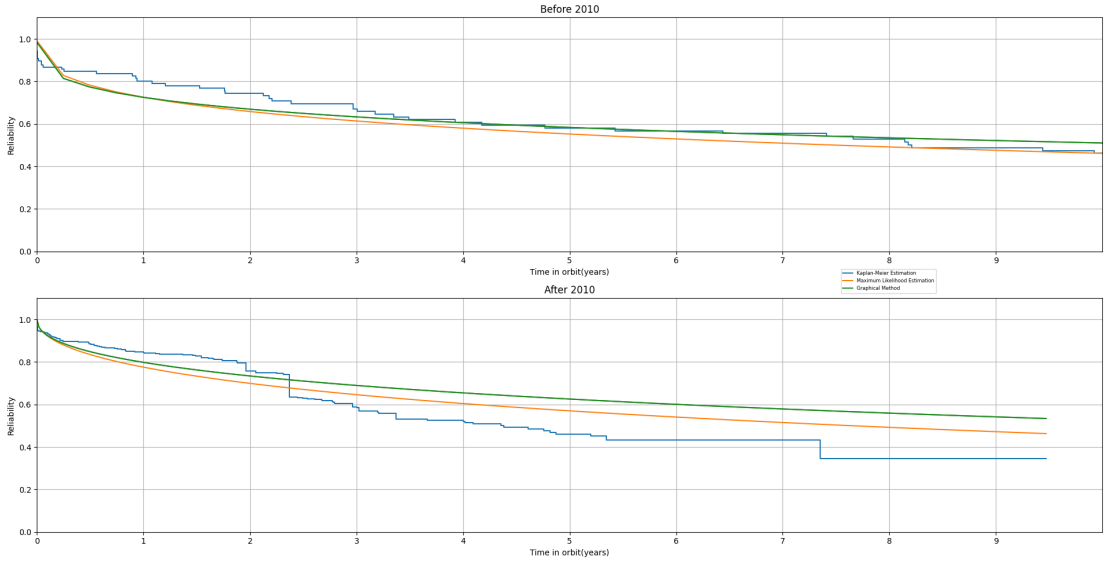

Figure 3.15: Reliability of small satellites < 40kg launched at different decades

reliability after five years in orbit. With regards to the mission influence of the satellite reliability, Earth observation satellites showed the highest reliability. Alternatively, Science Mission satellites had the highest infant mortality. As expected, the Commercial satellite developed

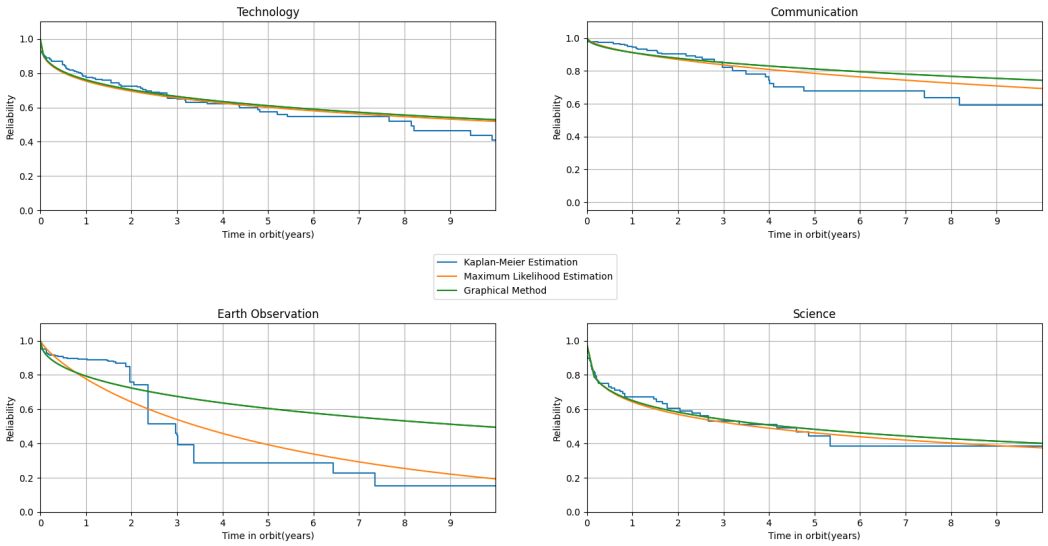

Figure 3.16: Reliability of small satellites < 40kg for different mission types

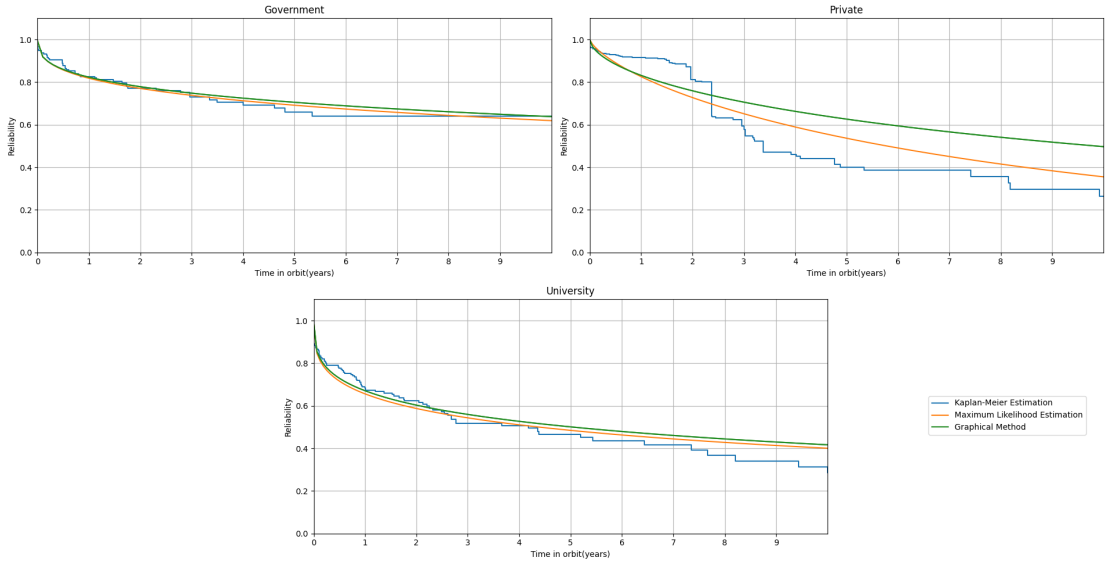

Figure 3.17: Reliability of small satellites < 40kg for different satellite developers

by Private developers had the highest survival rate, followed by the Government developed satellite. In terms of the operating condition, satellites operating in Polar orbit showed lower

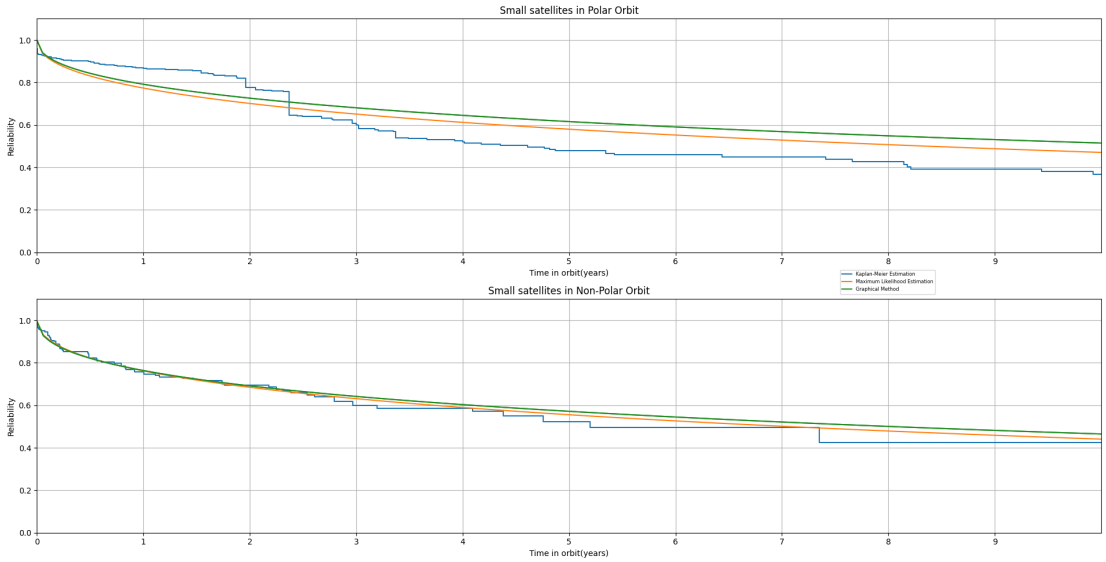

Figure 3.18: Reliability of small satellites < 40kg with different orbit inclination

infant mortality but degraded faster than the Non-Polar counterparts. A comparative analysis of subsystem failures was carried out at the end of the study. The failure reason for many satellites is unknown or undisclosed, impacting the possibility of identifying the legitimate "culprit subsystem". Nevertheless, within the known causes, the Power subsystem is identified as the primary contributor to satellite failures. The results from this Chapter provide the latest and effective reliability baseline for modern small satellites at system level.

The greatest challenge to any thinker is stating the problem in a way that will allow a solution.

Bertrand Russell

4

Reliability Allocation and Growth

Along with the reliability estimate from the statistical analysis and the reliability growth modelling, it is possible to estimate the resources needed to meet the reliability requirements. The standard practices to grow the reliability of a system[23] include

1. Incorporating highly reliable elements in place of less reliable elements (Reliability Allocation Problem)

2. Incorporating one or more redundant element (Redundancy Allocation Problem)

3. Combining the above two approaches (Reliability-Redundancy Allocation Problem)

Each strategy is helpful at different stages based on the maturity of the design. The Reliability Allocation Problem, which requires only sparse information of satellite's sub-level elements, is vital in the initial design stage. This strategy helps in refining the reliability requirements of sub-level elements and propagating these requirements to lower levels. As the design matures and establishes the relationships between the system and its lower-level elements, the Reliability-Redundancy Allocation Problem becomes beneficial. This strategy provides design alternatives to improve the overall reliability. At the lower levels, the reliability can be improved in a number of ways such as reducing the operational/environmental loads on equipment/parts, and improving design by testing and removing the causes of failure. This however is out of the scope of this research. This chapter provides different growth strategies to improve the reliability of the satellite.

4.1 Reliability Allocation Problem

Reliability Allocation Problem involves enhancing the reliability of sub-levels to meet the system level goals. This approach begins by assigning target reliabilities at each sub-level by employing Apportionment techniques. Then the sub-levels that do not meet the targets are identified and improved. This may appear simple but it may not be feasible in many scenarios. Any improvement effort usually requires resources. In most cases, it incurs a higher cost and does not comply with the budget. In other cases, reliability improvement may not be technically possible. Hence, the reliability allocation problem is not preferred anymore. However,

the apportionment techniques used in this approach is widely utilized during the initial design phase, especially for satellites. Designing for reliability is challenging in the early phases as there is not much information about the satellite design. Apportionment techniques are employed here to set reliability requirements for every major element in each subsystem. The subsystem designer can meet these requirements by selecting different products, redundancies and redundancy strategies. This selection is trivial in the early stages but as the design matures, the selection is not intuitive and other optimal reliability allocation approaches discussed in section 4.2 and 4.3 have to be used. Regardless of the type of allocation process, the primary goal is to solve the following.

$$f(R_1(t), R_2(t), ..., R_n(t)) \geq R_s(t) \tag{4.1}$$

where $R_i(t)$ is the reliability allocated to the i^{th} subsystem, $i = 1, 2, ..., n$ and $R_s(t)$ is the satellite system reliability requirement.

4.1.1 Reliability Apportionment

Reliability requirements at the satellite level are usually established before the initial design phase. During the initial design, Apportionment techniques are utilized to flow down the reliability to each sub-level, i.e. to determine the reliability required for each subsystem so that the satellite meets the specified reliability requirement. This is accomplished by using weighting factors to prioritize the sub-levels. The weighting factors are generally derived from heritage data and/or expert opinion. In Apportionment techniques, failure rates are assumed to be constant. Different Apportionment techniques are discussed below.

Element	Reliability
Attitude Determination and Control (ADC)	0.969
Propulsion (PROP)	0.969
Power (EPS)	0.969
Communication (COMM)	0.969
Structure (STR)	0.969
Thermal (TCS)	0.969
Onboard Computer (OBC)	0.969

Table 4.1: Reliability Allocation using EAT for reliability goal = 0.8

Equal Apportionment Technique

Equal Apportionment Technique (EAT) is the simplest of all apportionment techniques. As the name suggests, all the subsystems in the satellite are weighted equally and the reliability is distributed uniformly among all the elements[13]. The only input required is the number of subsystems. The mathematical model is as follows:

$$R_s = \prod_{i=1}^{n} R_i \tag{4.2}$$

$$R_i = (R_s)^{1/n} \tag{4.3}$$

Table 4.1 shows an example of allocation results using EAT. In order to meet the reliability goal of 0.8 each subsystem should have a reliability of 0.969. This method is useful only when there is no information available about the satellite.

Feasibility of Objectives

Feasibility of Objectives (FOO) is based on numerical assessments of design complexity (Cx), State of the Art (SoA), Operating time (Ot) and Environment (Env)[161]. Table 4.2 describes the input required for FOO. The assessments are done by a system expert or based on heritage data. Weighting factors are determined for each subsystem based on these inputs. The weighting factors are then used to allocate reliability. The mathematical model of FOO is as follows:

$$W_i = Cx_i \times SoA_i \times Ot_i \times Env_i \tag{4.4}$$

$$C_i = \frac{W_i}{\sum_{i=1}^{n} W_i} \tag{4.5}$$

$$\lambda_i = C_i \lambda_s \tag{4.6}$$

where W_i is the rating factor of i^{th} subsystem, $i = 1, 2, \ldots, n$, C_i is the weighting factor, λ_i is the failure rate of i^{th} subsystem and λ_s is the required failure rate of the satellite.

Table 4.3 shows the allocation results using FOO to obtain a system reliability of 0.8. Unlike EAT, FOO allocates reliability based on the weights assigned to each subsystem. Thus it results in meaningful and feasible targets.

Jeong and Koh Method

Jeong and Koh (KOH) method is based on the numerical assessments of Complexity factor (*CF*), System importance (*IF*) and impact on System Failure (*SF*). Table 4.4 describes the inputs needed. Similar to FOO, these inputs are used to calculate the weighting factors

Input Variable	Description
Complexity (Cx)	The Complexity of a SubElements (level n-1) is estimated considering both: • The probable number of components (level n-2) composing the SubElement • The complexity of their assembly/integration into the SubElement. *The SubElement with least complexity is assigned 1.* *The SubElement with maximum complexity is assigned 10.*
State of the Art (SoA)	The State of Art (SoA) denotes the current Engineering progress level (technology maturity) of the SubElement (level n-1). *The SubElement with a current high level of maturity is assigned 1.* *The SubElement with a current low level of maturity is assigned 10.*
Operating Time (OT)	*The SubElement that works for the entire mission is assigned 10.* *The SubElement that works for the lowest time in the mission is assigned 1.*
Environment (Env)	*The SubElement, which is subjected to the most severe environmental conditions, is assigned 10.* *The SubElement, which is subjected to the least severe environmental conditions, is assigned 1.*

Table 4.2: FOO Allocation Variables

	Cx	SoA	Ot	Env	W	C	λ	R
ADC	10	4	8	6	1920	0.251	6.39E-06	0.945
PROP	8	10	2	8	1280	0.168	4.26E-06	0.963
EPS	5	5	10	9	2250	0.295	7.49E-06	0.936
COMM	4	3	4	6	288	0.038	9.59E-07	0.992
STR	3	1	1	10	30	0.004	9.99E-08	0.999
TCS	1	1	10	7	70	0.009	2.33E-07	0.998
OBC	5	6	10	6	1800	0.236	5.99E-06	0.949

Table 4.3: Reliability Allocation using FOO for reliability goal = 0.8

Input Variable	Description
No. of Active Components (N_i)	The number of components (level n-2) needed to carry out nominal/main operations of the SubElement (level n-1).
System Importance (NF_i)	The number of System (level n) functions carried out by this SubElement (level n-1).
Impact on failure (K_i)	The estimated number of components (level n-2) in other SubElements (level n-1) affected due to a failure in the considered SubElement.

Table 4.4: KOH Allocation Variables

which is then used to assign reliabilities. The mathematical model is shown below.

$$CF_i = \frac{N_i}{\sum_{i=1}^{n} N_i} \tag{4.7}$$

$$SF_i = \frac{1 - \frac{K_i}{\sum_{i=1}^{n} K_i}}{n-1} \tag{4.8}$$

$$IF_i = \frac{1 - \frac{NF_i}{\sum_{i=1}^{n} NF_i}}{n-1} \tag{4.9}$$

$$W_i = CF_i \times SF_i \times IF_i \tag{4.10}$$

$$C_i = \frac{W_i}{\sum_{i=1}^{n} W_i} \tag{4.11}$$

$$\lambda_i = C_i \lambda_s \tag{4.12}$$

where W_i is the rating factor of i^{th} subsystem, $i = 1, 2, ..., n$, C_i is the weighting factor, N_i, K_i, NF_i are number of active components, impact on failure and importance respectively, CF_i is the complexity factor, SF_i is the failure scale factor, IF_i is the importance factor, λ_i is the failure rate of i^{th} subsystem and λ_s is the required failure rate of the satellite. Table 4.5 shows the reliability assigned to each subsystem to obtain a system reliability of 0.8 using

KOH method.

	CF	IF	SF	W	C	λ	R
ADC	1.37E-01	1.40E-01	1.41E-01	2.71E-03	0.136	3.47E-06	0.970
PROP	1.05E-02	1.58E-01	1.59E-01	2.65E-04	0.013	3.39E-07	0.997
EPS	6.32E-02	1.32E-01	1.45E-01	1.20E-03	0.061	1.54E-06	0.986
COMM	1.37E-01	1.40E-01	1.41E-01	2.71E-03	0.136	3.47E-06	0.970
STR	1.05E-01	1.58E-01	1.30E-01	2.17E-03	0.109	2.77E-06	0.975
TCS	3.68E-01	1.58E-01	1.34E-01	7.80E-03	0.392	9.98E-06	0.916
OBC	1.79E-01	1.14E-01	1.49E-01	3.03E-03	0.152	3.88E-06	0.967

Table 4.5: Reliability Allocation using KOH for reliability goal = 0.8

Failure rate over Value

In some cases, the most convenient starting point is the failure probability at design life. The failure probability can be taken from a similar mission, Equal Apportionment Technique or even the statistical results presented in the previous Chapter. Failure rate over Value (F/V) method allocates (re-allocates) reliability using the failure probability and estimated value[3]. Table 4.6 describes the required inputs. While cost is chosen as a value here, the same could be replicated with weight or any other resource. The mathematical model is presented below.

Input Variable	Description
Failure Rate (F)	An initial estimation/guess of the SubElement's (level n-1) failure rate.
Total Value (V)	The Total Value is the sum of all NRE + MAIT FM1 costs. • Non-recurring engineering (NRE) costs refer to the one-time costs to research, develop, design and qualify/test the new system (level n). • MAIT FM1 costs refer to the one-time costs for the Manufacturing, Assembly, Integration and Test of the Flight Model (first/unique).

Table 4.6: F/V Allocation Variables

	F	V	F/V	C	λ	R
ADC	3.63E-06	6	6.06E-07	0.064	1.64E-06	0.986
PROP	3.63E-06	5	7.27E-07	0.077	1.96E-06	0.983
EPS	3.63E-06	3	1.21E-06	0.128	3.27E-06	0.972
COMM	3.63E-06	4	9.09E-07	0.096	2.45E-06	0.979
STR	3.63E-06	2	1.82E-06	0.192	4.91E-06	0.958
TCS	3.63E-06	1	3.641E-06	0.385	9.82E-06	0.918
OBC	3.63E-06	7	5.19E-07	0.055	1.40E-06	0.988

Table 4.7: Reliability Allocation using F/V for reliability goal = 0.8

$$W_i = \frac{F_i}{V_i} \tag{4.13}$$

$$C_i = \frac{W_i}{\sum_{i=1}^{n} W_i} \tag{4.14}$$

$$\lambda_i = C_i \lambda_s \tag{4.15}$$

where W_i is the rating factor of i^{th} subsystem, $i = 1, 2, ..., n$, F_i is the initial failure rate i^{th} subsystem, V_i is the estimated cost of i^{th} subsystem, C_i is the weighting factor, λ_i is the failure rate of i^{th} subsystem and λ_s is the required failure rate of the satellite. The reliability allocated to each subsystem using F/V to obtain a system reliability of 0.8 is given in Table 4.7. The results from EAT are used as initial guess of failure rate and the subsystems are numerically rated based on total cost instead of actual cost figures.

Bracha Method

Bracha Method is similar to FOO method. Instead of using the numerical assessments directly to find the weights, these assessments are used to calculate different indexes which

Input Variable	Description
State of the Art (A)	The State of Art denotes the current Engineering progress level (technology maturity) of the SubElement (level n-1). *The SubElement with a current high level of maturity is assigned 1.* *The SubElement with a current low level of maturity is assigned 10.*
Operating Time (T)	*The SubElement that works for the entire mission is assigned 10.* *The SubElement that works for the lowest time in the mission is assigned 1.*
Environment (E)	*The SubElement, which is subjected to the most severe environmental conditions, is assigned 10.* *The SubElement, which is subjected to the least severe environmental conditions, is assigned 1.*
No. of Active Components (*na*)	The number of components (level n-2) needed to carry out nominal/main operations of the SubElement (level n-1).
No. of Redundant Components (*nr*)	The number of components (level n-2) added for redundancy for fail-safe/back up of the SubElement (level n-1).

Table 4.8: Bracha Allocation Variables

are then used to find the weights[13]. Bracha method is normally used when there is sufficient design information available from a similar mission in the past. Table 4.8 describes all the inputs need for Bracha Method. The mathematical model of Bracha method is presented below in equation (4.16 - 4.22).

$$K_1 = \frac{10np_i}{np_{max}} \tag{4.16}$$

$$K_2 = \frac{10nr_i}{nr_{max}} \tag{4.17}$$

$$Cx_i = 1 - e^{-K_1 + 0.6K_2} \tag{4.18}$$

$$E_i = 1 - \frac{1}{Env_i} \tag{4.19}$$

$$W_i = A_i(Cx_i + E_i + T_i) \tag{4.20}$$

$$C_i = \frac{W_i}{\sum_{i=1}^{n} W_i} \tag{4.21}$$

$$R_i = R_s^{C_i} \tag{4.22}$$

where np_i is the number of components (level n-2) i.e. active plus redundant in the i^{th} subsystem, $i = 1, 2, ..., n$, nr_i is the number of redundant components (level n-2) in the i^{th} subsystem, np_{max} and nr_{max} the maximum number of components and maximum number of redundant components, Cx_i, E_i, A_i, T_i are the index of Complexity, Environment, State of the Art and Operating time, W_i is the rating factor of i^{th} subsystem, C_i is the weighting factor, R_i and R_s is the reliability of i^{th} subsystem and satellite respectively. The results from Bracha to obtain a system reliability of 0.8 is given in Table 4.9.

The choice between the different allocation methods depends on the information available. These apportionment techniques are utilized in the decision support system, presented in Chapter 7.

	Cx	E	A	T	W	C	R
ADC	0.823	0.833	0.4	0.8	0.982	0.160	0.965
PROP	0.093	0.875	1	0.2	1.168	0.190	0.959
EPS	0.626	0.889	0.5	1	1.257	0.204	0.955
COMM	0.855	0.833	0.3	0.4	0.626	0.102	0.978
STR	0.806	0.900	0.1	0.1	0.181	0.029	0.993
TCS	0.982	0.857	0.1	1	0.284	0.046	0.990
OBC	0.920	0.833	0.6	1	1.652	0.269	0.942

Table 4.9: Reliability Allocation using Bracha for reliability goal = 0.8

4.2 Redundancy Allocation Problem

Redundancy Allocation Problem (RAP) involves evaluating the number and type of elemental redundancies required to increase system reliability. This approach entails the usage of multiple elements that increases weight, cost, and power. This method is ideal when the satellite design matured to a point where correlations between the design and actual components could be established. The inputs required for this method are satellite product tree and reliability plus physical parameters of all the elements in the product tree. These can be derived from previous missions, heritage data or even expert opinions. However, increasing the reliability of a complex system with numerous elements cannot be intuitively determined as it leads to numerous design choices. Therefore, the allocation problem is formulated as an optimization problem. The RAP is proved to be NP-hard[21].

4.2.1 Problem Description

The objective of the problem is to find the optimal number of redundancy levels and redundancy strategy to maximize the system reliability while respecting other budget constraints. The mathematical model of a satellite system s with m elements and subject to k

number of budget constraints are given as follows:

$$\begin{aligned} &\text{Max } R_s(n, nt) \\ &\text{Subject to } g_i(n, nt) \leq l_i,\ i = 1, 2, ...k \\ &n_j \in \mathbb{Z}^+,\ \ 1 \leq j \leq m \end{aligned} \tag{4.23}$$

where R_s is the system reliability, $n = (n_1, n_2, .., n_m)$ is a vector of number of redundancies, $nt = (nt_1, nt_2, .., nt_m)$ is a vector of redundancy types, g_i is the i^{th} budget constraint and l_i is the i^{th} available budget. Failure rate information of different elements are hard to come by and only a constant failure rate is available for each element from the heritage data. Even many suppliers indicate the performance of the element by using constant failure rates. Hence, for this work Exponential reliability distribution is used, even though it was clearly established in the previous Chapter that Exponential Distribution is not an accurate estimation of satellite reliability. Furthermore, since the satellite design is in the early design stage, a little variation in reliability and other parameters is acceptable. The overall reliability of the satellite is the product of all the element reliabilities. The elements can have any number of redundancies which can be active or standby.

4.2.2 Redundancy Strategies

The redundancy strategy considered for this optimization problem can either be active or cold. In the active redundancy, the redundant elements are energized throughout the entire mission duration. Instead, a cold-standby redundant system will have one primary element and one or more redundant elements that are switched ON only upon the failure of the primary element. The figure 4.1 shows the variation of reliability of active and cold standby

redundancy over time.

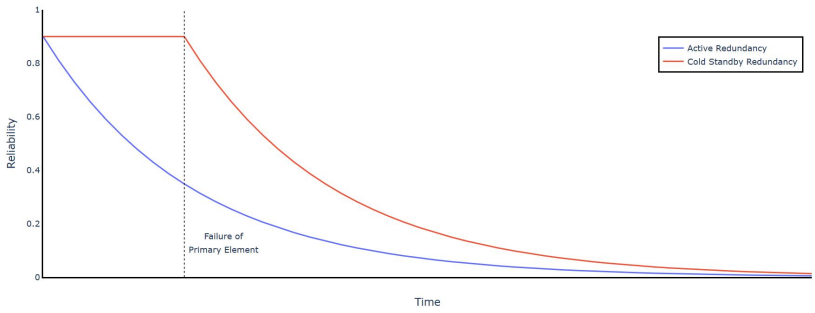

Figure 4.1: Reliability of Active and Cold Standby redundancy

In the active redundancy, the system will fail only if all the elements fail. That is, if at least one of the $n-1$ redundant elements remains operational, the mission is successful. The reliability of system R_s at time t, containing $n-1$ equal active redundant elements with constant failure rate λ is given by equation (4.24)[3,162]

$$R_s(t) = 1 - (1 - e^{-\lambda t})^n \tag{4.24}$$

A cold-standby redundant system requires a switch to energize a redundant element which reinstates the system operation. Failure of the switch before energizing the redundant element also causes the failure of the redundant element. In this study, it is assumed that the switch does not fail. The reliability R_s of the system at time t with one primary element plus $n-1$ standby elements and all elements having exponential time to failure with constant failure rate λ is given by equation (4.25)[162].

$$R_s(t) = e^{-\lambda t} \sum_{i=0}^{n-1} \frac{(\lambda t)^i}{i!} \tag{4.25}$$

4.2.3 RAP Optimization Results

Table 4.10 shows the list of all the elements and their parameters. In general, these parameters can be obtained from past missions or expert opinion. The design variables of the optimization are number of redundancies and redundancy strategy. RAP of satellite system is optimized using the APOPT solver from Gekko Optimization Suite[163]. The objective of RAP is to maximize its reliability subject to non-linear constraints such as weight, cost factor, and power. The mathematical model is presented in (4.23). The constraints of the optimization are as follows:

- Weight $\leq$ 150 kg
- Power $\leq$ 210 W
- Cost Factor $\leq$ 100,000

In addition to this, each element has a separate power constraint which influences the redundancy strategy and constraints on maximum & minimum elements possible. The results of the optimization are given in Table 4.11, 4.12.

The maximum possible reliability is 0.55 at the end of 3.5 years with the available set of elements. Increasing the reliability further requires more resources (cost, weight, etc). In this case, reliability growth while respecting the resource constraints is only possible by replacing the existing elements with more reliable ones. Adding this choice of element as a design variable to the optimization problem results in the Reliability-Redundancy Allocation Problem (RRAP), discussed in the next section.

RAP could be reformulated to minimize any resource while constraining the reliability.

Subsystem	Element	Acronym	Cost	Weight	Power	Failure Rate
Attitude Determination and Control	Reaction Wheel	RW	3960	6.38	16.4	6.95E-07
	Earth Sensor	ES	1260	3.14	4.1	4.39E-06
	Star Sensor	StS	3140	2.84	10.4	9.24E-06
	Inertial Measurement Unit	IMU	6400	4.14	33.6	6.99E-06
Propulsion	Propellant Tanks (valves)	PT	1810	3.56	1.1	2.11E-07
	Thrusters	ThR	1457	2.4	1.04	7.26E-06
Power	Battery	BAT	3620	9.52	0	1.63E-07
	Solar Panel Sections	SP	155	2	0	2.32E-05
	Power Conditioning Module	PCU	1460	3.44	2.44	4.93E-06
	Power Distribution Module	PDU	1660	2.08	1.92	8.36E-06
Telemetry, Telecommand and Ranging	Receiver	RCR	3280	3.22	11.6	7.23E-07
	Transmitter	TSR	2040	2.82	15.6	4.78E-06
	Antenna (switches)	ANT	2070	0.78	2.8	1.03E-05
Mechanism	Deployment	DPY	5620	3.58	10.4	2.47E-06
	Solar Array Drive Motor	SADM	3740	5.66	19.4	4.32E-06
Thermal	Radiator	RAD	2380	3.16	47.6	2.08E-06
Onboard Computer	Central Processing Unit	CPU	16160	1.54	3.82	8.83E-07
	Rad Hard Memory	DSU	13320	3.88	1.28	3.09E-06

Table 4.10: Satellite Elements and their parameters

For instance, the mathematical model to minimize the cost with constraint on reliability is given below.

$$\begin{aligned} &\text{Min } C_s(n, nt) \\ &\text{Subject to } g_i(n, nt) \leq l_i,\ i = 1, 2, ...k \\ &R_s \geq R \\ &n_j \in \mathbb{Z}^+,\ \ 1 \leq j \leq m \end{aligned} \tag{4.26}$$

The constraints are as follows. The optimization results are given in Table 4.13 and Table 4.14.

Elements	Element Count	Redundancy Type
RW	1	A
ES	2	A
StS	2	A
IMU	1	A
PT	2	C
ThR	4	C
BAT	1	A
SP	16	A
PCU	2	A
PDU	2	A
RCR	1	A
TSR	2	C
ANT	2	C
DPY	1	A
SADM	2	C
RAD	2	C
CPU	1	A
DSU	1	A

Table 4.11: Max Reliability: Optimized Redundancy and Redundancy Strategy

	Weight	Power	Cost	Reliability
Satellite	129	202	99784	0.553

Table 4.12: RAP Resultant satellite parameters to maximize Reliability

- Power $\leq$ 210 W
- Cost Factor $\leq$ 100,000
- Reliability $\geq$ 40%

Elements	Element Count	Redundancy Type
RW	1	A
ES	2	A
StS	2	A
IMU	1	A
PT	1	C
ThR	3	C
BAT	1	A
SP	8	A
PCU	2	A
PDU	2	A
RCR	1	A
TSR	2	C
ANT	2	A
DPY	1	A
SADM	1	C
RAD	1	C
CPU	1	A
DSU	1	A

Table 4.13: Min Cost: Optimized Redundancy and Redundancy Strategy

	Weight	Power	Cost	Reliability
Satellite	98	205	89158	0.437

Table 4.14: Results: Resultant satellite parameters to minimize cost

4.3 Reliability-Redundancy Allocation Problem

4.3.1 Problem Formulation

Satellite System

Generally, a satellite mission consists of four phases namely, Launch, Orbit Transfer, On-orbit operation and Disposal. This system is an exemplary type of Phased Mission Systems (PMS). A specific set of equipments/elements is crucial for the successful operation of the

system in a particular phase. However, this set of elements may vary from phase to phase. Therefore, a detailed model of each phase is necessary for modelling the reliability of a PMS.

Each phase of a satellite has a distinct reliability requirement which requires a phase-specific reliability analysis for every phase. The satellite mission fails if any of the phases is unsuccessful, which suggests that the phases are connected in series. This implies that the event of failure of one phase leads to the failure of the subsequent phases. The primary satellite subsystem required for a successful launch is the Structure subsystem. The satellite structure has to withstand static and dynamic launch loads. Statistical analysis of on-orbit data, from the previous Chapter, indicates that the failure rate of Satellite structure is negligible and hence the launch phase is not considered for this analysis. Table 4.15 shows all the critical elements considered for each subsystem as well as the phases they are required. The satellite details in Table 4.15 are used to construct a fault tree diagram which contains logic gates and basic events, such as failures.

Subsystem	Element	Acronym	Orbit Transfer	On-orbit operation	Disposal
Attitude Determination and Control	Reaction Wheel	RW	x	x	x
	Earth Sensor	ES	x	x	x
	Star Sensor	StS		x	
	Inertial Measurement Unit	IMU		x	
Propulsion	Propellant Tanks	PT	x	x	x
	Thrusters	ThR	x	x	x
Power	Battery	BAT	x	x	x
	Solar Panel Sections	SP		x	
	Power Conditioning Module	PCU		x	
	Power Distribution Module	PDU	x	x	x
Telemetry, Telecommand and Ranging	Receiver	RCR	x	x	
	Transmitter	TSR	x	x	
	Antenna	ANT	x	x	
Mechanism	Deployment	DPY		x	
	Solar Array Drive Motor	SADM		x	
Thermal	Radiator	RAD	x	x	
Onboard Computer	Central Processing Unit	CPU	x	x	x
	Rad Hard Memory	DSU		x	

Table 4.15: Critical Satellite Elements and mission phases

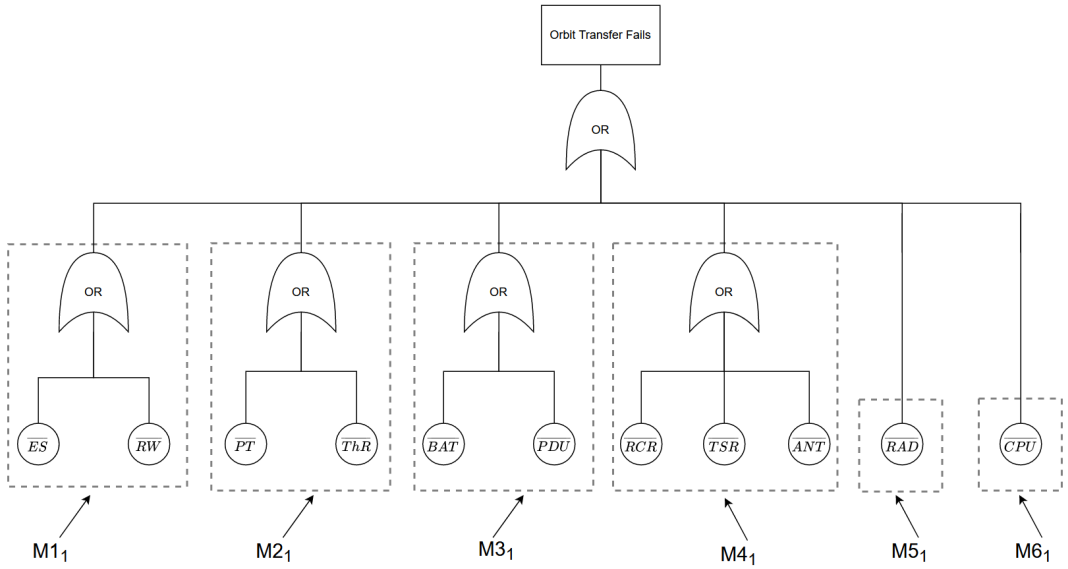

Figure 4.2: Fault tree of satellite system during orbit transfer

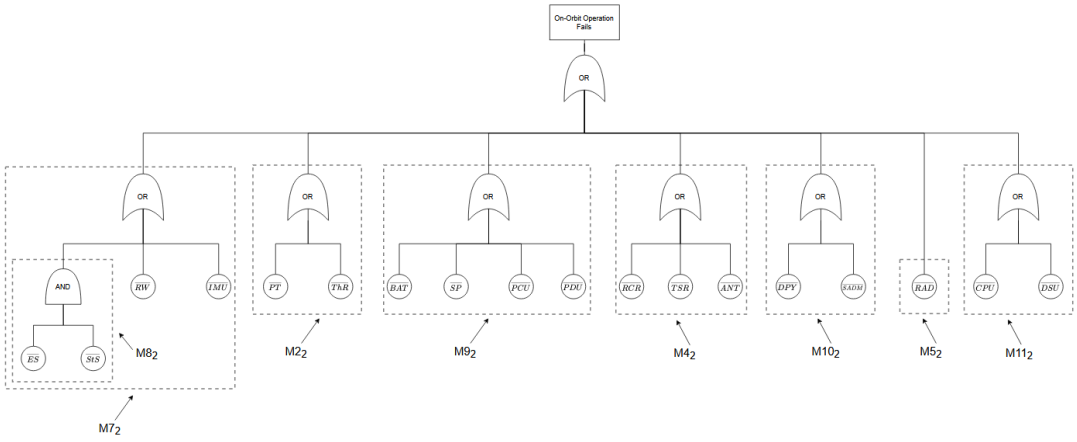

Figure 4.3: Fault tree of satellite system during on-orbit operations

A fault tree shows the logical relationships between the events and the causes leading to failure events. The fault trees corresponding to the three phases of the satellite mission are presented in Figure 4.2, 4.3 and 4.4. The notation $\overline{Element}$ represents the failure of the *Element*. To apply the modular approach[39] the first step is to identify independent subtree

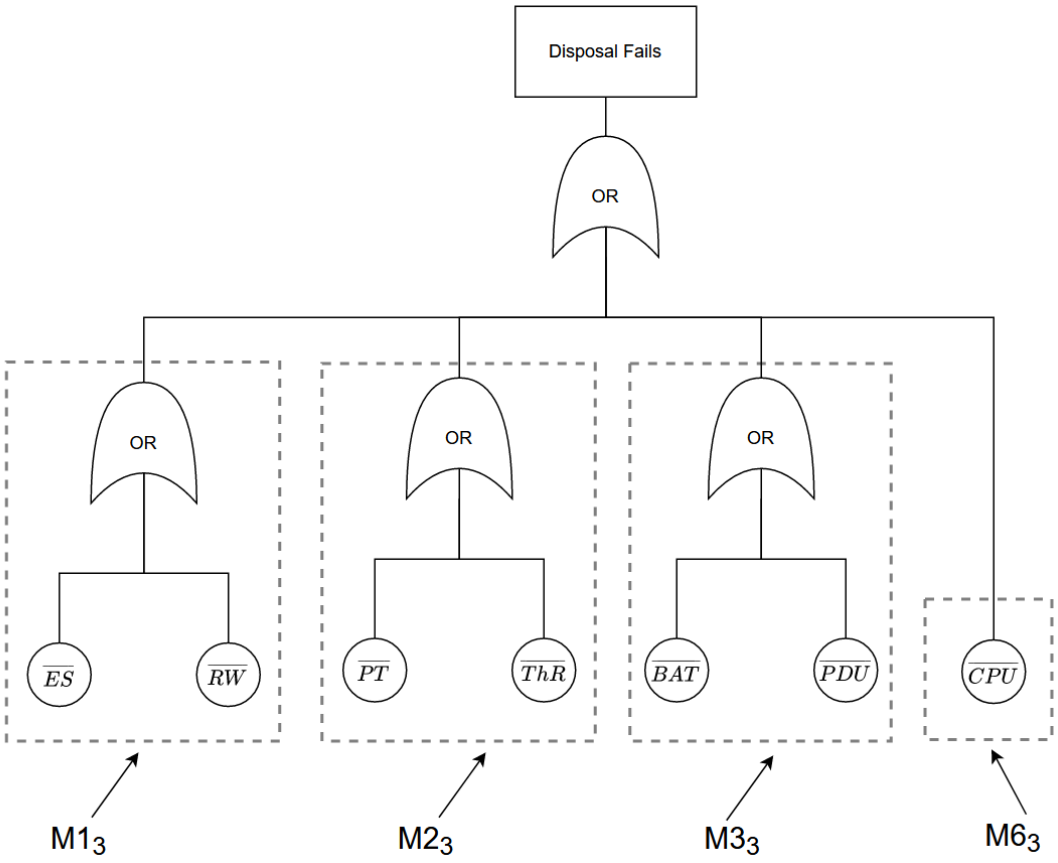

Figure 4.4: Fault tree of satellite system during end of life disposal

in each phase of the fault tree (Figure 4.2 - 4.4). Kohda et al.[164] define *an independent subtree composed of at least two events as a part of the fault tree which has no input from the rest of the tree and no outputs to the rest except from its output event*. The subtrees $M1 - M11$ are identified as shown in Figures 4.2 - 4.4. Each subtree is treated as a phase module and its functions and requirements may vary from one phase to another. The modularized fault tree of the satellite system is shown in Figure 4.5. $\overline{M1_1}, \overline{M1_3}$ represents the failure of phase module $M1$ during the first phase (orbit transfer) and failure of phase module $M1$ during the third phase (disposal), respectively. Because there are 18 individual lowest level failing

elements in the satellite system under consideration, 18 basic events (failure) are possible as given in equation (4.27).

$$\mathcal{B} = \{\overline{ES}, \overline{StS}, \overline{RW}, \overline{IMU}, \overline{PT}, \overline{ThR}, \overline{BAT}, \overline{SP}, \overline{PCU}, \overline{PDU}, \overline{RCR}, \overline{TSR}, \overline{ANT}, \overline{DPY}, \overline{SADM}, \overline{RAD}, \overline{CPU}, \overline{DSU}\} \tag{4.27}$$

The Basic event of the subtree or phase modules across every phase is given in equations (4.28-4.30).

$$\mathcal{P}_1 = \left\{\left\{\overline{ES}, \overline{RW}\right\}, \left\{\overline{PT}, \overline{ThR}\right\}, \left\{\overline{BAT}, \overline{PDU}\right\}, \left\{\overline{RCR}, \overline{TSR}, \overline{ANT}\right\}, \left\{\overline{RAD}\right\}, \left\{\overline{CPU}\right\}\right\} \tag{4.28}$$

$$\mathcal{P}_2 = \left\{\left\{\overline{ES}, \overline{StS}, \overline{RW}, \overline{IMU}\right\}, \left\{\overline{PT}, \overline{ThR}\right\}, \left\{\overline{BAT}, \overline{SP}, \overline{PCU}, \overline{PDU}\right\}, \left\{\overline{RCR}, \overline{TSR}, \overline{ANT}\right\}, \left\{\overline{DPY}, \overline{SADM}\right\}, \left\{\overline{RAD}\right\}, \left\{\overline{CPU}, \overline{DSU}\right\}\right\} \tag{4.29}$$

$$\mathcal{P}_3 = \left\{\left\{\overline{ES}, \overline{RW}\right\}, \left\{\overline{PT}, \overline{ThR}\right\}, \left\{\overline{BAT}, \overline{PDU}\right\}, \left\{\overline{CPU}\right\}\right\} \tag{4.30}$$

Modularization is a recursive process and any subtree identified within the phase module must be further modularized such as $M8$. The overall system reliability is computed using the joint probabilities of the modules. Therefore, the system reliability (R_s) for the satellite system becomes:

$$R_s = P\left\{\bar{\mathcal{P}}_1 \bar{\mathcal{P}}_2 \bar{\mathcal{P}}_3\right\} \tag{4.31}$$

where $\bar{\mathcal{P}}_1, \bar{\mathcal{P}}_2, \bar{\mathcal{P}}_3$ is the probability of success during orbit transfer, on-orbit operation, and disposal phase respectively. The probability of success can be calculated by translating the modularized fault tree into a Binary Decision Diagram (BDD)[37,165,166], as shown in Figure

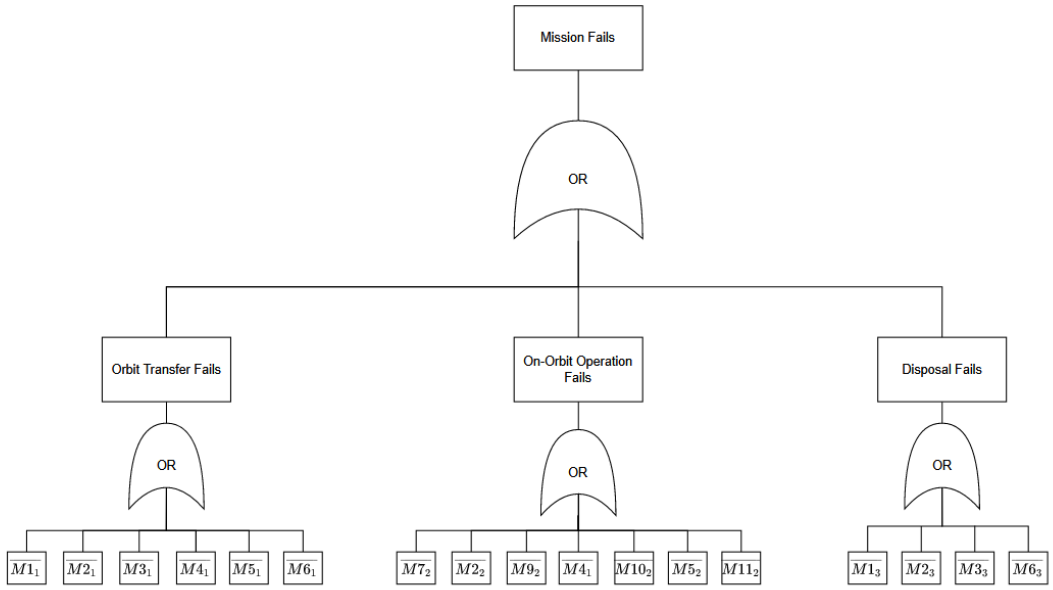

Figure 4.5: Modularized Fault Tree

4.6.

A BDD is a directed acyclic graph and all the paths in BDD flow in one direction. A BDD is composed of root vertex, intermediate node and terminal vertex. All the paths start from the root vertex and end at the terminal vertex. In this case, the terminal vertex can be either 1 (Failure) or 0 (Success). All the disjoint paths that lead to 0 is the cut set of the fault tree and the sum of the identified paths is used to calculate the system reliability (i.e) $P\left\{\bar{\mathcal{P}}_1\bar{\mathcal{P}}_2\bar{\mathcal{P}}_3\right\}$. For the considered satellite system there is only one path that leads to a successful mission that is evaluated as

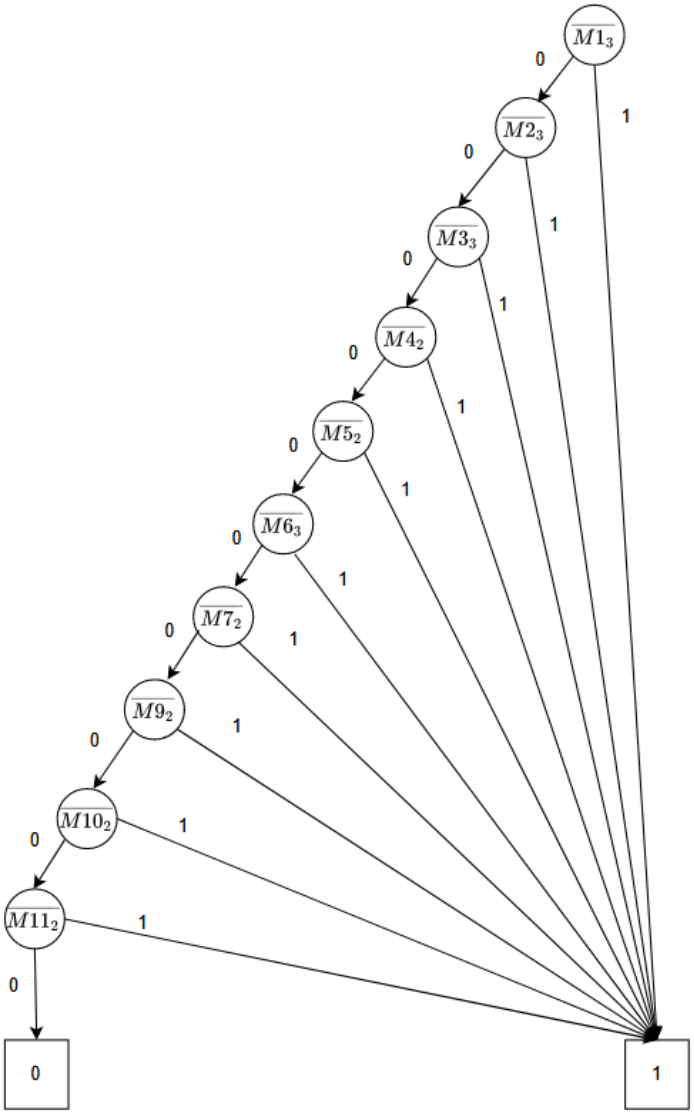

Figure 4.6: BDD of multi-phase satellite system

$$R_s = P\left\{\overline{M}1_3\overline{M2}_3\overline{M3}_3\overline{M4}_2\overline{M5}_2\overline{M6}_3\overline{M7}_2\overline{M9}_2\overline{M10}_2\overline{M11}_2\right\} \tag{4.32}$$

$$\begin{aligned} R_s(t) = & R_{M1}(T_1+T_3)\, R_{M2}(T_1+T_2+T_3)\, R_{M3}(T_1+T_3)\, R_{M4}(T_1+T_2) \\ & R_{M5}(T_1+T_2)\, R_{M6}(T_1+T_3)\, R_{M7}(T_2)\, R_{M9}(T_2)\, R_{M10}(T_2)\, R_{M11}(T_2) \end{aligned} \tag{4.33}$$

where T_1, T_2 and T_3 represent the duration of three phases respectively, $\overline{Mi_j}$ represents the probability of success of phase module Mi at phase j. The phase duration are predefined and assumed as $T_1 = 20\,days$, $T_2 = 3\,years$, $T_3 = 310\,days$ for this application. Now to find the reliability of each module, the respective phase modules is translated into BDD. For example the reliability of phase module $M7$ during on-orbit operations is calculated by translating the phase module $M7_2$ into BDD as shown in figure (4.7a). The disjoint paths leading to 0 vertex are presented in equation (4.34). Similarly, the reliability of subtree $M8$ inside $M7$ is given in equation (4.36) and Figure (4.7b) shows the BDD.

$$R_{M7_2} = P\left\{\overline{M8_2}\,\overline{RW}\,\overline{IMU}\right\} \tag{4.34}$$

$$R_{M7_2}(T_2) = R_{M8_2}(T_2)\; R_{RW}(T_2)\; R_{IMU}(T_2) \tag{4.35}$$

$$R_{M8_2} = P\left\{\overline{ES}\right\} + P\left\{ES\,\overline{StS}\right\} \tag{4.36}$$

$$R_{M8_2}(T_2) = R_{ES}(T_2) + (1 - R_{ES}(T_2))\; R_{StS}(T_2) \tag{4.37}$$

Since ES, StS, RW, IMU are the lowest level of elements considered, their reliabilities can be calculated from their constant failure rate (λ) as shown in equation (4.38). All the elements are assumed to follow an Exponential failure distribution. There are different choices available for ES, StS, RW, IMU and the elements can have any number of redundancies which can be active or cold-standby. In such cases the redundancy equations (4.24, 4.25) are used to calculate the reliability.

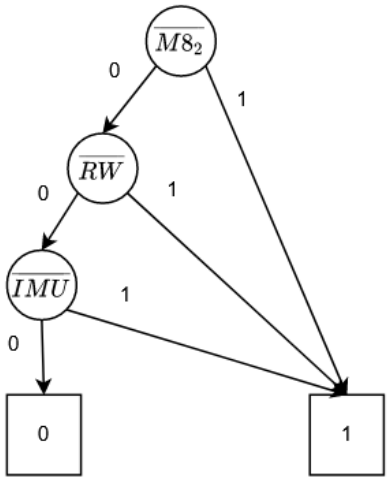

(a) BDD of phase module M7 during on-orbit operations

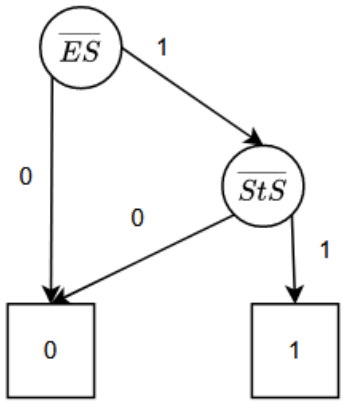

(b) BDD of phase module M8 during on-orbit operations

Figure 4.7: Binary Decision Diagram

$$R(t) = e^{-\lambda t} \tag{4.38}$$

Reality Factors

As mentioned already, RRAP is known to be NP-Hard[21] which makes a highly sophisticated system like the satellite mission extremely difficult to be solved. To deal with the complexity, only the main elements are considered. The main elements defined here constitutes the essential elements, most expensive elements and elements with a high failure rate. However, this choice leads to a substantial deviation of calculated reliability from the actual reliability. An aspect called 'Reality factors' is introduced to overcome this shortcoming. Reality

factors for a subsystem are identified by averaging out the reliabilities of elements accompanying main elements, captured from its heritage and historic data.

For example let us consider the Telemetry, Telecommand and Ranging (TT&R) subsystem of a satellite. The TT&R subsystem enables the ground operator to communicate with the satellite. It sends telemetry and receives telecommands sent from the ground stations. The main elements of TT&R include transmitters, receivers, and transmitting and receiving antennas. It also has various other ancillary elements such as couplers, waveguides, and latching current limiters. Table 4.16 shows the comparison of actual reliability - calculated considering every element in TT&R, calculated reliability - considering only the main elements of TT&R and calculated reliability multiplied with reality factor. It can be seen that the ancillary elements have a significant impact on reliability.

	Actual Reliability	Calculated Reliability	Reliability with Reality Factor
TT&R A	0.9868	0.8809	0.9734
TT&R B	0.9870	0.8643	0.9550
TT&R C	0.9941	0.8824	0.9750

Table 4.16: Comparison of TT&R reliability

The ancillary elements associated with every main element are identified and their reliability is calculated separately. This process is done for the actual TT&R subsystem from ten different satellites. The average reliability of ancillary elements for each subsystem constitutes the 'Reality factor' of that subsystem. After introducing the reality factors, the reliability values are closer to the actual values.

4.3.2 RRAP Optimization Results

RRAP of the satellite system is optimized using the APOPT solver from Gekko Optimization Suite[163]. The APOPT solver is based on a branch and bound algorithm and it is the most common solver for NP-hard optimization problems. The satellite system architecture and the available choices for each element, along with its resource information, are modelled in Neo4j[167] in Figure 4.8. The satellite architecture consists of the central satellite system, SAT, containing the satellite bus or Platform, PF, which encloses every subsystem. The elements belonging to every subsystem are denoted by their acronyms that are previously established in Table 4.15. This problem considers five different choices for each of the elements as the basis for the selection. The choice elements are denoted as E_ck, where E is the element's acronym, c indicates the choice element, and $k = 1to5$ is the element's choice. The RRAP is then formulated into two cases for optimizing reliability and cost. Within each case, the same problem is implemented for PMS and for the traditional Single Phased Mission System (SPMS) to compare against one another.

Case (i): Maximize Satellite Reliability

The objective of the first case is to optimize the problem to have maximum reliability. Here, the RRAP of the satellite system is formulated to maximize its reliability subject to non-linear constraints such as cost, power, and weight. Assuming that a satellite system, s consists of m number of elements subject to q different constraints (g) then the mathematical

model to optimize the system reliability, R_s is given by the following:

$$\begin{aligned} \max \quad & R_s = f(r, n, nt) \\ \text{s.t.} \quad & g_i(g, n, nt) \leq l_i, \quad 1 \leq i \leq q \\ r = (r_1, r_2, .., r_m) \quad & n = (n_1, n_2, .., n_m) \\ nt = (nt_1, nt_2, .., nt_m) \quad & g = (g_1, g_2, .., g_q) \\ & 0 \leq r_j \leq 1, \quad r_j \in \Re, \quad n_j \in \mathbb{Z}^+, \quad 1 \leq j \leq m \end{aligned} \tag{4.39}$$

The subscript j represents any system element from 1 to m such that r_j is a real number between 0 and 1, and n_j is a positive integer. Then, for a system consisting of m elements, each having k choice elements, r is the reliability vector, n is the required number of redundancies, and nt is the redundancy strategy of the corresponding system elements. For example, if RW is the j^{th} system element and RW_C_k is the selected choice for RW, then r_j is the reliability of RW_C_k, n_j is the number of redundancy of RW, and nt_j is the redundancy strategy for RW, respectively.

The design variables considered for the optimization are (i) element choice, (ii) number of redundancies, and (iii) redundancy strategy. The constraints g of the optimization and its limits, l are as follows:

- Weight $\leq$ 150 kg
- Power $\leq$ 210 W
- Cost Factor $\leq$ 100,000

Table 4.17 shows the design variables and their corresponding parameters obtained for

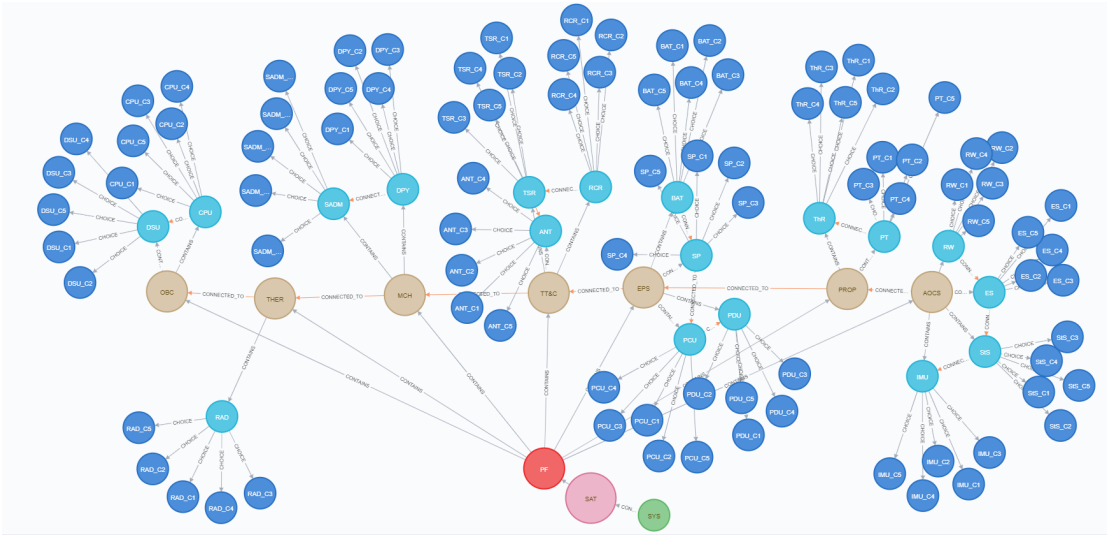

Figure 4.8: Satellite Data Model in Neo4j

both PMS and SPMS. The resultant satellite configuration for PMS is distinct from that of SPMS. Out of 18 system elements considered for this problem, nine elements remained the same in both the configurations, while element choices and/or redundancies are different for the remaining ten elements. The reliability of elements required for more than one phase, such as ThR, PDU, RCR, TSR, ANT, and RAD, have higher reliability in PMS than in SPMS as expected. However, the reliabilities of RW, PT, BAT, and CPU remain constant in both configurations as they are the best available choices.

In theory, increasing the reliability of an element required only for a single-phase increases the overall satellite reliability. Though, in reality, it is an over-kill without making a significant difference in overall reliability. For instance, Solar Panels (SP) are used only during on-orbit operations, whereas PDU is required for all the phases. In the configuration from SPMS formulation, many redundancies for SP and, a comparatively less reliable variant of PDU were selected. Investing considerable resources in SP while selecting a cheaper, less reliable

Elements	Choice		Element Count		Redundancy Type		Failure Rate		Weight(kg)		Power(W)		Cost(EUR)	
	PMS	SPMS	PMS	SPMS	PMS	SPMS	PMS	SPMS	PMS	SPMS	PMS	SPMS	PMS	SPMS
RW	RW_C3	RW_C3	1	1	A	A	6.95E-07	6.95E-07	6	6	13	13	4600	4600
ES	ES_C1	ES_C1	1	2	A	A	4.39E-06	4.39E-06	3.7	3.7	4.5	4.5	1500	1500
StS	StS_C3	StS_C3	2	2	A	A	9.24E-06	9.24E-06	3	3	9	9	2550	2550
IMU	IMU_C1	IMU_C1	1	1	A	A	2.73E-06	2.73E-06	5.6	5.6	32	32	7000	7000
PT	PT_C5	PT_C5	1	1	A	A	2.11E-07	2.11E-07	4.3	4.3	1	1	1700	1700
ThR	ThR_C2	ThR_C5	3	3	C	C	7.26E-06	1.60E-05	1.5	1.5	1.1	1.3	1416	1366
BAT	BAT_C4	BAT_C4	2	2	A	A	1.63E-07	1.63E-07	8.9	8.9	0	0	3200	3200
SP	SP_C1	SP_C1	8	15	A	A	2.32E-05	2.32E-05	3	3	0	0	131	131
PCU	PCU_C2	PCU_C2	2	2	A	A	4.93E-06	4.93E-06	3.4	3.4	3	3	1650	1650
PDU	PDU_C3	PDU_C2	2	2	A	A	8.11E-06	8.36E-06	2.4	1.5	2.5	1.9	2150	900
RCR	RCR_C5	RCR_C4	1	2	A	A	7.23E-07	4.90E-06	3.8	3.5	13	9	3050	2950
TSR	TSR_C2	TSR_C5	2	2	C	C	3.58E-06	4.78E-06	3.2	3.5	18	14	2250	1850
ANT	ANT_C2	ANT_C5	2	2	C	C	1.30E-06	5.70E-06	1.3	0.5	3.5	2.3	1700	2200
DPY	DPY_C4	DPY_C5	1	1	A	A	2.47E-06	2.82E-06	2.3	3.9	13	11	6200	5800
SADM	SADM_C5	SADM_C1	2	2	C	C	4.32E-06	9.40E-06	6.2	4.6	15	16	4200	3200
RAD	RAD_C4	RAD_C2	2	2	C	C	2.08E-06	5.22E-06	2.5	2.9	47	48	2800	1950
CPU	CPU_C4	CPU_C4	1	1	A	A	8.83E-07	8.83E-07	0.9	0.9	2.9	2.9	17500	17500
DSU	DSU_C2	DSU_C2	1	1	A	A	3.09E-06	3.09E-06	4.1	4.1	1.8	1.8	12100	12100

Table 4.17: Results: Max Reliability

choice for PDU is not optimal. This clearly shows the inefficiency of SPMS. Meanwhile, in PMS formulation, PDU is prioritized by selecting highly reliable alternative. Ideally, a small part of the resources allocated to SP is used to improve the reliability of other elements.

The overall system parameters for PMS and SPMS are presented in Table 4.18. At the end of the mission (i.e. 3.9 years), the system reliability obtained for the PMS is 0.727 and for the SPMS formulation is 0.640. With the given constraints, the optimized reliability of PMS is higher than the SPMS. Although the resultant weight and power is lower in PMS, the resultant cost is higher than the SPMS.

As a step further, the resultant satellite configurations of PMS is computed using SPMS formulation and vice versa and their results are given in Table 4.19. For the same set of input parameters, the reliability calculated using the SPMS formulation is far less than the reliability calculated using the PMS formulation. Therefore, a system using SPMS formulation would need to employ more resources to reach the same target reliability.

Type	Reliability	Weight	Power	Cost	Availability
PMS	0.727	121	195	99946	0.9999
SPMS	0.640	145	198	98663	0.9999

Table 4.18: Resultant System Parameters

	PMS Formulation	SPMS Formulation
PMS configuration	0.727	0.563
SPMS configuration	0.714	0.640

Table 4.19: Resultant reliability for each configuration with the both formulations

Case (ii): Minimize Satellite Cost

The mathematical model is modified and the objective is to minimize the cost of the satellite which is subject to non-linear constraints. The mathematical model to optimize the cost of a satellite system s with m elements and subject to q number of budget constraints are given as follows:

$$\begin{aligned} \min \quad & C_s = f(C, n, nt) \\ \text{s.t.} \quad & g_i(W, n, nt) \leq l_i, \quad i = 1, 2, ...q \\ & R_s \geq R \\ & W_j \in \Re, \quad n_j \in \mathbb{Z}^+, \quad 1 \leq j \leq m \end{aligned} \tag{4.40}$$

where C_s is the system cost, $C = (C_1, C_2, .., C_m)$ is a vector of choice element cost, $n = (n_1, n_2, .., n_m)$ is a vector of number of redundancies, $nt = (nt_1, nt_2, .., nt_m)$ is the redundancy strategy, g_i is the i^{th} budget constraint, l_i is the i^{th} available budget, R_s is the system reliability and R is the minimum required reliability. The constraints of the optimization are as follows:

- Weight $\leq$ 150 kg
- Power $\leq$ 210 W
- Reliability $\geq$ 0.5

The design variables and obtained system parameters for PMS and SPM formulations are given in Table 4.20. Ten of the system elements remain the same, and eight of them vary in both satellite configuration. SPMS underestimates the actual reliability and therefore to achieve the target reliability, redundancies of the system elements are increased. This increase in redundancies of elements directly increases the cost of the satellite. Table 4.21 presents the optimization outcome for PMS and SPMS. Since the cost is the objective function and reliability is a constraint here, the reliability corresponding to the optimized cost is presented for each case. Unlike in case (i), the increase in reliability of PMS to that of SPMS is not proportional to the cost increase.

Elements	Choice		Element Count		Redundancy Type		Failure Rate		Weight(kg)		Power(W)		Cost(EUR)	
	PMS	SPMS	PMS	SPMS	PMS	SPMS	PMS	SPMS	PMS	SPMS	PMS	SPMS	PMS	SPMS
RW	RW_C3	RW_C3	1	1	A	A	6.95E-07	6.95E-07	6	6	13	13	4600	4600
ES	ES_C3	ES_C3	2	2	A	A	1.07E-05	1.07E-05	1.9	1.9	3.9	3.9	650	650
StS	StS_C3	StS_C3	1	2	A	A	9.24E-06	9.24E-06	3	3	9	9	2550	2550
IMU	IMU_C3	IMU_C1	1	1	A	A	6.99E-06	2.73E-06	3.3	5.6	36	32	5300	7000
PT	PT_C5	PT_C5	1	1	A	A	2.11E-07	2.11E-07	4.3	4.3	1	1	1700	1700
ThR	ThR_C5	ThR_C3	3	3	C	A	1.60E-05	1.19E-05	1.5	2.8	1.3	0.8	1366	1383
BAT	BAT_C4	BAT_C4	1	1	A	A	1.63E-07	1.63E-07	8.9	8.9	0	0	3200	3200
SP	SP_C1	SP_C1	8	11	A	A	2.32E-05	2.32E-05	3	3	0	0	131	131
PCU	PCU_C1	PCU_C1	2	2	A	A	9.54E-06	9.54E-06	3.9	3.9	2	2	1100	1100
PDU	PDU_C2	PDU_C2	2	2	A	A	8.36E-06	8.36E-06	1.5	1.5	1.9	1.9	900	900
RCR	RCR_C5	RCR_C5	1	1	A	A	7.23E-07	7.23E-07	3.8	3.8	13	13	3050	3050
TSR	TSR_C5	TSR_C5	1	1	A	A	4.78E-06	4.78E-06	3.5	3.5	14	14	1850	1850
ANT	ANT_C2	ANT_C3	1	2	C	C	1.30E-06	1.03E-05	1.3	0.6	3.5	2.6	1700	1300
DPY	DPY_C4	DPY_C5	1	1	A	A	2.47E-06	2.82E-06	2.3	3.9	13	11	6200	5800
SADM	SADM_C4	SADM_C1	2	2	C	C	1.40E-05	9.40E-06	5.9	4.6	23	16	3050	3200
RAD	RAD_C4	RAD_C2	1	2	A	C	2.08E-06	5.22E-06	2.5	2.9	47	48	2800	1950
CPU	CPU_C4	CPU_C4	1	1	A	A	8.83E-07	8.83E-07	0.9	0.9	2.9	2.9	17500	17500
DSU	DSU_C2	DSU_C2	1	1	A	A	3.09E-06	3.09E-06	4.1	4.1	1.8	1.8	12100	12100

Table 4.20: Results: Minimize Cost

Type	Reliability	Weight	Power	Cost	Availability
PMS	0.524	98.8	194.1	79100	0.9999
SPMS	0.504	119.2	191.3	85694	0.9999

Table 4.21: Resultant System Parameters

4.4 Summary

This Chapter investigated the Reliability Allocation Problem, Redundancy Allocation Problem (RAP), and Reliability-Redundancy Allocation Problem (RRAP) for a satellite system. At first, the reliability allocation models based on various apportionment techniques were developed to allocate the satellite reliability during the initial design phase. Then a RAP model was developed to utilize the heritage data and estimate the number of redundancies required to improve the reliability. Later, a detailed model, fault tree and binary decision diagram of the satellite were developed for each phase to solve RRAP. Next, the idea of reality factors was introduced to deal with the complexity of satellites. Then, the system reliability equation was calculated using the modular method. Finally, the satellite system model was optimized to identify the optimal elements, number of redundancy and redundancy strategies. Comparison between the optimization results of Phased Mission System (PMS) and Single Phase Mission System (SPMS) formulation showed that PMS provided a more precise estimation of reliability.

All models are approximations. Essentially, all models are wrong but some are useful.

George Box

5

Satellite System Design

The interactions among the different subsystems in the satellite is necessary for a good design. Multidisciplinary Design Optimization (MDO), sometimes referred to as Multidisciplinary Design Analysis and Optimization (MDAO), is a field of engineering that is used to solve optimization problems involving more than one discipline.

Like any other optimization, the primary focus of MDO is to identify an optimal solution in a specified design space subject to constraints. Optimization of individual subsystems can conflict with each other when assembled. Therefore, the entire system has to be optimized holistically. In this Chapter, the mathematical foundation of system analysis and optimization using MDO is introduced and is then used to optimize a Distributed Space System.

5.1 Fundamentals of Multidisciplinary Design Optimization

The key aspect of MDO is to enable system optimization where the inherent couplings between the various disciplines are appropriately modelled. Constraints of the optimization reflect the requirement of the design and the objective function represents the system design preference. The foundation of the MDO is built on the intersection of three distinct yet related fields: **Non-linear Optimization**, **Model Construction** and **Model Differentiation**[168].

5.1.1 Non-linear Optimization

Non-linear optimization converts the problem with infinite solutions (under-defined problem) into a problem with single solution (well-defined). The objective function distinguishes between different system design alternatives and identifies the optimal design that maximizes or minimizes the desired system attribute. Optimization algorithms/Optimizer identifies the optimum design in several ways. The three main classes of optimization algorithms are as follows:

Brute Force Method In the Brute Force method, all possible solutions in the design space are enumerated, and the best design that satisfies a given problem is identified. The continuous design variables in the problem are discretized and sampled. This method is effective when the objective function of the problem is simple and involves a small number of design variables. It is the simplest and the only method that guarantees the global optimum or the best design. However, it falls short of optimizing real-world complex systems such as satellites with numerous design variables and computationally expensive objective functions.

Gradient-free Method The Gradient-free method includes mathematically rigorous algorithms such as Constrained Optimization BY Linear Approximation (COBYLA) and evolutionary algorithms such as Genetic Algorithms that are heuristic in nature. It does not require the gradient information of the functions to find the optimal solution. The advantages of the Gradient-free method are that it is straightforward to implement, runs the optimization in parallel, and can be used even when the design variables are discrete. However, the method requires a large number of function evaluations to get a reasonable answer. Moreover, the optimization becomes extremely difficult to solve when external tools such as Nastran-Patran for structural analysis are used as discipline models.

Gradient-based Method The Gradient-based method finds the optimal solution with the search directions given by the gradients of the function at the current point. Gradient-based methods are orders of magnitude faster than gradient-free method if the gradients are easy to compute. The gradient method is excellent in handling numerous design variables and the computational cost is reasonable even when external tools are used as discipline models. If the external tools do not provide gradients, they can be estimated through finite-difference

or complex step approximations. The main drawback of the gradient method is that it can be used only for continuous functions and continuous design space. Besides, this method often results in local optima and is highly dependent on the starting points. In many cases, the main justification for using the gradient method is that a local optimum for models that closely represent reality may be more valuable than a global optimum for low fidelity models. Hence the gradient method will be used in this research for satellite design. Although analytical models are used for the design problem in this research, the models can be easily upgraded to high fidelity models in the future. SLSQP and SNOPT are some good examples of gradient based optimizers.

5.1.2 Model Construction

Model construction is a process of formulating all the satellite subsystems and their interactions. The combination of problem formulation and organizational strategy is called the MDO Architecture. Chapter 2 introduced different types of MDO Architectures used for various applications. The models that represent a system is either explicit or implicit. For example, if the dependent variable y is given in terms of an independent variable x such that $y = f(x)$, the function is explicit. Equation (5.1) is simple example of an explicit function.

$$y = x^2 + 3x + 8 \tag{5.1}$$

On the other hand, the implicit function is defined in terms of both dependent and independent variables. The implicit functions are expressed by residual equations, $r = R(x, y) = 0$ where x is the input and y is the output. For a given value of x, the value of y can be calculated such that the residual equation is equal to zero. All explicit functions can be expressed

as implicit functions. The main difference between explicit and implicit functions is in the output computation. A non-linear solver such as a Newton solver is required to compute the outputs of an Implicit Function. Equation (5.2) is simple example of an implicit function. Implicit functions are required to model the disciplinary coupling and are discussed in the following section.

$$y - x^2 - 3x - 8 = 0 \tag{5.2}$$

NEWTON'S METHOD Newton's method is an iterative method of approximating the roots of a function using Taylor's expansion to solve Implicit functions. For example, consider a vector-valued implicit function $R(x, y)$, with the goal to solve for the parameter y. Then, Taylor's expansion for small variations in y for this equation is given by,

$$R(x,\ y + \Delta y) = R(x, y) + \frac{\Delta y \left[\frac{\partial R}{\partial y}\right]}{1!} + \ldots \tag{5.3}$$

Converting equation (5.3) to residual form and rearranging gives,

$$\Delta y \left[\frac{\partial R}{\partial y}\right] \approx -R(x, y) \tag{5.4}$$

Ignoring the infinitesimal higher order terms gives a linear equation as shown below that is straightforward to solve,

$$\Delta y \approx -R(x, y) \left[\frac{\partial R}{\partial y}\right]^{-1} \tag{5.5}$$

Equation (5.5) is the Newton's method and it is iteratively solved until Δy reaches the required level of accuracy. At each successive iteration, y in the equation is replaced by a new term, y^{k+1} such that $y^{k+1} = y^k + \Delta y^k$ where k and k+1 are the current and successive approximations, respectively.

5.1.3 Model Differentiation

The gradients required for the Gradient-based optimizer can be computed in several ways. These approaches are classified into Numerical, Algorithmic and Analytical Differentiations. The two main methods in Numerical Differentiations are Finite Difference and Complex-step method. The Finite difference does not require access to the source code and therefore is the easiest method to implement. The first-order finite difference approximation is derived from Taylor's expansion as follows:

$$f(x+h) = f(x) + \frac{hf'(x)}{1!} + \frac{h^2 f''(x)}{2!} + \ldots \tag{5.6}$$

$$hf'(x) = f(x+h) - f(x) - \frac{h^2 f''(x)}{2!} - \ldots \tag{5.7}$$

$$f'(x) \approx \frac{f(x+h) - f(x)}{h} \tag{5.8}$$

The value of h in the above equation must be sufficiently small to get approximations of the derivatives closer to the actual values. Therefore, all the terms in multiplication with h are infinitesimally smaller and are neglected. While, in theory, it is possible to get accurate gradients with small values of h, it is not practical after a specific lower limit of h, as the error in the approximation grows with it. The lower limit of h comes from the ability of computers to store the significant digits of floating-point numbers. There is limit to how small of a differ-

ence can be resolved in two numbers. This phenomenon is called Catastrophic cancellation or Subtractive cancellation, which is an inherent problem in numerical subtraction.

An excellent workaround to reach higher accuracy is to implement the Complex-Step approximation. Like Finite difference, the Complex step approximations is also derived from Taylor's expansion but uses complex arithmetic functions as shown below.

$$f(x+ih) = f(x) + \frac{ihf'(x)}{1!} - \frac{h^2f''(x)}{2!} - \frac{ih^3f'''(x)}{3!} + \dots \tag{5.9}$$

Equating the real and imaginary parts in equation (5.9) gives complex step approximation as shows in equation (5.13).

$$Re\, f(x+ih) = f(x) - \frac{h^2f''(x)}{2!} + \dots \tag{5.10}$$

$$Im\, f(x+ih) = \frac{hf'(x)}{1!} - \frac{h^3f'''(x)}{3!} + \dots \tag{5.11}$$

$$hf'(x) = Im\, f(x+ih) + \frac{h^3f'''(x)}{3!} + \dots \tag{5.12}$$

$$f'(x) \approx \frac{Im\, f(x+ih)}{h} \tag{5.13}$$

As there is no subtraction involved in equation (5.13), this method does not suffer from Catastrophic cancellation. Moreover, it offers second-order convergence as the largest neglected term is of order h^2. However, the main drawback with the complex-step method is that the source code must be compatible with complex arithmetics. Numerical approximations, in general, are computationally expensive as the approximation must be computed once per variable in the gradient.

Algorithmic Differentiation computes the derivative of a given model with respect to a specified variable, producing a new model as its output. This method provides more accurate derivatives than numerical approximations yet is computationally expensive than Analytical Differentiation.

The best option to improve the accuracy and reduce the computational cost is to use Analytical Differentiation that uses manually calculated derivatives. Therefore, in this research, Analytical Differentiation is used for gradient-based optimization. The relationship between total and partial derivatives of a coupled system is given in Figure 5.1. Here, the derivatives obtained from discipline models are partial derivatives and the derivatives obtained from a system model that combine the discipline models are the total derivatives.

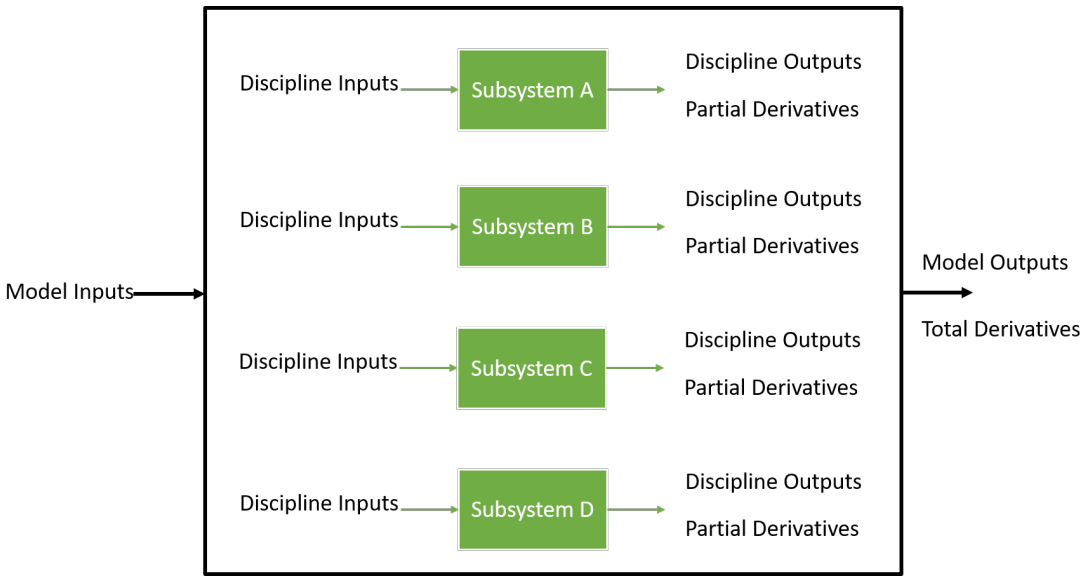

Figure 5.1: Relationship between total and partial derivatives of a coupled system

5.1.4 MDO Frameworks

MDO Frameworks assist in model development, differentiation and optimization. OpenMDAO[169] is an open-source MDO framework for optimizing complex coupled systems. OpenMDAO combines the discipline model as implicit functions to efficiently compute the total derivatives of the coupled model. When the model consists only of explicit functions, the total derivatives can be calculated using basic calculus. However, when there are implicit functions due to coupling between the models, the computation of the total derivatives becomes challenging.

Consider a function $F(x, y)$, where x is a vector of n inputs and y is a vector of m variables that depend implicitly on x. Then the total derivative ($\frac{df}{dx}$) of model output (f) with respect to model input (x) is calculated in openMDAO as follows[169]:

$$\frac{df}{dx} = \frac{\partial F}{\partial x} + \frac{\partial F}{\partial y}\frac{dy}{dx} \tag{5.14}$$

The partial derivatives in equation (5.14) is straightforward to calculate. However, the derivative dy/dx that captures the change in y with respect to x is calculated by differentiating the residual function $R(x, y) = 0$ as follows:

$$\frac{\partial R}{\partial x} + \frac{\partial R}{\partial y}\frac{dy}{dx} = 0 \tag{5.15}$$

The equation (5.15) is rearranged, and the resultant linear equation (5.16) is solved for n times (once for each inputs in vector x) find dy/dx. The calculated dy/dx is then substituted in equation (5.14) to compute the total derivatives.

$$\underbrace{\frac{\partial R}{\partial y}}_{m\times m}\underbrace{\frac{dy}{dx}}_{m\times n} = -\underbrace{\frac{\partial R}{\partial x}}_{m\times n} \tag{5.16}$$

This approach is called the direct method or forward method, and it scales linearly with the number of inputs. Therefore, the computational cost of this approach is directly proportional to the number of inputs. Another way of calculating total derivatives is to directly substitute the equation (5.16) in equation (5.14).

$$\frac{df}{dx} = \frac{\partial F}{\partial x} + \overbrace{\underbrace{\frac{\partial F}{\partial y}}_{1\times m}\underbrace{\left[\frac{\partial R}{\partial y}\right]^{-1}}_{m\times m}}^{\psi^T}\frac{\partial R}{\partial x} \tag{5.17}$$

where ψ is the adjoint vector of size m and is calculated as follows.

$$\psi^T = \underbrace{\frac{\partial F}{\partial y}}_{1\times m}\underbrace{\left[\frac{\partial R}{\partial y}\right]^{-1}}_{m\times m} \tag{5.18}$$

$$\underbrace{\left[\frac{\partial R}{\partial y}\right]^T}_{m\times m}\underbrace{\psi}_{m\times 1} = \underbrace{\left[\frac{\partial F}{\partial y}\right]^T}_{m\times 1} \tag{5.19}$$

The vector ψ in this linear equation can be solved and is then used to compute the total derivatives. This approach is called the adjoint method or reverse method, which scales linearly with the number of outputs and is independent of the number of inputs. Therefore, the direct method is advantageous if the number of inputs is less than the number of out-

puts and the adjoint method is advantageous when the number of outputs is less than the number of inputs in a given model. However, it is challenging to integrate this choice into the MDO framework. Hwang et al.[170] developed a Modular Analysis and Unified Derivatives (MAUD) architecture to overcome this challenge. MAUD architecture provides the mathematical framework that generalizes all analytical derivative methods using the Unified Derivatives Equation as presented in equation (5.20)[171].

$$\left[\frac{\partial R}{\partial u}\right]\left[\frac{du}{dr}\right] = \mathrm{I} = \left[\frac{\partial R}{\partial u}\right]^{T}\left[\frac{du}{dr}\right]^{T} \tag{5.20}$$

where u is the vector containing inputs, implicit variables and outputs, R is the residual functions and du/dr is the required total derivative. The left equality of equation (5.20) corresponds to the direct method, while the right equality corresponds to the adjoint method. OpenMDAO leverages the MAUD architecture to efficiently compute the derivatives. However, it is challenging to formulate the problem with Distributed Architectures using OpenMDAO. In a Distributed Architecture, the problem is decomposed into sub-problems that are optimized separately under a top-level optimization. The top-level optimization requires derivatives from the sub-problems, which is outside the scope of MAUD. While it is true that Distributed architectures perform well for a specific application, there is no conclusive evidence that it would outperform monolithic architecture for the same application. Moreover, the conclusion from previous researches[94,99], that compared monolithic and distributed architectures for various applications, favoured monolithic architectures. Therefore, in this research, only monolithic architectures are considered for optimization.

5.2 Distributed Space System

In the emerging NewSpace industry, driven by the advancements and miniaturization of electronics, the capabilities and application of small satellites are growing tremendously. Small satellites offer unique benefits such as shorter development time, lower cost, relatively simple maintenance, and mass producibility. As a result, small satellites are currently considered for almost every space application[172]. Small satellites are predominant in Low Earth Orbits (LEO)[173]. The ground coverage capacity of a small satellite operating in LEO is limited and therefore, often operate in a group to accomplish a commercial mission. Distributed Space Systems (DSS) is a system in which several satellites work together to achieve a common goal which is not feasible with a single small satellite. Nowadays, there is a growing demand for cost-effective DSS operable in LEO. Previous researches on DSS[174–177] were focused on optimizing the geometric configuration of the satellite constellation to improve coverage and reduce the overall cost. However, the satellite subsystems and their parameters were not considered for the optimization. The long-term success of a DSS hinges on substantial cost reduction. This is possible only when the connection between the constellation configuration and satellite subsystems are fully exploited. Therefore, design of DSS considering all the disciplines with interdisciplinary coupling needs to be optimized. Because of its disciplinary boundaries, DSS cannot be optimized as a standard constrained non-linear programming problem and has to be considered as a Multidisciplinary Design Problem.

The optimum solution to a multidisciplinary design problem can be achieved not only by considering the design of individual disciplines in the system but also their interactions. Modelling of subsystem interactions with each other in a DSS complicates the optimization

problem as the subsystem compatibility has to be maintained along with the objective function minimization. There are several ways to overcome this challenge with problem formulation procedure called MDO architecture.

The goal here is to compare three different Monolithic architectures: Multidisciplinary Feasible (MDF), Individual Discipline Feasible (IDF) and Simultaneous ANalysis and Design (SAND) for the DSS design problem. The various disciplines and their interactions of DSS are modelled in OpenMDAO [169], which is a specialized framework for MDO optimization. The usage of such framework removes most of the human-factors in programming of the architectures. Therefore, the results remain unbiased and depend only on the nature of the problem.

5.3 Problem Description

This section describes a DSS model to compare the selected architectures. A DSS is a complex multidisciplinary system consists of following subsystems: (i) Constellation model, (ii) Payload, (iii) Power, (iv) Thermal, (v) Structure, (vi) Attitude Determination and Control (ADC), (vii) On-board Computer (OBC), (viii) Telemetry, Tracking and Command (TT&C), and (ix) Propulsion. For the initial study, only Constellation, Payload, Power, Thermal and Structure subsystems are considered. It is assumed that ADC, OBC, TT&C, and Propulsion subsystems are readily available and their mass and power budgets are estimated based on design estimation relationships [155,178,179]. The multidisciplinary design optimization problem requires a set of design variables and subsystem inputs to generate subsystem states by solving the respective analysis model. The calculated subsystem states are either needed to compute the objective/constraints or needed by other subsystems (coupling). The

connections between the subsystems of modelled DSS is illustrated in Figure. 5.2. The set of design variables used in this problem, and their permissible ranges are presented in Section 5.5.

The difference between the MDO architectures lies in their handling of coupling variables. Most of the design variables in this problem are continuous while some of them are discrete. If both types of variables are considered, then the optimization problem becomes a Mixed Integer Non-Linear Problem (MINLP) which are very hard to solve. The discrete variables such as the number of satellites and orbital planes are important for reducing the launch cost but they are not directly coupled to any other subsystem. While these discrete variables will impact the resultant satellite design and the computation time, it will not affect the comparison between the architectures. Therefore, in this section the number of satellites and orbital planes are fixed to reduce MINLP to Non-Linear Problem (NLP), and optimize only the Altitude, Inclination and Elevation angle in the constellation model.

The DSS considered in this research is an earth observation constellation operating in LEO. The constellation consists of 25 satellites evenly distributed over five orbital planes. The satellites in the constellation are assumed to be identical to each other and have the same optical payload. The primary constraint enforced in this DSS optimization problem is to provide at least 70% coverage over Luxembourg, Belgium, and Germany. The objective of the optimization problem is to minimize the overall mass of the DSS system subject to various constraints. The mass of DSS m_{sys} is calculated using equation (5.21).

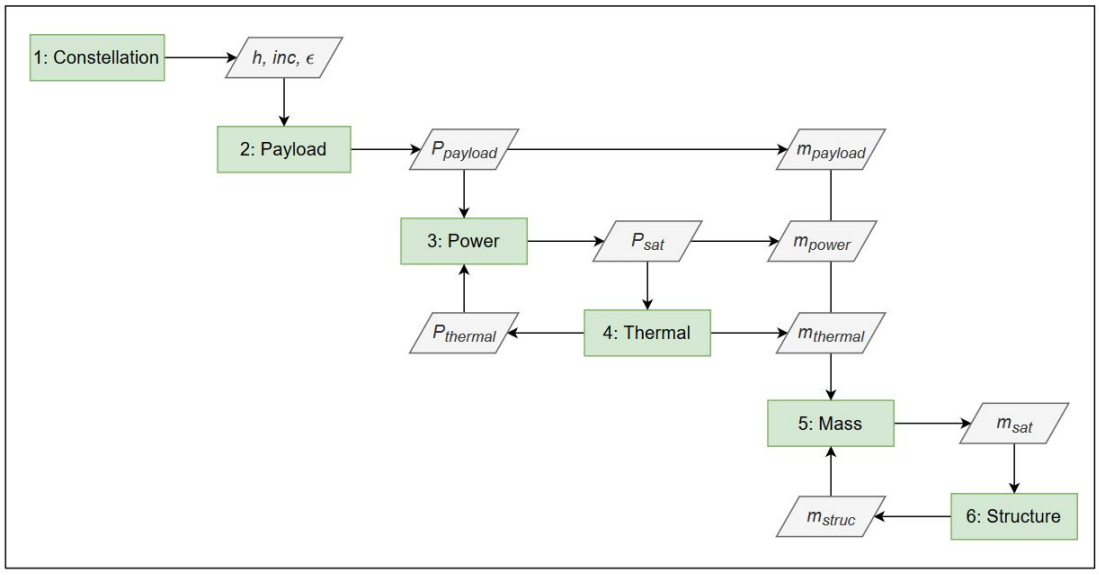

Figure 5.2: Coupling of DSS (MDO) disciplines

$$m_{sys} = N_s \times (m_{struc} + m_{payload} + m_{power} + m_{thermal} + m_{remaining}) \tag{5.21}$$

where N_s is the number of satellites, m_{struc} is the mass of satellite structure, $m_{payload}$ is the mass of payload, m_{power} is the mass of power subsystem, $m_{thermal}$ is the mass of thermal subsystem and $m_{remaining}$ is the mass of remaining subsystems.

5.4 DSS Subsystems

In this section, the mathematical models for all the considered disciplines in the Distributed Space System are detailed. Here the parent element is DSS and the children elements

are Constellation, Payload, Power, Thermal and Structure subsystems.

5.4.1 Constellation Model

Coverage goal of the DSS can be achieved by numerous constellation patterns. However, Walker Delta pattern is considered for its simplicity and cost-effectiveness[180,181]. The constellation parameters i, N_s, p, and f define the distribution of the satellites in space, where i is the inclination, N_s is the total number of satellites, p is the number of orbital planes, and f is the phase difference between satellites in the adjacent plane. Walker Delta constellation pattern is denoted by $i : N_s/p/f$. The number of satellite in each orbit is given by $s = \frac{N_s}{p}$ where $p \mid N_s$ (p divisible by N_s). To avoid collisions between satellites, the phase difference between adjacent satellites in a single plane is calculated by $f \times \frac{360^\circ}{N_s}$, where f is an integer between 0 to $(p - 1)$.

The orbital parameters of a satellite in the three-dimensional space include the six Keplerian elements: semi-major axis (a), eccentricity (e), inclination (i), the longitude of ascending node (Ω), the argument of perigee (ω), and true anomaly (ν). Since the Walker Delta constellation consists of circular orbits, $e = 0$ and $\omega = 0$. Therefore, a is equal to the radius of the orbit, and ν becomes the angle from the ascending node to the satellite's position vector. The right ascension of ascending node is given by $\Omega = \frac{360^\circ}{p}$. At epoch $\nu_n = f_n$ where $n = 1, 2, \ldots, N_s$. The optimization design variables for the constellation discipline are the Altitude (h), inclination (i) and Elevation angle (ε). The constraints set for this problem is to achieve total temporal coverage of at least 70%.

At first, the satellite's initial state is determined from the orbital parameters. Then, the satellite state is propagated around the Earth over a defined time, 12 days in this case. Finally,

the coverage is computed and updated for each satellite. Detailed descriptions of these steps are as follows:

Satellite State Determination The state ($\vec{Y}$) of the satellite at any a given point in space is determined by the position and velocity vectors of the satellite. Equations (5.22-5.24) represent the state ($\vec{Y}_{PQW}$), position ($\vec{r}_{PQW}$), and velocity ($\vec{v}_{PQW}$) vectors in the Perifocal coordinate system, PQW, and μ is the standard gravitational parameter. Here, P axis is towards perigee (ω), Q axis is 90° from P in the direction of satellite motion, and W axis is normal to the orbit plane.

$$\vec{Y}_{PQW} = \begin{bmatrix} \vec{r}_{PQW} \\ \vec{v}_{PQW} \end{bmatrix} \tag{5.22}$$

$$\vec{r}_{PQW} = \begin{bmatrix} \frac{acos(\nu)}{1+ecos(\nu)} \\ \frac{asin(\nu)}{1+ecos(\nu)} \\ 0 \end{bmatrix} \tag{5.23}$$

$$\vec{v}_{PQW} = \begin{bmatrix} -\sqrt{\frac{\mu}{p}} sin(\nu) \\ \sqrt{\frac{\mu}{p}}(e + cos(\nu)) \\ 0 \end{bmatrix} \tag{5.24}$$

Since $\omega = 0$, the perifocal frame of reference becomes obsolete for further calculation. Therefore, using coordinate transformation, the state variables are transformed into the Earth-Centred Inertial (ECI) system, IJK, where I axis points towards the vernal equinox direction, J axis is 90° towards the east in the equatorial plane and K axis goes through the north pole.

Satellite State Propagation With the gravitational attractions between the satellite and the Earth, the movement of a satellite in an orbit around the Earth is considered as a two-body problem. In an ideal case, this is represented by simple equations of motion. However, in an actual case, there are perturbations due to the following: (i) Non-homogeneity and oblateness of Earth, (ii) Third-body effects, (iii) atmospheric drag, and (iv) solar pressure. The effect of the perturbations in the satellite cannot be neglected in a real-world scenario. Cowell's Formulation [182] accounts for these effects by adding the perturbing accelerations to the two-body equation of motion, as shown in equation (5.25).

$$\ddot{\vec{r}} = -\frac{\mu}{r^3}\vec{r} + \vec{a}_p \tag{5.25}$$

where perturbing acceleration, $\vec{a}_p$, is the total acceleration caused by all other forces acting on the satellite and $\ddot{\vec{r}}$ is the resultant satellite acceleration. The specific form of $\vec{a}_p$ depends on the number of perturbation sources considered in the problem. A simplified acceleration model that includes perturbations due to the non-spherical central body is assumed. This perturbing acceleration on the satellite is obtained from the gradient of the gravitational potential of the non-spherical Earth that is modelled using spherical harmonics [183]. The perturbations arising from the second (J2), third (J3) and fourth (J4) harmonics are considered for the calculation. The components of the perturbing acceleration vector due to J2, J3, and J4 harmonics used for the calculation are found in *Fundamentals of astrodynamics and applications* [184] and are added linearly to equation (5.25).

Combining the state vector equation (5.22) and Cowell's second order equation of motion, the state of the satellite is reformulated into a first-order system as follows:

$$\dot{\vec{Y}} = \begin{bmatrix} \vec{v} \\ -\frac{\mu\vec{r}}{r^3} + \vec{a}_p \end{bmatrix} \tag{5.26}$$

Equation (5.26) is known as the variation of Cowell's formulation and is solved by using numerical integration methods.

Coverage Analysis The satellite observational area is the field of view from the satellite that projects a circular or rectangular footprint on the Earth. Access between the satellite and a target point in the footprint area at a given time represents the instantaneous coverage of the satellite. With the latitudes and longitudes of the sub-satellite point (Θ_s, Λ_s), and the latitudes and longitudes of the target (Θ_t, Λ_t), the value of Earth Central angle λ is calculated using equation (5.27)[3].

$$cos\lambda = sin\Theta_s sin\Theta_t + cos\Theta_s cos\Theta_t cos|\Lambda_s - \Lambda_t| \tag{5.27}$$

Then the nadir η is calculated using the design variable ε from equation (5.28) which is used to calculate the maximum Earth Central angle λ_{max}.

$$sin\ \eta_{max} = cos\ \varepsilon_{min} \frac{R_E}{h + R_E} \tag{5.28}$$

$$\lambda_{max} = 90^\circ - \varepsilon_{min} - \eta_{min} \tag{5.29}$$

A total of three hundred grid points, evenly distributed among the intended region (Luxembourg, Belgium and Germany) are selected as targets for this study. The condition for the

coverage, $\lambda < \lambda_{max}$ is checked for each grid point. The total temporal coverage is determined by equation (5.30).

$$C = \frac{\sum_{i=1}^{n} \sum_{j=1}^{m} T_{ij}}{nm} \tag{5.30}$$

where C indicates the coverage performance of the constellation, n is the number of time points considered, m is the number of grid points and T_{ij} is the coverage matrix. C should be at least 70% as per the constraints set for the problem.

5.4.2 Payload

Payload, being the most important subsystem of a satellite, drives the system design. Therefore, payload parameters such as size, weight and power requirements are needed at the initial stage of the satellite design. Usually for constellation missions, the payload is well defined and needs to be populated properly in orbit. However, in this case, the payload design is also optimized. It is unlikely to know the exact value of the payload parameters at the early stage. Therefore, viable estimation techniques are used to find their approximate values[179]. For earth observation mission, an optical payload is considered. Given the satellite altitude, the size of the payload is estimated using the relation in the following equations[179].

$$f = \frac{hd_x}{X/N_{samp}} \tag{5.31}$$

$$D = \frac{Bf}{Qd_x} \tag{5.32}$$

where h is the altitude, f is the focal length, D is the aperture diameter, d_x is the width of cross-track detectors, X is the cross-track ground pixel resolution, N_{samp} is the cross-track detector

samples in one pixel, B is the operating wavelength and Q is the quality factor for imaging. Based on the estimated aperture diameter $D_{payload}$, the mass $m_{payload}$, and power $P_{payload}$ of the payload are determined by sub-scaling from a reference payload using following relations[179].

$$R = D_{payload}/D_0 \tag{5.33}$$

$$m_{payload} \approx KR^3 W_0 \tag{5.34}$$

$$P_{payload} \approx KR^3 P_0 \tag{5.35}$$

where R is the aperture ratio, D_0, W_0, and P_0 are the aperture diameter, mass, and power of the reference payload respectively and K is the scaling factor which is 2 when R is less than 0.5, and 1 otherwise.

To increase the overall system coverage, the overlap of satellite footprints must be ensured. Therefore, the swath of a satellite must be greater than the successive node crossings at the Equator. This implies that the orbits maintain substantial margins at higher latitudes which ultimately increases the coverage. The swath of the satellite is given by $2\lambda_{max}$. Successive node crossings are determined from the perpendicular separation between the orbits as given in equation below.

$$S = sin^{-1}(sin(\Delta L)sin(i)) \tag{5.36}$$

where ΔL is the longitudinal shift per orbit and i is the orbit inclination angle.

5.4.3 Power Subsystem

The electrical power required to operate the satellite is generated by the Power subsystem with the help of solar panels. In addition to power generation, the power subsystem is also responsible for storing, distributing, and regulating the electrical power to each subsystem as needed. The area of solar panels influences the power generation as well as the size of the satellite. The size and capacity of the rechargeable battery to store the generated power depend on the power consumption and the duration of the satellite in eclipse.

Solar Panel Sizing The solar arrays must be sized such that the power generated by them is greater than the power required by the satellite. The area of the solar panel is determined based on the amount of power required by the satellite. The power required by the satellite is calculated as follows:

$$P_{req} = \frac{P_{payload}T_{payload} + P_{thermal}T_e + P_{batt}T_e + P_{others}T}{T - T_e} \tag{5.37}$$

where $P_{payload}$ is the power required by the payload in time $T_{payload}$, $P_{thermal}$ is the power required by the thermal subsystem operated during eclipse T_e, P_{batt} is the power required to charge the battery, P_{others} is the combined power required by the remaining for the total orbital period T. The power generated by the solar panel depends on various factors as given in the following equation[90].

$$P_{gen} = S_0 X_i X_s X_e X_0 A_s \eta F_c (\beta_p \Delta T + 1) cos(\chi) \tag{5.38}$$

where $S_0 = 1367\ W/m^2$ is the solar constant, $X_i = 0.95$, $X_s = 0.9637$, $X_e = 1$ and $X_0 =$

0.98 are the correction factors, A_s is the area of solar panel, η is the photoelectric conversion efficiency, F_c is the solar array loss coefficient, β_p is the power temperature coefficient, χ is the worst-case sun vector deviation from the solar panel normal. Using required and generated power, the surplus power is calculated as follows[90]:

$$P_{surplus} = (1 - d_y)^{L_t} P_{gen} - (1 + 5\%) P_{req} \tag{5.39}$$

where d_y is the annual power degradation of the solar panels and L_t is the mission lifetime.

Battery Sizing During the eclipse, the power generated by the solar panel is zero. A rechargeable battery is required to maintain the supply of power to the satellite. The discharge capacity, C of the battery depends on the duration of the eclipse and the power required during the eclipse. The Depth-of-Discharge, DOD of the battery, is taken as 80% of the rated capacity C_{rated}.

With the area of the solar panels as design variable and the estimated battery capacity, the mass of the power subsystem, m_{power} is calculated from equation 5.40.

$$m_{power} = \rho_s A_s + C_{rated}.V_{DB}/\mu_b \tag{5.40}$$

where ρ_s is the areal density of solar array, V_{DB} is the battery voltage and μ_b is the specific energy of the battery.

5.4.4 Thermal Subsystem

The satellite in an orbit is subject to radiation from the sun, thermal radiation from the Earth, and albedo. The temperature within the satellite must be maintained to keep the electronics in their operational range. Excess heat collected inside the satellite is ejected to the outer space by the radiators located in sun-facing direction. The common heat sources are external environment and internal heat generation, while the common heat sinks are controlled heat rejection from the radiator and heat leaks from the insulation. Initially, the satellite is assumed to be in steady-state equilibrium. The heat balance equation for the satellite is given by equation (5.41)[3,178].

$$Q_{source} = Q_{sink}$$

$$Q_{external} + Q_{internal} = Q_{Radiator} + Q_{MLI} \tag{5.41}$$

It is assumed that the predominant source of radiation is the sun and the other external radiations are negligible. The entire satellite is encapsulated by Multi-Layer Insulation (MLI) except the faces where the radiators are mounted. The heat leaks from MLI are insignificant and is neglected in the calculation. Therefore, using Stefan-Boltzmann law the heat balance equation is rewritten as follows:

$$\alpha S_0 A_R + Q_{internal} = \varepsilon A_R \sigma T^4 \tag{5.42}$$

where α is the Absorbity of the material, ε is the Emissivity of the material, S_0 is the solar constant, σ is the Stefan-Boltzmann constant, T is the satellite temperature, A_R is the radiator

area and $Q_{internal}$ is the internal heat generation. With equation (5.42) and A_R as the design variable, the temperature T is calculated for hot and cold cases. $Q_{internal}$ is assumed as 60% of the satellite power during hot case and 40% of the satellite power during cold case. The temperature during the hot case must not exceed 340K and the temperature during the cold case must not be less than 263K. Finally, the mass and power of the thermal subsystem are estimated by equations (5.43,5.44) respectively.

$$m_{thermal} = A_R \rho_R \tag{5.43}$$

$$p_{thermal} = \varepsilon \sigma A_R T^4 \tag{5.44}$$

where ρ_R is the areal radiator density.

5.4.5 Structure Subsystem

The structure of the satellite is the mechanical enclosure enveloping the satellite subsystems to protect them from the launch and space environments. The structural elements are treated as a separate subsystem for design and analysis purposes. This subsystem stays in contact with a launch vehicle, and it experiences severe static and dynamic loads. The load-carrying capacity of a satellite depends on the strength and stiffness of the structure subsystem that can be improved by careful selection of materials, and adequate reinforcement. However, it is necessary to keep the mass of the satellite as light as possible to reduce the launch cost. The shape of the satellite has significant importance, especially when solar panels, radiators or any other elements are mounted on its surfaces. Satellite exists not only in regular shapes such as cylinder, cuboid, sphere but also in irregular shapes.

Table 5.1: AL7075 T6 material properties

E (GPa)	ν	G (GPa)	ρ (kg/m^3)	σ (MPa)	τ (MPa)
71.7	0.33	26.9	2810	503	331

Table 5.2: Launch loads considered

Launch load	Longitudinal	Lateral
Acceleration (g)	$\pm$ 10g	$\pm$ 7.5g
Frequency (Hz)	$\geq$ 90Hz	$\geq$ 60Hz

The satellite considered here is a semi-monocoque cuboid whose length in X and Y directions are equal as shown in Figure 5.3. It has four side panels, four stiffeners at the corners, and four trays/frames perpendicular to the stiffeners. The launch adapter in the launcher is attached to the outside of the bottom tray, A. The trays B and C hold payload and other subsystems, while the tray D covers the cuboid. The number of elements in the structural design is fixed and its dimensions are optimized. The space-grade aluminium alloy - AL7075 T6 is selected as the material for the design. Its material properties is indicated in Table 5.1. The structural model presented here is based on the analytical structural design methodologies provided in the literature[44,178,185,186]. The design variables and constraints for structural optimization are the geometric dimensions and launch loads, respectively. The magnitude of launch loads varies with the launchers. A launcher with severe launch loads shown in Table 5.2 is considered for this study.

Static Model A static model or time-invariant satellite model is used to evaluate the structure under quasi-static limit loads imposed by the launcher. For preliminary calculations, the satellite structure is considered as a cantilever beam fixed at the base through the

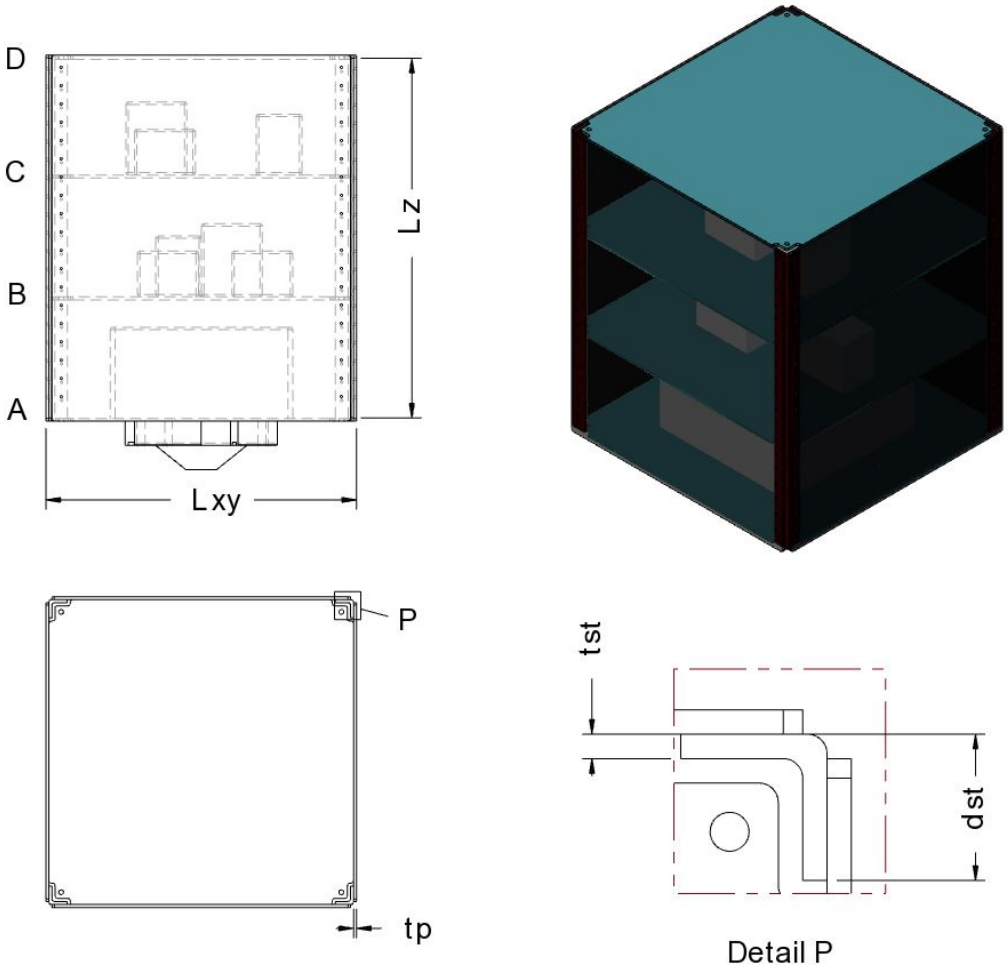

Figure 5.3: Satellite cross section

launch adapter. The satellite experiences the maximum axial load of 10g and a uniform lateral load of 7.5g. Then the maximum normal stress, σ_{max} and maximum shear stress, τ_{max} are calculated from following equations.

$$A_{sat} = 4[A_b + t_p(L_{XY} - t_p)] \tag{5.45}$$

$$\sigma_{max} = \frac{M_{max} h_p}{2I_x} + \frac{F_{long}}{A_{sat}} \tag{5.46}$$

$$\tau_{max} = \frac{V_{max} Q}{I_x L_{XY}} \tag{5.47}$$

where A_{sat} is the cross sectional area of the satellite, L_{XY} is the satellite dimension in X and Y direction, t_p is the thickness of the side panels, I_x is the satellite moment of inertia, M_{max} is the maximum bending moment and V_{max} is the maximum shear force. The Lateral load, F_{lat} and longitudinal load, F_{long} is obtained by substituting lateral acceleration a_{lat} and longitudinal accelerations a_{long} in $F = m_{sat} \times a$, respectively. The calculated stress should be less than the yield strength of the material indicated in Table 5.1.

Dynamic Model The satellite should withstand both static and dynamic load applied to it. The classical methodology is to design for static loads and verify the design for dynamic loads or vice versa. However, in this optimization, a set of design variables is iteratively checked against both static and dynamic loads. A dynamic model of the satellite predicts the natural frequency of the satellite in the given load conditions. The dynamic model here is a four degrees-of-freedom spring-mass system. The mass m_1, m_2, m_3, and m_4 represent the lumped masses for trays A, B, C, and D respectively. The launch adapters and structural elements between the trays act like spring. The equations of motion in longitudinal and lateral

directions are given by equations (5.48, 5.49) respectively.

$$\begin{bmatrix} m_1 & 0 & 0 & 0 \\ 0 & m_2 & 0 & 0 \\ 0 & 0 & m_3 & 0 \\ 0 & 0 & 0 & m_4 \end{bmatrix} \begin{bmatrix} \ddot{z}_1 \\ \ddot{z}_2 \\ \ddot{z}_3 \\ \ddot{z}_4 \end{bmatrix} + \begin{bmatrix} k_1 + k_2 & -k_2 & 0 & 0 \\ -k_2 & k_2 + k_3 & -k_3 & 0 \\ 0 & -k_3 & k_3 + k_4 & -k_4 \\ 0 & 0 & -k_4 & k_4 \end{bmatrix} \begin{bmatrix} z_1 \\ z_2 \\ z_3 \\ z_4 \end{bmatrix} = \begin{bmatrix} 0 \\ 0 \\ 0 \\ 0 \end{bmatrix} \tag{5.48}$$

$$\begin{bmatrix} I_m & 0 & 0 & 0 \\ 0 & m_2 & 0 & 0 \\ 0 & 0 & m_3 & 0 \\ 0 & 0 & 0 & m_4 \end{bmatrix} \begin{bmatrix} \ddot{\phi} \\ \ddot{x}_2 \\ \ddot{x}_3 \\ \ddot{x}_4 \end{bmatrix} + \begin{bmatrix} k_\phi & 0 & 0 & 0 \\ 0 & k_5 + k_6 & -k_6 & 0 \\ 0 & -k_6 & k_6 + k_7 & -k_7 \\ 0 & 0 & -k_7 & k_7 \end{bmatrix} \begin{bmatrix} \phi \\ x_2 \\ x_3 \\ x_4 \end{bmatrix} = \begin{bmatrix} 0 \\ 0 \\ 0 \\ 0 \end{bmatrix} \tag{5.49}$$

where k_1, k_ϕ are the longitudinal and lateral stiffness of the launch adapter. k_{2-4} are the longitudinal stiffness, and k_{5-7} are the lateral stiffness of the structural elements between the trays

A-B, B-C and C-D, respectively. I_m is the mass moment of inertia of the satellite.

With the mass and stiffness matrices, the angular frequency of the satellite is obtained by solving the eigenvalue problem, $([K] - \omega_n^2[M]) = 0$. The first natural frequency is calculated by $f_n = \omega_n / 2\pi$. The calculated first lateral frequency and the first longitudinal frequency must be greater than launcher constraints shown in Table 5.2.

5.5 MDO Architectures

The MDO problem of the DSS is formulated to have a single objective function that is to minimize the mass of DSS, with continuous design variables described in Table 5.3. The problem is solved using three different architectures MDF, IDF, and SAND. The main difference between the architecture lies in the handling of interdisciplinary coupling. For a fair comparison, all the architectures use the Sequential Least-Squares Quadratic Programming (SLSQP) optimizer[187] and the convergence tolerance of the optimizer set to 1×10^{-3}.

To describe the sequence of operation and data interactions within the architecture, an extended Design Structure Matrix (XDSM) proposed by Martin and Lambe[188] is used. The conventions used in XDSM are as follows: (i) Rounded rectangle denotes the optimizer that controls the entire optimization. (ii) Rectangular-shaped nodes represent discipline modules and are placed along the diagonal. (iii) Parallelogram shaped nodes depict data and results. (iv) Thick grey lines indicate data flow and thin black lines indicate process flow. (v) Data flow in vertical direction represents the input to the module while the data flow in horizontal direction represents the output from the module. (vi) In addition to the thin black lines, a numbering system is used to indicate the process flow. (vii) The process flows from module-0 and continues in sequential order up to module-n. (viii) $i \rightarrow j$ represents loops executed

Table 5.3: Design Variables of Optimization

Variable	Symbol	Unit	Range	Initial Guess
Altitude	h	km	[800,1000]	900
Inclination	i	deg	[53, 55]	53.5
Elevation Angle	ε	deg	[15, 25]	15
Length in X & Y direction	L_{xy}	m	[0.5, 1.2]	1
Length in Z direction	L_z	m	[0.5, 1.2]	1
Thickness of panel	t_p	m	[0.001, 0.005]	0.005
L-bar Width	d_{st}	m	[0.02, 0.05]	0.03
L-bar Thickness	t_{st}	m	[0.001, 0.005]	0.005
Length Ratio between plate A and B	AB	-	[0.25, 0.5]	0.325
Length Ratio between plate B and C	BC	-	[0.25, 0.375]	0.25
Area of Solar Panel	A_s	m^2	[1, 5]	2
Area of Radiator	A_r	m^2	[0.1, 2]	1.06
Mass of Structure*	m_{struc}	kg	[4, 50]	15
Mass of Satellite*	m_{sat}	kg	[65, 150]	100
Power required by Satellite*	P_{sat}	W	[300, 750]	400
Power required by Thermal Subsystem*	$P_{thermal}$	W	[30, 200]	90
Power required by Payload**	$P_{payload}$	W	[20, 200]	40

* Needed by IDF and SAND
** Needed by SAND

within the architecture such that a process i is followed by process j until a specified condition is met. (ix) Data external to the optimizer, such as design variable initial guesses $x^{(0)}$, variables at their optimum x^*, and discipline-specific variables are placed in the outer nodes.

IDF and SAND are decoupled while, MDF requires a solver to handle the coupling. The following sub-sections present a brief description of problem formulations in MDF, IFD, and SAND architectures and their respective XDSM diagrams for the given DSS model.

5.5.1 Simultaneous Analysis and Design (SAND)

As the name suggests, the SAND architecture simultaneously analyses and designs the system. This is performed by including state variables ($\bar{y}$) and coupling variables (y) from each discipline to the set of design variables (x). The analysis models are reformulated to provide residuals for each disciplinary equations. These residuals are treated as equality constraints for this architecture. The general mathematical formulation of SAND architecture[92] is shown below.

$$\begin{aligned} \min \quad & f(x, y) \\ \text{w.r.t.} \quad & x, y, \bar{y} \\ \text{s.t.} \quad & g_i(x_0, x_i, y_i) \geq 0 \quad \text{for } i = 1, \ldots, N \\ & R_i(x_0, x_i, y, \bar{y}_i) = 0 \quad \text{for } i = 1, \ldots, N \end{aligned} \tag{5.50}$$

The XDSM of the DSS problem implementation in SAND architecture is shown in Figure 5.4. The design variables and their acceptable range are given in Table 5.3.

5.5.2 Multidisciplinary Feasible (MDF)

MDF architecture consists of Multidisciplinary Analysis (MDA) modules over which the optimizer is placed. This implies that at each iteration of MDF, a multidisciplinary feasible solution is present. The set of design variables (x) are passed into the MDA modules which iterate over the discipline analysis models until a consistent set of coupling variables (y) is generated. Then the design variables and the resultant coupling variables are used to compute the objective and constraints. Typical iterative solvers such as Block Gauss-Seidel, Newton solver are used to solve the MDA. The general mathematical formulation of MDF

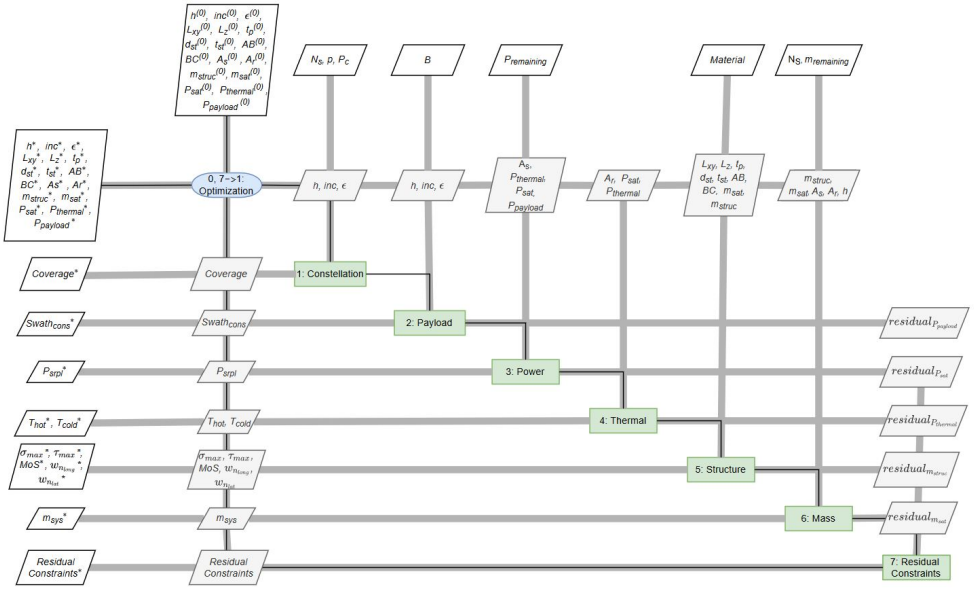

Figure 5.4: DSS XDSM diagram for SAND

architecture[92] is shown below.

$$\begin{aligned} \min \quad & f(x, y(x, y)) \\ \text{w.r.t.} \quad & x \\ \text{s.t.} \quad & g_i(x_0, x_i, y_i(x_0, x_i, y_i)) \geq 0 \quad \text{for } i = 1, \ldots, N \end{aligned} \tag{5.51}$$

The XDSM of the DSS problem implementation in MDF architecture is shown in Figure 5.5. Nonlinear Block Gauss-Seidel iterative solver (NLBGS) and Newton solver is used to solve the MDA of the DSS.

5.5.3 Individual Discipline Feasible (IDF)

Decoupling the MDF architecture results in IDF architecture. To decouple the MDF, copies of coupling variables ($\hat{y}$) are added to the design variable set (x). This design variable

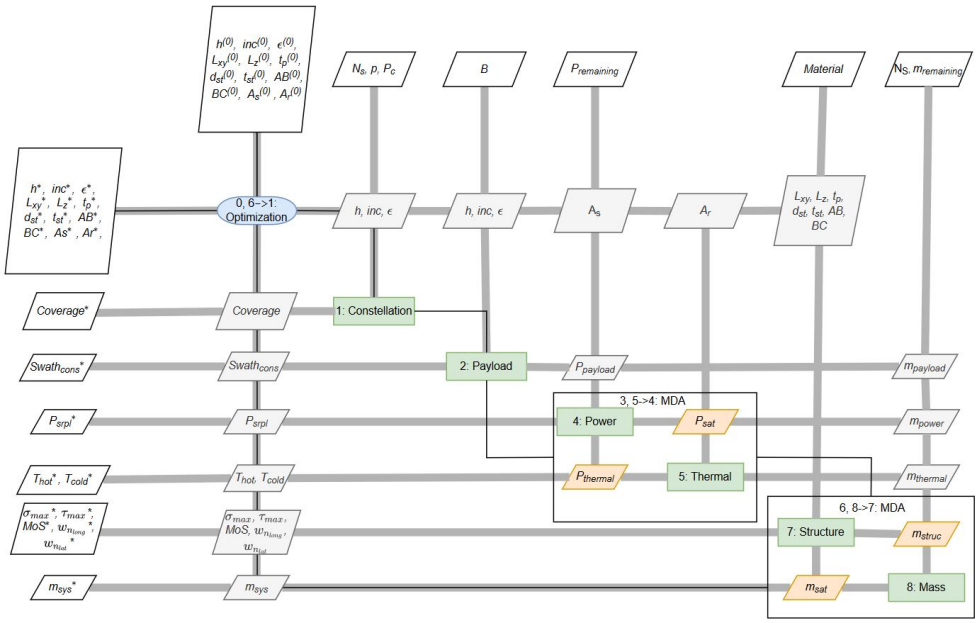

Figure 5.5: DSS XDSM diagram for MDF

set is then used to compute the objective and constraints at each iteration. Multidisciplinary feasibility is ensured by the usage of consistency constraints, $g_c = \hat{y} - y$. The general mathematical formulation of IDF architecture[92] is given by:

$$\begin{aligned} \min \quad & f(x, y(x, \hat{y})) \\ \text{w.r.t.} \quad & x, \hat{y} \\ \text{s.t.} \quad & g_i(x_0, x_i, y_i(x_0, x_i, \hat{y}_i)) \geq 0 \quad \text{for } i = 1, ..., N \\ & g_c = \hat{y}_i - y_i(x_0, x_i, \hat{y}_i)) = 0 \quad \text{for } i = 1, ..., N \end{aligned} \tag{5.52}$$

The XDSM of the DSS problem implementation in IDF architecture is shown in Figure 5.6.

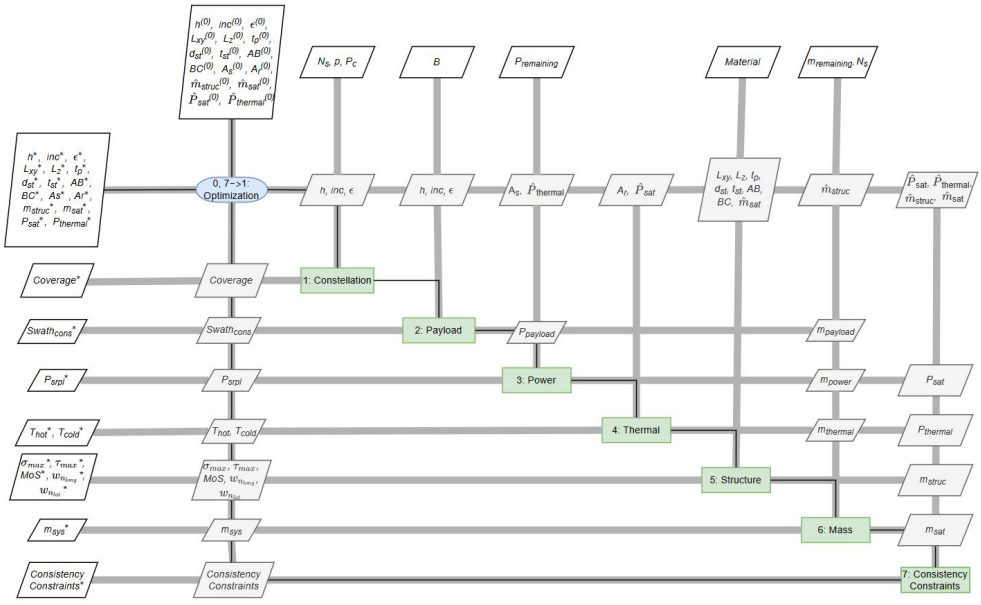

Figure 5.6: DSS XDSM diagram for IDF

5.6 Results and Discussions

The DSS design problem was solved successfully in all three architectures. IDF, SAND, and MDF are optimized using SLSQP optimizer. For MDF, a solver is needed to handle the coupling between the disciplines. For completeness, the MDF architecture is optimized for two cases: (i) using a gradient-free Non-linear Block Gauss-Seidel (NLBGS) solver and (ii) using a gradient-based Newton solver. Additionally, a Linear Direct solver is used for the Newton solver to compute to the derivatives. Comparison between the solvers demonstrates the differing performance of the same problem within the architecture. The optimization results obtained from each architecture are shown in Table 5.4. There are multiple ways to measure the effectiveness of an architecture. The most obvious way is to compare the optimum Objective Values attained by each architecture. However, other metrics such as Total

Function Calls and Convergence Characteristics are also important for useful comparison.

5.6.1 Objective Value

IDF provided the minimum objective value, i.e. m_{sys}. However, there are no significant changes in m_{sat} between the architectures. The nonlinear solvers used in MDF introduces a noise during convergence which causes the variations of the results. Since the resultant mass of DSS is only an estimation, minor variations do not significantly impact the DSS design. However, the accumulation of error grows with the addition of subsystems. It is possible to minimize the error by using analytical derivatives instead of numerical approximation, in the later stages.

5.6.2 Total Function Calls

The computation power required by the architecture is indicated by the number of functions evaluated/called while optimization. The calls to calculate the derivatives are also included in the functional call counts recorded for each subsystem. The number of function calls to each subsystem for every architecture is shown in Table 5.5. IDF supersedes the other architectures with the lowest function calls. Since MDF converges to a multidisciplinary feasible design at each iteration it has the most function calls. Additionally, the presence of Direct solver induces a spike in function calls of MDF_{Newton}.

The optimizations were run on an intel CORE i7 7th Gen processor. The computational time required for each architecture is given in Table 5.4. Due to careful selection of design variable ranges combined with the calculation of DSS coverage for a period of 12 days, the computation time required is significantly lower than the time generally required to solve

Table 5.4: Optimization results

	Unit	IDF	SAND	MDF_{Newton}	MDF_{NLBGS}
m_{sys}	kg	2477	2502	2560	2660
m_{sat}	kg	99.11	100.09	102.40	106.43
h	km	917.2	913.3	918.92	964.2
i	deg	55.00	55.00	53.57	53.50
ε	deg	18.64	18.56	17.83	18.88
L_{xy}	m	0.54	0.66	0.55	0.56
L_z	m	0.80	0.66	0.80	0.79
t_p	m	0.001	0.001	0.001	0.001
d_{st}	m	0.050	0.050	0.050	0.049
t_{st}	m	0.001	0.001	0.001	0.003
AB	-	0.250	0.250	0.250	0.366
BC	-	0.250	0.250	0.250	0.316
A_s	m	2.38	2.36	2.36	2.38
A_r	m	0.876	0.877	0.878	0.887
m_{struc}	kg	9.374	10.590	9.470	11.763
$P_{thermal}$	W	55.75	55.78	55.89	56.43
$P_{payload}$	W	99	98	106	109
P_{sat}	W	566.96	567.25	568.37	565.84
$Coverage$	%	70	70	70	70
P_{srpl}	W	5.48	1.13	0.00	6.80
T_{hot}	K	340	340	340	340
T_{cold}	K	276.55	276.55	276.56	275.00
MoS	-	1.8	2.2	1.9	3.6
$w_{n_{long}}$	Hz	74	74	73	71
$w_{n_{lat}}$	Hz	60	72	60	62
Execution time	h	≤ 1	~ 1	~ 6	~ 2

Table 5.5: Function evaluation counts

Architecture	Constellation	Payload	Power	Thermal	Structure	Mass	Total
IDF	122	82	162	64	122	122	674
SAND	226	198	310	170	254	254	1412
MDF_{Newton}	3020	3020	17362	11072	23813	23813	82100
MDF_{NLBGS}	964	964	2181	2181	2380	2380	11050

a problem of this size. In the actual scenario, the design variable have wide ranges and the temporal coverage is calculated for the entire mission lifetime. This exponentially increases the computational time. However, the results obtained are sufficient for the comparison of architectures. The execution times given in Table 5.4 are consistent with the number of function calls. As expected, the MDF_{Newton} had the highest execution time and IDF had the lowest.

5.6.3 Convergence Characteristics

The path taken for the optimization problem to arrive at the optimum value is given by the convergence characteristics of the problem. Due to the complexity, the exact optimal solution for the DSS problem is not known. Therefore, the lowest objective value calculated is considered as the exact optimal solution for this comparison. The relative error is calculated using the following equation.

$$\text{Relative Error} = \frac{|f - f_{min}|}{f_{min}} \tag{5.53}$$

where f is the objective of the targeted architecture and f_{min} is the corresponding objective from the architecture with the lowest objective value. The convergence rate of optimization

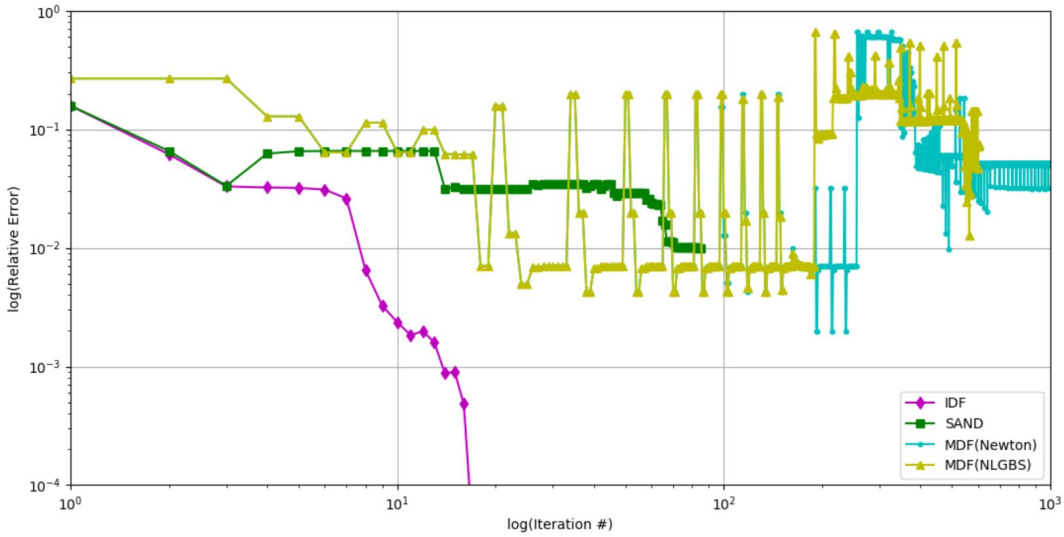

Figure 5.7: Objective Convergence

for each architecture is shown in Figure 5.7. IDF architecture exhibits a clear convergence trend while MDF_{Newton} required more iterations to converge. The convergence behaviour will be different when analytical derivatives are used instead of numerical approximation[94].

5.7 Summary

In this chapter, a Distributed Space System was modelled. The three MDO architectures MDF, IDF and SAND implementation of the DSS problem were then optimized. The results from the optimization showed that MDF needed the highest computational resources compared to other architectures. MDF solved using NLBGS introduced noise in the objective value while MDF solved using Newton solver had highest function calls. SAND had better results compared to MDF, in terms of optimality, computation, and convergence. However, IDF outperformed all architectures in terms of optimality, computational efficiency,

and convergence rate. Based on the comparison it can be concluded that IDF is preferable for the conceptual design of DSS followed by SAND. At later stages of the DSS design, the simple analytical models are not sufficient. More detailed design has to be developed considering all the subsystems and using high fidelity simulation models. This further complicates the optimization and makes it more expensive to compute. From an engineering design context, it might be beneficial to get an improved design that need not be an optimal one in a strict mathematical sense. In such cases, MDF architecture is advantageous, provided that the optimization maintains the feasible design path, as it offers a multidisciplinary feasible solution at each iteration.

Optimization is an automatic process to find all the bugs, holes, and weaknesses in your model.

"Enlightened" MDO Analyst

6

Reliability Based Multidisciplinary Design Optimization

Reliability has a crucial implication on the design of satellites. Numerous tests are carried out to ensure the satellite will work as intended in the orbit. With the grow-

ing capabilities of small satellites, reliability is considered as a cornerstone of their design. Consequently, to effectively design a reliable satellite, reliability must be incorporated in the early design phases. So far, the researches on Reliability-based design follow a sequential decomposition approach where the satellite model is optimized first, followed by the reliability analysis. The traditional sequential method often produces a sub-optimal or infeasible design due to the lack of coupling relations between the satellite and the reliability model. In this chapter these issues are addressed by coupling the reliability model developed in Chapter 4 with the satellite model developed in Chapter 5 to leverage the synergy.

6.1 Background

As presented in the State of the Art, the literature on Reliability-Based Optimization (RBO) includes very few publications that discuss satellite design optimization in the context of reliability. Similar to the previous efforts, the work presented in this chapter aims to optimize the design of small satellites (microsatellites) by prioritizing their reliability. However, the problem and model formulation in this study differ from that of the literature in many ways as follows: First, most previous efforts employ the Sequential approach, where the satellite model and reliability model are optimized sequentially. In contrast, in this study both the satellite design and reliability analysis are considered as a single optimization problem (Simultaneous Approach). Second, the reliability models in the literature formulate satellite as a Single Phase Mission System (SPMS), whereas in this study the satellite is considered as a Phased Mission System (PMS) using the reliability model discussed in Chapter 4. Third, in the previous works, technology choices, redundancy levels or both are considered as design variables for optimization. In this work, redundancy levels and element choices instead of

technology choices are considered. As the element choices are gathered from heritage data, this would result in a tangible relationship between the satellite model and the actual satellite elements. Moreover, unlike in the literature, this work uses gradient-based method for the satellite model instead of non-gradient search method. Finally, with 94 discrete/integer design variables, the problem size in this study is significantly larger than the problems in the literature. RBMDO of small satellites with the context of PMS and its correlation with satellite elements is a unique optimization problem. The work presented here introduces an approach to incorporate reliability assessments within the MDO of a satellite. The proposed approach is demonstrated for the design of a Earth Observation small satellite in Low Earth Orbit. The results from Sequential and the Simultaneous optimization approaches are finally compared.

The developed satellite and reliability model are optimized using A Mixed Integer Efficient Global Optimization algorithm - Multiple Infill via a Multi-Objective Strategy (AMIEGO-MIMOS)[137–139]. Figure 6.1 illustrate the AMIEGO algorithm. The red blocks denote the exploration of integer design space, and the blue block represents the exploration of continuous design space. The algorithm starts by separating the integer and continuous design variables. Next, a set of initial integer starting points that satisfy the integer constraints are generated. With the generated set of integer variables, a complete gradient-based optimization with respect to continuous variables is performed in the next step. Then, a surrogate model is built with the integer type design variables and the output response of the objective function with respect to continuous design variables. Kriging is combined with Partial Least Square regression[189] to reduce the number of hyper-parameters and efficiently train the surrogate model. In the next step, the integer is solved by maximizing the expected improvement

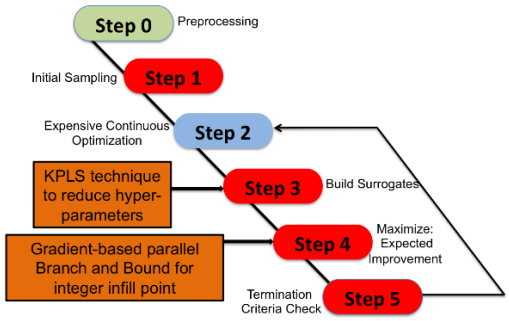

Figure 6.1: Overview of AMIEGO algorithm [139]

function. This solution is the next infill point that is used as the next iteration input for continuous optimization. The MIMOS part further extends this step by adding two additional objectives to maximize the distance from the existing point and maximize the generalized expected improvement function. This provides multiple-infill points instead of a single point to further explore the design space. Finally, the optimization is terminated when the expected improvement value falls below a specified percentage of the present best solution.

6.2 Problem Description

The Reliability Based Multidisciplinary Design Optimization (RBMDO) framework presented in this chapter seeks to formulate the relationship between reliability and the satellite conceptual design. The objective of the optimization problem is to minimize the overall mass and cost of the satellite to meet its target reliability within the available resource budgets. As evident from the state of the art, most previous efforts in RBMDO employ the Sequential approach, where the satellite model and reliability model are optimized sequentially. In this study, both the satellite design and reliability analysis are considered as a single optimization problem (Simultaneous Approach) and are optimized simultaneously. The proposed ap-

proach is demonstrated for the design of an Earth Observation small satellite in Low Earth Orbit.

The satellite model and reliability model is used to formulate the satellite design problem. Then this problem is solved using two approaches, namely Sequential Approach and Simultaneous Approach, to have a basis of comparison and investigate the impact on coupling the two models. The results from the Sequential and the Simultaneous optimization approaches are finally compared.

6.2.1 Sequential Approach

In the sequential approach, there is no explicit coupling between the satellite and reliability models. The satellite model is optimized first, and the results are used as constraints to optimize the reliability model. The satellite design optimization is carried out in OpenMDAO[169] using a gradient-based nonlinear optimizer, SNOPT[190,191]. Analytical gradients are specified for every subsystem in the satellite model. The couplings between the disciplines are handled by formulating the problem using Multidisciplinary Feasible (MDF) architecture. IDF was identified as the best architecture in terms of optimality in the previous chapter. However, there is an increased chance that the optimization may terminate early without obtaining a feasible design for a complex problem such as RBMDO. Hence, it is advantageous to use MDF in this study to obtain a feasible design at each iteration. The problem formulations for the sequential approach is shown in Table 6.1.

Figure 6.2 shows the extended design structure matrix (XDSM)[188] of satellite MDO in MDF architecture. The resultant mass and power of every subsystem are used as constraints for optimizing the reliability model. If a satellite system, s consists of m number of elements

Satellite Design Optimization (NLP)	
Minimize	Satellite mass
With respect to	Area of solar panel
	Area of radiator
	Altitude
	Structural dimensions
Subject to	Allowed Maximum Stress
	Natural Frequency
	Operational temperature
	Power constraints
	Payload specific constraints

Mathematically,

$$
\begin{aligned}
\min \quad & m_{sat} = f(A_s, A_r, h, L_{xy}, L_z, t_p, d_{st}, t_{st}, AB, BC) \\
\text{s.t.} \quad & \sigma_{max} < \sigma_{Al}, \\
& \tau_{max} < \tau_{Al}, \\
& MoS > 1 \\
& w_{n_{long}} > 55 \\
& w_{n_{lat}} > 60 \\
& S_w > S \\
& P_{surplus} > 0 \\
& T_{hot} < 340 \\
& T_{cold} > 263
\end{aligned}
$$

Table 6.1: Satellite Design Optimization (NLP)

subject to q different constraints (g), then the mathematical representation to optimize the system cost, C_s is given in Table 6.2.

The subscript j represents any system element from 1 to m such that its reliability r_j is a real number between 0 and 1, and n_j is a positive integer. Then, for a system consisting of m elements, each having k choice elements, r is the reliability vector, and n is the required number of redundancies of the corresponding system elements.

The element's reliabilities, along with its resource information such as mass, cost, power, and the available choice of elements, are modelled in a graph database management system,

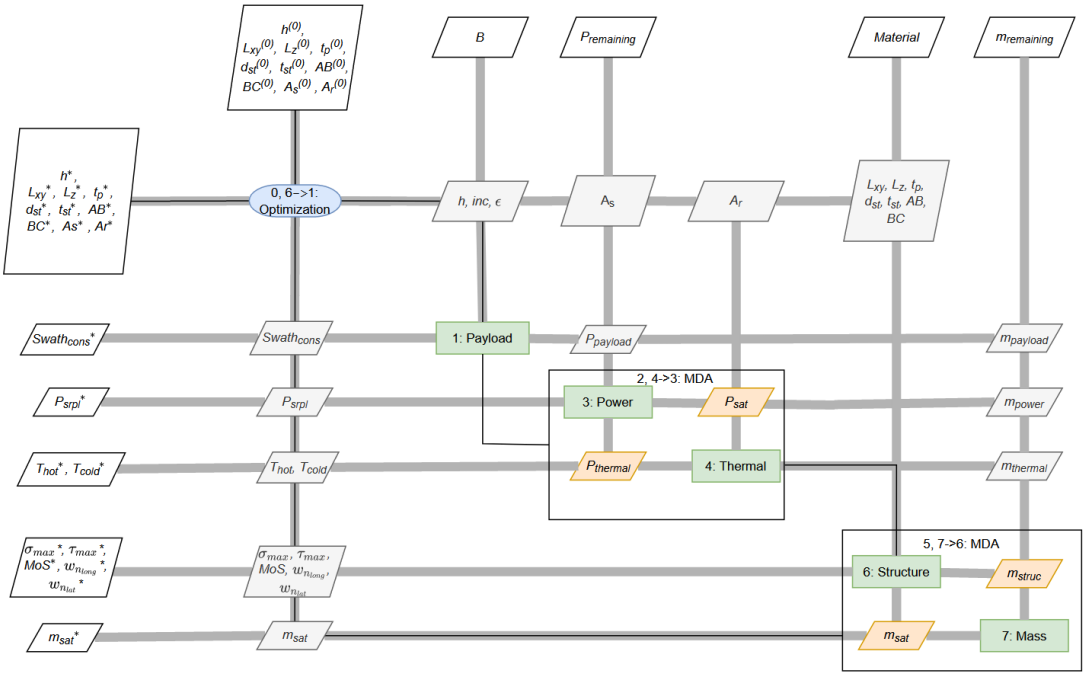

Figure 6.2: Extended Design Structure Matrix of Satellite MDO model in Multidisciplinary Feasible architecture

Reliability-Redundancy Allocation Problem (ILP)

Minimize	Satellite Cost
With respect to	Element Choice
	Redundancy Level
Subject to	Reliability
	Mass Budget
	Power Budget

Mathematically,

$$
\begin{aligned}
\min \quad & C_s = f(c, n) \\
\text{s.t.} \quad & g_i(g, n) \leq l_i, \quad 1 \leq i \leq q \\
& C = (c_1, c_2, .., c_m) \\
& n = (n_1, n_2, .., n_m) \\
& g = (g_1, g_2, .., g_q) \\
& 0 \leq r_j \leq 1, \quad r_j \in \Re, \quad n_j \in \mathbb{Z}^+, \quad 1 \leq j \leq m
\end{aligned}
$$

Table 6.2: Reliability-Redundancy Allocation Problem (ILP)

Neo4j[167]. The structure of the modelled graph database is presented in Figure 4.8. The data architecture consists of the central satellite system, SAT, containing the satellite bus or Platform (PF), which encloses every subsystem. The elements belonging to every subsystem are denoted by their acronyms that have been previously established in Table 4.15. The real data for each element is gathered from proprietary heritage data. Therefore, the resource values are scaled, and cost factors are used in place of actual costs.

This problem considers five different choices for each of the elements as the basis for the selection. The choice elements are denoted as E_ck, where E is the element's acronym, c indicates the choice element, and k = 1 to 5 is the element's choice. For example, if RW is the j^{th} system element and RW_C_k is the selected choice for RW, then c_j is the cost of RW_C_k, and n_j is the number of redundancy of RW respectively. The parameters of each subsystem constrain the selection of elements, and the resource constraints are implemented at the subsystem level. For instance, the sum of mass of the selected choices for the main elements of the power subsystem must not exceed the resultant mass of the power subsystem from MDO. The reliability model/Reliability - Redundancy Allocation Problem (RRAP) is optimized using the APOPT solver from Gekko Optimization Suite[163].

6.2.2 Simultaneous Approach

The satellite and reliability models are coupled and posed as a single optimization problem in the simultaneous approach, also called as RBMDO. Coupling the models results in MINLP. The problem formulation for the simultaneous approach is given in Table 6.3.

Figure 6.3 shows the extended design structure matrix (XDSM) of the satellite RBMDO in MDF architecture. The mass and power constraints are flown down to each subsystem

Satellite RBMDO (MINLP)

Minimize	Satellite Parameters (mass and cost)
With respect to	Area of solar panel
	Area of radiator
	Altitude
	Structural dimensions
	Element Choice
	Redundancy Level
Subject to	Allowed Maximum Stress
	Natural Frequency
	Operational temperature
	Power constraints
	Payload Specific constraints
	Satellite Cost
	Reliability
	Mass Budget
	Power Budget

Mathematically,

$$
\begin{aligned}
\min \quad & W_{sys} = f(A_s, A_r, h, L_{xy}, L_z, t_p, d_{st}, t_{st}, AB, BC, n, c) \\
\text{s.t.} \quad & \sigma_{max} < \sigma_{Al}, \\
& \tau_{max} < \tau_{Al}, \\
& MoS > 1 \\
& w_{n_{long}} > 55 \\
& w_{n_{lat}} > 60 \\
& S_w > S \\
& P_{surplus} > 0 \\
& T_{hot} < 340 \\
& T_{cold} > 263 \\
& g_i(g, n) \leq l_i, \quad 1 \leq i \leq q \\
& n = (n_1, n_2, .., n_m) \\
& g = (g_1, g_2, .., g_q) \\
& 0 \leq r_j \leq 1, \quad r_j \in \Re, \quad n_j \in \mathbb{Z}^+, \quad 1 \leq j \leq m
\end{aligned}
$$

Table 6.3: Satellite RBMDO (MINLP)

and directly influence their design. The RBMDO model has a total of 94 integers/discrete design variables and 10 continuous design variables. To solve the MINLP RBMDO problem, a mixed-integer efficient global optimization algorithm (AMIEGO-MIMOS) is used. AMIEGO-MIMOS combines the ability of a gradient-based approach with the ability of Efficient Global Optimization (EGO)[139]. As a result, it helps in handling large-scale design optimization problems in the continuous space while globally exploring the integer design space. More details on the theory and the algorithm implementation of AMEIGO-MIMOS can be found in [137–139].

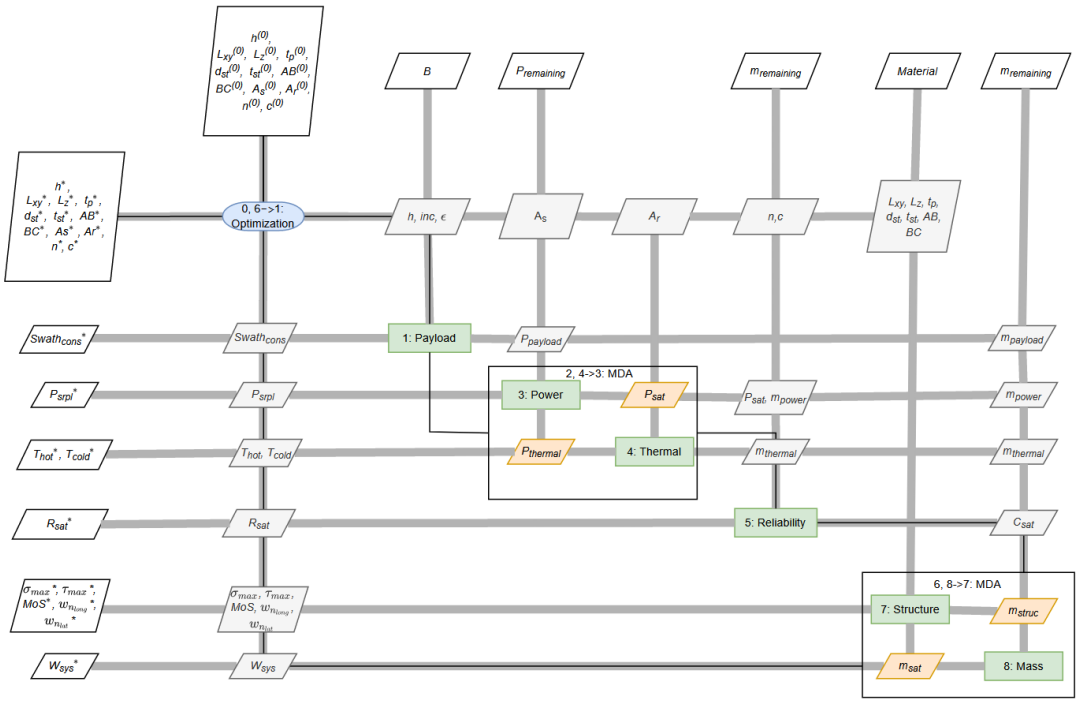

Figure 6.3: Extended Design Structure Matrix of Satellite RBMDO model in Multidisciplinary Feasible (MDF) architecture

6.3 Results and Discussion

Initially, the optimization problem is solved by using the Sequential Approach. As the first step in this approach, the MDO of the problem is performed. Then, the mass values calculated from MDO are frozen, and these values are used as constraints for RRAP. As a next step the reliability model is optimized to identify the optimal configuration that minimizes the overall cost and meets the target reliability requirements within the mass limit set by MDO. The reliability requirement for the satellite considered in this research is that the satellite shall have a reliability of at least 0.5 after 3.9 years (i.e. the sum of all three phases in PMS).

Next, the optimization problem is solved by employing the Simultaneous Approach and the problem is simultaneously optimized for mass and cost with constraints on reliability. Unlike, sequential approach, the correlation between the satellite design and its reliability is well established in the RBMDO problem giving additional freedom to adapt the design with respect to reliability and cost.

The results show apparent changes among the two approaches in the continuous subsystem variables. Similarly, the integer design variables obtained from the sequential approach also radically differ from the simultaneous approach.

6.3.1 Continuous Variables

The optimization results of the continuous variables in Sequential and Simultaneous Approaches are presented in MDO and RBMDO columns of the Table 6.4, respectively. The mass of the power ($m_{power}*$) and thermal ($m_{thermal}*$) subsystem is marginally higher for RBMDO compared to MDO. A slight increase in the mass of the structural subsystem, $m_{struc}*$

is seen in RBMDO to support the changes in the power and thermal subsystem. Therefore, the total mass of the satellite, $m_{sat}*$ is also higher in RBMDO compared to MDO.

Subsystem	Parameters	Unit	MDO	RBMDO
	$m_{sat}*$	kg	88.6	91.5
Payload	h	km	800	800
Structure	L_{xy}	m	0.531	0.537
	L_z	m	0.824	0.819
	t_p	m	0.001	0.001
	d_{st}	m	0.05	0.05
	t_{st}	m	0.0012	0.0012
	AB	-	0.25	0.25
	BC	-	0.25	0.25
	$m_{struc}*$	kg	9.1	9.2
Power	A_s	m	2.357	3.307
	$m_{power}*$	kg	11.0	13.7
Thermal	A_r	m	0.876	0.879
	$m_{thermal}*$	kg	2.8	2.9

*Resultant parameter from the optimization

Table 6.4: Resultant objective and continuous design variables for MDO and RBMDO

6.3.2 Integer variables

Table 6.5 presents the integer variables in Sequential and Simultaneous Approaches in RRAP and RBMDO columns, respectively. RRAP and RBMDO have chosen different element choice and number of elements to meet the same reliability requirement. Table 6.5 shows the cost factor comparison for every subsystem. The subsystem costs obtained using the Simultaneous Approach are less than the Sequential Approach.

The resultant masses of the power subsystem is 11 kg and that of thermal subsystems is 2.8 kg in the Sequential Approach. In RRAP, the elements are selected such that their

masses are less than 11 kg and 2.8 kg for power and thermal subsystem, respectively, while satisfying the reliability requirement. At the same time, RBMDO identified another set of slightly heavier elements that considerably reduced the overall cost. This however, violates the mass constraints of power and thermal subsystem set by MDO. As RBMDO simultaneously optimizes both models, it is able to modify the mass of power and thermal subsystem by varying the continuous design variables, to accommodate the heavy configuration. This causes a 3% increase in overall mass but reduces the overall cost by 7.5% as shown in Table 6.6. The result clearly proves the advantage of coupling the satellite and reliability model.

Subsystem	Elements	Element Count		Redundancy Type		Choice		Failure Rate		Unit mass(kg)		Unit Power(W)		Unit Cost Factor	
		RRAP	RBMDO	RRAP	RBMDO	RRAP	RBMDO	RRAP	RBMDO	RRAP	RBMDO	RRAP	RBMDO	RRAP	RBMDO
Attitude Determination and Control	RW	1	1	C	C	RW_C3	RW_C3	6.95E-07	6.95E-07	6	6	13	13	4600	4600
	ES	2	2	A	A	ES_C3	ES_C3	1.07E-05	1.07E-05	1.9	1.9	3.9	3.9	650	650
	StS	1	1	A	A	StS_C5	StS_C3	1.22E-05	9.24E-06	2	3	15	9	2900	2550
	IMU	1	1	C	C	IMU_C1	IMU_C3	2.73E-06	6.99E-06	5.6	3.3	32	36	7000	5300
Power	BAT	1	1	A	A	BAT_C4	BAT_C4	1.63E-07	1.63E-07	4.5	4.5	0	0	3200	3200
	SP	8	8	A	A	SP_C1	SP_C1	2.32E-05	2.32E-05	0.3	0.3	0	0	131	131
	PCU	2	2	A	A	PCU_C4	PCU_C1	1.06E-05	9.54E-06	1.2	1.9	2.8	2	1700	1100
	PDU	1	2	A	A	PDU_C2	PDU_C2	8.36E-06	8.36E-06	1.5	1.5	1.9	1.9	900	900
Telemetry, Telecommand and Ranging	RCR	1	1	A	A	RCR_C5	RCR_C5	7.23E-07	7.23E-07	3.8	3.8	13	13	3050	3050
	TSR	2	1	C	C	TSR_C4	TSR_C5	1.25E-05	4.78E-06	2.7	3.5	17	14	1450	1850
	ANT	2	1	C	C	ANT_C3	ANT_C2	1.03E-05	1.30E-06	0.6	1.3	2.6	3.5	1300	1700
Mechanism	DPY	1	1	C	C	DPY_C4	DPY_C5	2.47E-06	2.82E-06	2.3	3.9	13	11	6200	5800
	SADM	2	2	C	C	SADM_C1	SADM_C4	9.40E-06	1.40E-05	4.6	5.9	16	23	3200	3050
Thermal	RAD	1	1	C	C	RAD_C4	RAD_C2	2.08E-06	5.22E-06	2.5	2.9	47	48	2800	1950
Onboard Computer	CPU	1	1	C	C	CPU_C4	CPU_C4	8.83E-07	8.83E-07	0.9	0.9	2.9	2.9	17500	17500
	DSU	1	1	C	C	DSU_C2	DSU_C2	3.09E-06	3.09E-06	4.1	4.1	1.8	1.8	12100	12100

Table 6.5: Resultant integer design variables and resources for RRAP and RBMDO

Approach	Mass	Reliability	Cost Factor
Sequential	88.6	0.504	77900
Simultaneous	91.5	0.512	72050

Table 6.6: Comparison of results from Sequential and Simultaneous Approach

The mass of ADC, TT&R, Mechanism and OBC estimated based on design estimation relationships are added together and represented as $m_{remaining}$. This remaining mass is used as a mass constraint for the sum of elements selected for these subsystems. Although different choices and redundancy levels are selected for these subsystems in RRAP and RBMDO, their total mass remain constant.

6.4 Summary

Reliability Based Multidisciplinary Design Optimization (RBMDO) is intensely complex as it involves multiple disciplines with numerous interactions. Although highly crucial, it is challenging to estimate the reliability of a satellite system in early design stages. The developed reliability model was coupled with the satellite model and posed as a single optimization problem. This led to a Mixed Integer Nonlinear Programming (MINLP) problem formulation which is optimized using AMIEGO-MIMOS. The couplings between the disciplines were formulated as Multidisciplinary Feasible architecture (MDF).

The results showed the considerable impact of synergism between the two models, and an optimal design may not be achieved without leveraging the couplings between the two models. The Simultaneous Approach produced a better design choice than the Sequential counterpart. Even though the satellite's mass from the Simultaneous Approach is 3% heavier than the Sequential Approach, the overall cost factor in the Simultaneous Approach was 7.5% lower than the latter.

Design is not just what it looks like and feels like. Design is how it works.

Steve Jobs

7

DESIRA

The knowledge and experience accumulated from the previous chapters provide the basis for developing the DEcision Support system for Incorporating Risk/Reliability Assessments (DESIRA) for the early stages of the satellite design. Inputs from Chapter 3 are used for allocation of initial reliability using apportionment techniques that are discussed

in Section 4.1. Depending on the stage of the satellite design, reliability growth strategy can be considered either as a Redundancy Allocation Problem as discussed in Section 4.2 or as a Reliability-Redundancy Allocation problem as discussed in Section 4.3. Chapter 5 presents the mathematical formulation for Multidisciplinary Design Optimization (MDO) of the satellite system. The coupling between the Reliability and the Multidisciplinary Design Optimization is incorporated in Chapter 6. Some of the unique features of the DESIRA tool are listed below:

- Allocation of initial reliability to the subsystems.
- Development of optimal reliability growth strategy.
- Multidisciplinary Design Optimization of the satellite system.
- Reliability-Based Multidisciplinary Design Optimization of the satellite system.

A graphical user interface (GUI) is developed to support the first two features of DESIRA. This Chapter presents the design methodology, architecture of the DESIRA tool and demonstrates DESIRA's capabilities by applying it to a satellite system to provide a first reliability analysis of a complex satellite system in the early design phase.

7.1 Architecture Design

Typically, every satellite is unique, meaning only limited previous life data is available to assist its design. It is evident from the state of the art presented in Section 2.4 that most of the available tools are either based on expert opinion or statistical data. Allocation based on expert opinion could result in biased results based on their personal experiences. On the

other hand, translating the general statistical results to a unique design is not possible for a satellite system as a whole. A more realistic allocation during the early design stage is possible by combining the statistical data with expert opinion.

DESIRA offers this realistic allocation by combining the favourable traits from statistical data and expert opinion. The Reliability Allocation Module in DESIRA performs this task. The allocated reliability is then improved by the Reliability Mapping Module of the tool that utilizes the models developed in Chapter 4.2. The process flow of reliability allocation and reliability mapping features of the tool are explained in Section 7.2. The tool employs a graphical database management system, Neo4j[167], to manage data and model information required for reliability allocation, mapping and optimization. As a support tool for decision making, DESIRA helps system engineers to develop reliability requirements and optimal strategies for reliability growth.

7.1.1 Software Architecture

A model-view-controller design pattern is employed to decouple the user interface (view), model (data) and application logic (controller). The user interface is entirely developed using PyQt5. The controller connects with the user interface and graphical database to carry out the analysis by utilizing the developed reliability models. The functionality of DESIRA and its interaction with the user is presented with a use case diagram in Figure 7.1. Figure 7.2 is the activity diagram that shows the process flow of transforming the design inputs into decision aids.

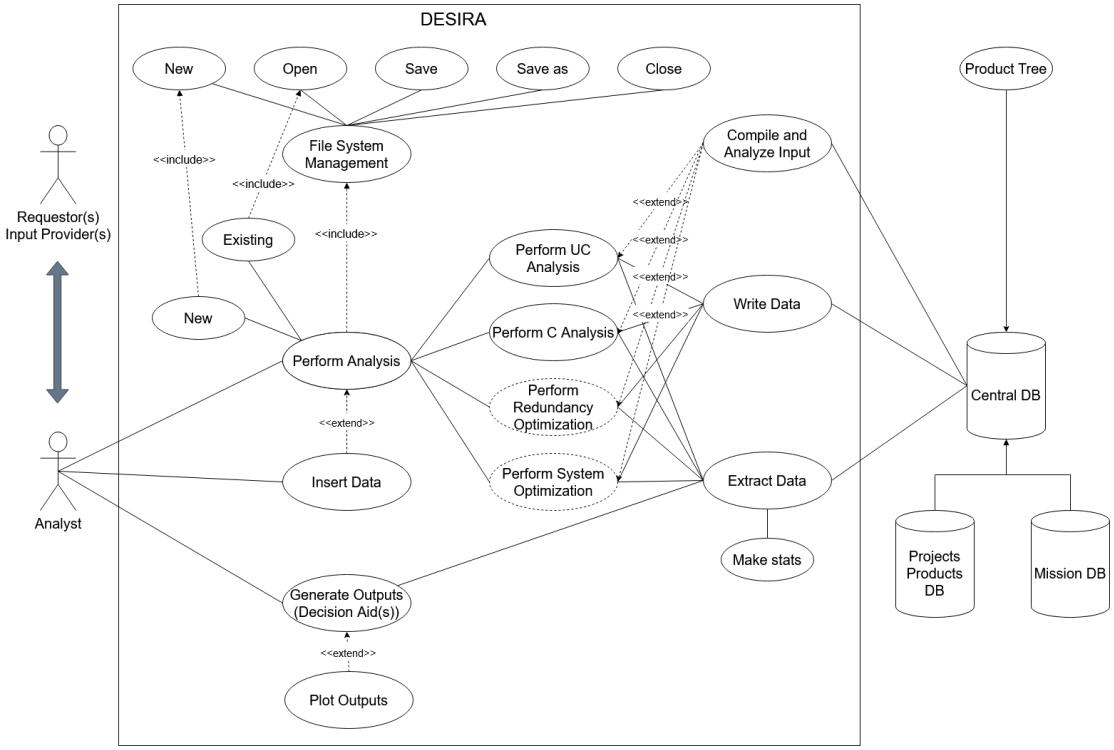

Figure 7.1: DESIRA Use Case Diagram

7.2 Application to Satellite Design

In this section, the features of reliability allocation module and reliability mapping module in DESIRA are illustrated. The satellite reliability requirement is 0.75 at the end of 4 years.

7.2.1 Reliability Allocation Module

The product tree of the satellite is required to start the reliability analysis. In the initial design stage, a detailed product tree is usually not available and the decomposition of the satellite into subsystems will suffice. As the design matures, the subsystem can be further de-

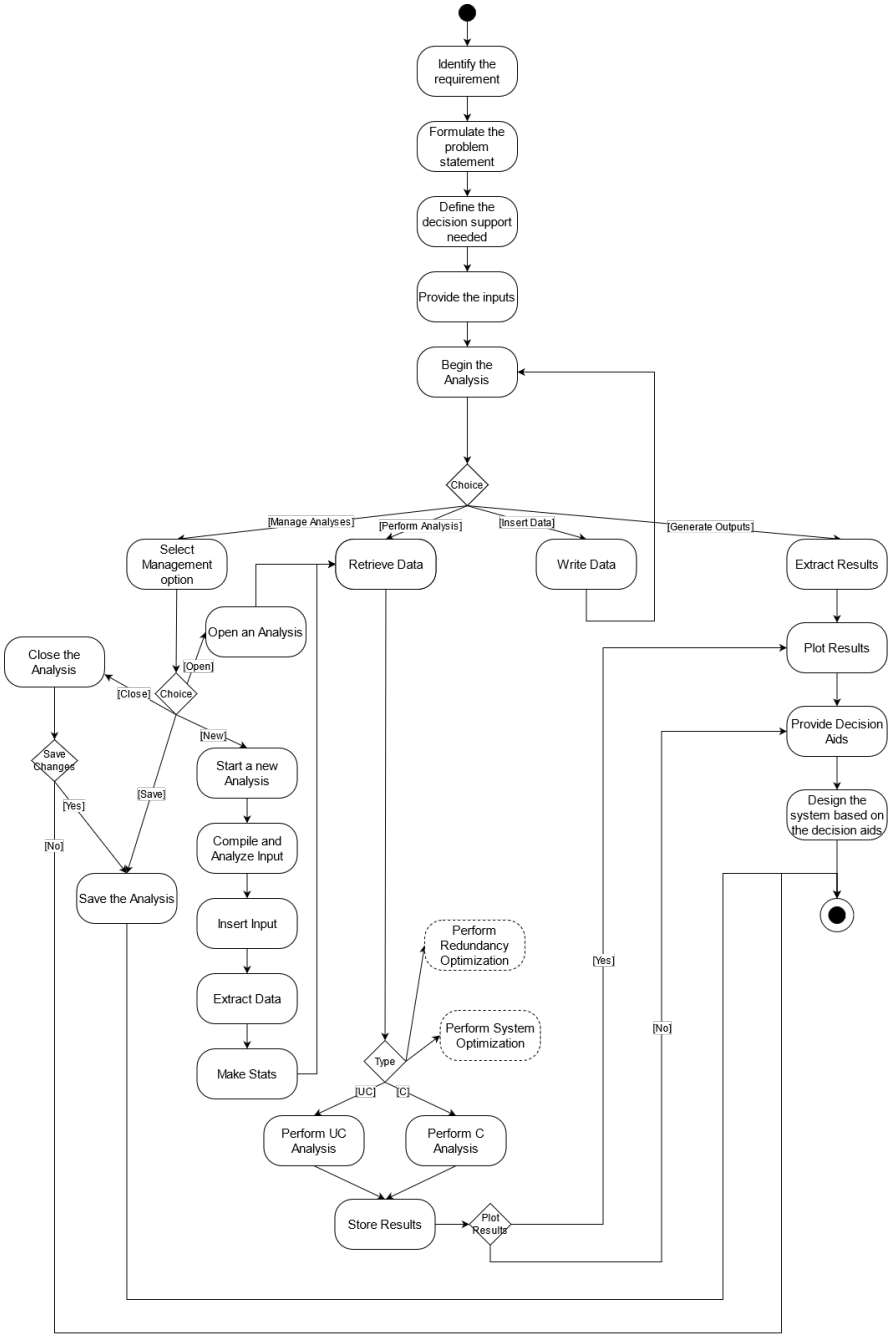

Figure 7.2: DESIRA Activity Diagram

composed into lower levels, and more detailed reliability analysis can be carried out. DESIRA accepts the product tree information in XML or CSV file types. A sample generic satellite product tree is given in the Listing 7.1. The product tree data is stored in the graph database in the form of graph as shown in Figure 7.3.

Listing 7.1: Satellite Generic Product Tree

```
<?xml version="1.0" encoding="utf-8" standalone="yes"?>
<Element>
  <Element level="1" name="Project" acronym="N/A" Id="0">
    <Element level="2" name="Space Segment(Satellite)" acronym="S/C" Id="0-">
      <Element level="3" name="Payload (P/L) Module/Assembly" acronym="P/L" Id="1-"></Element>
      <Element level="3" name="Platform (P/F) Module/Assembly (or Service Bus)" acronym="P/F" Id="2-">
        <Element level="4" name="On-Board Data Handling S/S" acronym="DAT" Id="21"></Element>
        <Element level="4" name="Electrical Power S/S" acronym="EPS" Id="22"></Element>
        <Element level="4" name="Communications S/S" acronym="COM" Id="23"></Element>
        <Element level="4" name="Harness S/S" acronym="HAR" Id="24"></Element>
        <Element level="4" name="Structure and Mechanisms S/S" acronym="STM" Id="25"></Element>
        <Element level="4" name="Thermal Control S/S" acronym="TCS" Id="26"></Element>
        <Element level="4" name="Attitude Determination and
```

```
            Control S/S" acronym="ADC" Id="27"></Element>
14          <Element level="4" name="Orbit Determination and Control
            (Propulsion) S/S" acronym="ODC" Id="28"></Element>
15        </Element>
16      </Element>
17    </Element>
18 </Element>
```

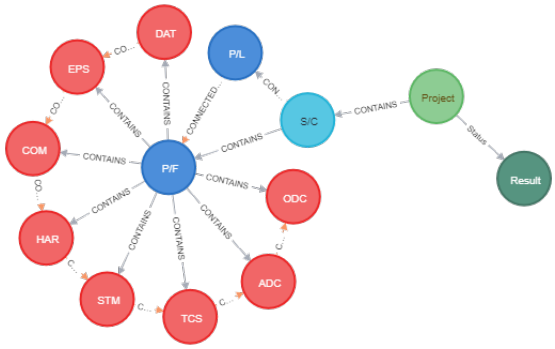

Figure 7.3: Product tree graph in the database

The next step is to obtain expert opinion on various satellite parameters using the template shown in Table 7.1. A detailed explanation of each column in the template is given in Chapter 4.1. There is no limit on the number of experts providing the inputs. However, the coefficient of variation for a particular parameter from different experts must not exceed 50%. Figure 7.4 presents the radar chart containing the variation in the user inputs. The green, red and blue lines in the plots represent lower, upper and average input values. In Figure 7.4, most of the subsystems overshoot this threshold and the inputs must be revised to advance to the next steps. Then, based on the expert opinion, weights are assigned to the individual elements using the apportionment techniques.

Table 7.1: Template for acquiring expert opinion

Subsystem	Complexity	SoA	Operating Time	Environment	Total Value	Failure Rate	No. of components	No. of Active components	No. of redundant components	No. of System Functions performed	No. of affected elements due to failure in this sublevel	Cost for improvement
DAT												
EPS												
COM												
TCS												
STM												
ADC												
ODC												
HAR												

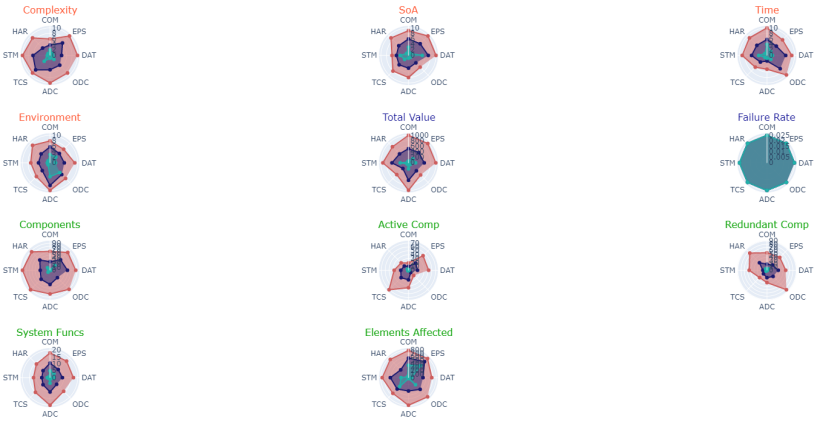

Figure 7.4: User input variation

Next, based on the mission, satellite type and orbit information, an appropriate statistical reliability category from the results presented in Chapter 3 is chosen for the satellite of interest. Then an initial reliability value for the satellite from the statistical reliability data is obtained as input for further steps. For the satellite considered in this study, the collective reliability of 0.648 obtained for small satellites at 4 years from Figure 3.1 is taken as the initial reliability. Then this initial reliability is allocated to the subsystems based on their previously calculated weights. Since different apportionment techniques are used to assign the weights of the subsystems, the obtained reliability is a range of values instead of a single value. Figure 7.5 shows the initial reliability and failure rate flow down to the subsystems of the considered satellite. The initial reliability is then used as a baseline to calculate the improvement need in

each subsystem to reach the target reliability. This step is crucial because it is generally challenging to obtain the initial reliability for the satellite under development. Satellite developers often know their required reliability but seldom know the reliability during the design phase. Hence, the baseline reliability estimated in DESIRA, provides an early understanding of the system and subsystem reliabilities.

Figure 7.5: Initial reliability flown down to each subsystem

After each allocation (top-down approach), a reliability validation is carried out using the Monte-Carlo simulation by propagating the reliability of the individual subsystems to the system level (bottom-up approach). The mean of the normal reliability distribution after the Monte-Carlo simulation represents the most probable system reliability. Figure 7.6 shows the resultant probability density function of the satellite by propagating the allocated reliability range values.

In the next step, the required target reliability is allocated to the subsystems based on the weights derived from expert opinion. The target reliability of the considered satellite is 0.75, and its allocation is shown in Figure 7.7. Similar to initial reliability, the target reliability is

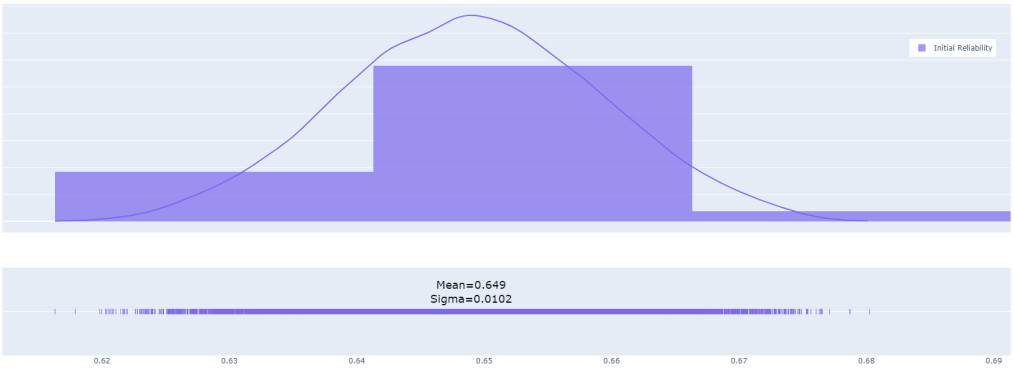

Figure 7.6: Propagated reliability using Monte-Carlo simulations

also a range of values.

Figure 7.7: Target reliability flown down to each subsystem

In the next step, an optimization is carried out to find the optimal reliability for each subsystem to meet the target system reliability. In addition to the initial and target reliability ranges, the cost index of improvement (obtained from experts) for every subsystem is required

as inputs for the optimization. Then the cost for improvement can be quantified in terms of reliability with the cost function given in Equation (7.1)[192].

$$C_i(R_i) = e^{(1-f)\frac{R_i - R_{i.min}}{R_{i.max} - R_i}} \tag{7.1}$$

where C_i is the cost function, f is the cost index for improving element reliability relative to other elements, $R_{i.min}$ is the minimum reliability and $R_{i.max}$ is the maximum reliability of i^{th} element from the allocation. The goal of this optimization is to reach the target reliability (R_{tgt}) with a minimum cost of improvement. The mathematical formulation of this reliability optimization is given below.

$$\begin{aligned} \min \quad & \sum_{i=1}^{n} C_i(R_i) \\ \text{s.t.} \quad & R_{sys} \geq R_{tgt} \\ & R_{i.min} \leq R_i \leq R_{i.max}, i = 1, 2, \ldots, n \end{aligned} \tag{7.2}$$

After following the above steps, the resultant reliabilities of each subsystem corresponding to the minimal cost of improvement are obtained and are shown in the Figure 7.8. Since DESIRA combined expert opinion and statistical data to compute the reliabilities, realistic reliability requirements for subsystems are obtained.

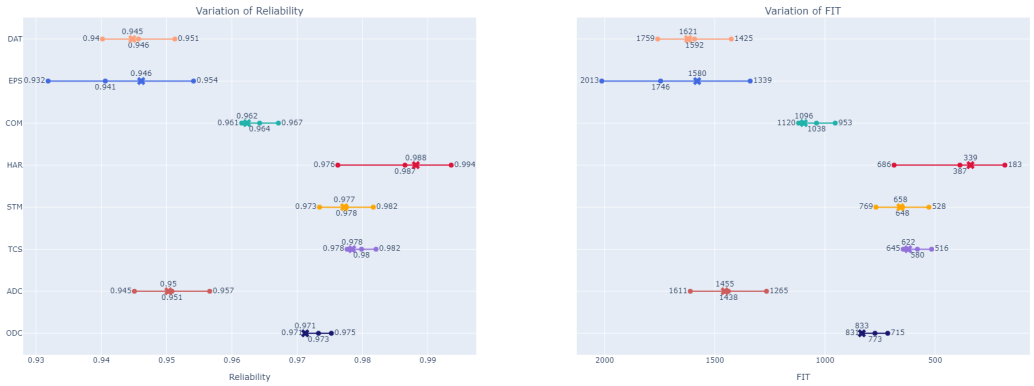

Figure 7.8: Optimal reliability (marked with 'x') flown down to each subsystem

7.2.2 Reliability Mapping Module

The next step is to determine the redundancies and/or choices for the lower level elements such that subsystem reliability requirements set at the previous step are met. DESIRA's reliability mapping module examines all possible combinations and lists the results that satisfy the target. This is computationally expensive and is recommended to be used for smaller systems or an individual subsystem. For instance, this model is used to find the optimum number of redundancies of elements in Power subsystem. The different elements and their reliability, weight, cost, power, maximum allowed redundancies and redundancy type are given in Table 7.2. DESIRA examines all the different reliability combinations and the results can be plotted between any two parameters. The plot between Reliability and Cost is shown in figure 7.9. The redundancy combination that gives the highest reliability value is selected. For an entire satellite with many elements, the developed RAP and RRAP models should be used to minimize the resources required to reach the target reliability. In this case, the required inputs are directly taken from the product database.

Acronym	FIT	Weight	Cost	Power	Max Redundancy	Redundancy Type	Reality Factors
SA	100	0.92	222	2.5	1	C,H	1
PDU	540	1.8	400		4	C,H	1
BAT	440	1.5	308	18.9	4	C,H	1

Table 7.2: Inputs Required for Reliability Mapping

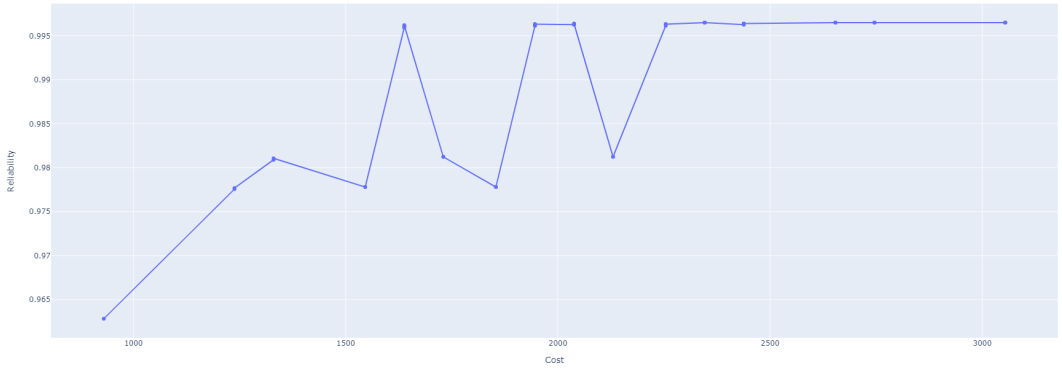

Figure 7.9: Reliability vs Cost for different levels of redundancies and redundancy types

7.2.3 Additional features

As the satellite design matures, MDO and RBDMO shall be performed to get a more detailed design. The graphical user interface (GUI) of DESIRA is yet to support the developed MDO and RBMDO. The inputs and outputs of the optimization are stored in the same database to ensure continuity and enable potential integration in the future.

7.3 Summary

In this Chapter the software architecture of DESIRA is described and its application was illustrated with a simple use case. DESIRA can be employed by a satellite developer in the early design phase when the available data is scarce. It can be adapted for every increment of

the design progress. The novelty of DESIRA is substantiated by its ability to produce realistic results starting from the early design phase and its continued support as the design matures. A few screenshots of the graphical user interface of DESIRA are shown in Appendix C.

It is difficult to say what is impossible, for the dream of yesterday is the hope of today and reality of tomorrow.

Robert Goddard

8

Discussion and Conclusion

The motivation of this thesis was to improve the design of microsatellites by incorporating risk/reliability assessments during the conceptual design phase. To that goal, a decision support system, DESIRA, was developed that enables designing for reliability and informed decision making during the early design stage. All the

identified research questions are answered through out this thesis. The important findings and contributions are summarized below.

8.1 Research Questions Revisited

Research Question 1: How to estimate the reliability of satellite during the initial design phase?

Chapter 3 answered this question. Reliability is an important aspect of small satellite performance, and the reliability analysis must be performed as early as the preliminary design phase. Unfortunately, reliability information is sparse or not available during this phase. Statistics-based approaches that used empirical failure data and estimated the collective on-orbit reliability of small satellites are outdated and inadequate for contemporary small-satellite design. This research carried out a survival analysis of around 2000 small satellites weighing less than 500kg and extended the existing literature. The results helped to understand the reliability trends in small satellites and crucial factors contributing to the satellite's failure. Additionally, reliability was analyzed for small satellites based on mission, developer type, launch date, and orbit inclination. These results provided baseline reliability of the satellite system for their propagation to lower levels using various apportionment methods. Next, with these initial reliability estimates, it is of interest to answer the following question:

Research Question 2: How to improve the reliability of satellite while minimizing the resources?

At first, the baseline reliability and required reliability for the satellite design were taken as the initial and the target reliabilities, respectively. Then, the problem was formulated with

an objective to move the reliability from the initial to the target. Later, the Redundancy Allocation Problem (RAP) for the satellite design was modelled that identified the ideal number of element redundancies required to reach the reliability target. Although this method did not consider the element choices, it provided an initial estimate of the resources required to satisfy the reliability requirements. Next, the Reliability-Redundancy Allocation Problem (RRAP) for the satellite design was applied that determined the choice of elements and the redundancies required to improve the reliability with minimum resources. Additionally, when the satellite was modelled as a Phased Mission System (PMS), the mission-critical elements were prioritized to reach the target reliability with minimum resources. The methods presented in Chapter 4 answered this question in more detail.

Research Question 3**:** How to identify the best satellite design during the early design stage?

The satellite subsystems and their interactions were modelled in OpenMDAO. The interactions between the subsystems were formulated in three different monolithic architectures, namely Multidisciplinary Feasible (MDF), Individual Discipline Feasible (IDF), and Simultaneous Analysis and Design (SAND). Then, the Multidisciplinary Design Optimization (MDO) was performed using a gradient-based solver for each architecture to identify the best design as presented in Chapter 5.

Research Question 4**:** How to incorporate reliability in the early satellite design?

The reliability was incorporated in the early satellite design using two design approaches, namely Sequential Approach and Simultaneous Approach presented in Chapter 6. The approaches coupled the reliability model in Chapter 4 with the satellite model in Chapter 5 in

different ways. In the Sequential Approach, the satellite model was optimized first, followed by the reliability model. The results from the satellite model were used as constraints in the reliability model to produce a feasible design that satisfied the reliability requirements. On the other hand, the Simultaneous Approach simultaneously optimized the satellite model and the reliability model. It was inferred that the Simultaneous Approach produced a better design choice than the Sequential counterpart.

The models and approaches developed to answer the research questions constituted the building block of the decision support system, DESIRA, that incorporates risk/reliability assessments in the early satellite design, fulfilling the primary goal of this research. A graphical user interface was developed for ease of operation and supported few features provided by DESIRA. The architecture of DESIRA and the various features offered are discussed in Chapter 7.

8.2 Summary of Unique Contributions

The broad scope of this thesis examined various fields such as Satellite System Design, Reliability Analysis, Statistics, Software Engineering and Multidisciplinary Design Optimization. The work carried out in this research produced significant contributions in several areas and are summarized below.

1. The results from the statistical analysis of empirical data from the last three decades revealed the on-orbit reliability trends to improve the design of future satellites.

2. The satellite was modelled as a Phased Mission System (PMS), which enabled priori-

tizing the elements that substantially impacted the reliability.

3. A Distributed Space System (DSS) was modelled and optimized with different MDO implementations.

4. The intensely complex Reliability-Based Multidisciplinary Design Optimization (RB-MDO) of satellites with over 100 design variables was performed.

5. The proposed methods provided innovative approaches to incorporate reliability analysis from the initial stages of satellite design.

8.3 Future Work

Several interesting areas and directions of future research are identified to strengthen the design approaches proposed in this research.

1. DESIRA lays a solid foundation to design satellites in the conceptual design phase and is scalable to suit the Detailed design phase. Therefore, the next step is to perform Multidisciplinary Design Optimization (MDO) with high-fidelity discipline models to enable the Detailed design features in DESIRA. For instance, FEM solvers such as TACS[193] that provides gradients can be wrapped into DESIRA to perform a more detailed structural analysis.

2. The deterministic reliability values currently used in Reliability-Based Multidisciplinary Design Optimization (RBMDO) shall be replaced with probabilistic reliability models to improve the accuracy of estimated reliabilities. Combining probabilistic reliability

models with high-fidelity discipline models will significantly increase the computational cost but has the highest potential to provide valuable results.

3. The satellite design process in DESIRA shall be enhanced by combining the advantages of Model-Based Systems Engineering (MBSE) with Multidisciplinary Design Optimization (MDO). Integrating these two shall enable DESIRA in extensive evaluations of different system configurations while efficiently managing the complexities.

References

[1] National Research Council. *Reliability Growth: Enhancing Defense System Reliability*. The National Academies Press, Washington, DC, 2015.

[2] Ajit Kumar Verma, Srividya Ajit, Durga Rao Karanki, et al. *Reliability and safety engineering*, volume 43. Springer, 2010.

[3] Wiley J Larson and James Richard Wertz. Space mission analysis and design. Technical report, Torrance, CA (United States); Microcosm, Inc., 1992.

[4] Jean-Francois Castet and Joseph H Saleh. Satellite reliability: statistical data analysis and modeling. *Journal of Spacecraft and Rockets*, 46(5):1065–1076, 2009.

[5] Jean-Francois Castet and Joseph H Saleh. Satellite and satellite subsystems reliability: Statistical data analysis and modeling. *Reliability Engineering & System Safety*, 94(11):1718–1728, 2009.

[6] Jean-Francois Castet and Joseph H Saleh. Beyond reliability, multi-state failure analysis of satellite subsystems: a statistical approach. *Reliability Engineering & System Safety*, 95(4):311–322, 2010.

[7] Jean-Francois Castet and Joseph H Saleh. Single versus mixture weibull distributions for nonparametric satellite reliability. *Reliability Engineering & System Safety*, 95(3):295–300, 2010.

[8] Gregory F Dubos, Jean-Francois Castet, and Joseph H Saleh. Statistical reliability analysis of satellites by mass category: Does spacecraft size matter? *Acta Astronautica*, 67(5-6):584–595, 2010.

[9] Jian Guo, Liora Monas, and Eberhard Gill. Statistical analysis and modelling of small satellite reliability. *Acta Astronautica*, 98:97–110, 2014.

[10] Teri Hamlin, Bruce Reistlea, and Michael Stewarta. Large satellite bus reliability. *Probabilistic Safety Assessment and Management PSAM 14*, 2018.

[11] Jose A Cruz. Applicability and limitations of reliability allocation methods. 2016.

[12] *Electronic Reliability Design Handbook, MIL-HDBK-338B*. US Department of Defense, 1998.

[13] Dimitri Kececioglu. *Reliability engineering handbook*, volume 2. DEStech Publications, Inc, 2002.

[14] Fabio De Felice, D Falcone, A Silvestri, and G Di Bona. Proposal of a new reliability allocation methodology: the integrated factors method. *International Journal of Operations and Quantitative Management*, 16(1):67–85, 2010.

[15] Yiqiang Wang, Richard CM Yam, Ming J Zuo, and Peter Tse. A comprehensive reliability allocation method for design of cnc lathes. *Reliability Engineering & System Safety*, 72(3):247–252, 2001.

[16] Peng Li, Chuanri Li, and Tao Li. A new reliability allocation method based on fuzzy numbers. *International Journal of Medical and Health Sciences*, 9(5):277–281, 2015.

[17] Frank A Tillman, Ching-Lai Hwang, and Way Kuo. Optimization techniques for system reliability with redundancy□a review. *IEEE Transactions on Reliability*, 26(3):148–155, 1977.

[18] Joon-Eon Yang, Mee-Jung Hwang, Tae-Yong Sung, and Youngho Jin. Application of genetic algorithm for reliability allocation in nuclear power plants. *Reliability Engineering & System Safety*, 65(3):229–238, 1999.

[19] AK Rajeevan, PV Shouri, and Usha Nair. Markov modeling and reliability allocation in wind turbine for availability enhancement. *Life Cycle Reliability and Safety Engineering*, 7(3):147–157, 2018.

[20] Yongchun Miao, Rongxue Kang, and Xuefeng Chen. Research on reliability modeling, allocation and prediction of chemical production system. In *MATEC Web of Conferences*, volume 220, page 02006. EDP Sciences, 2018.

[21] Maw-Sheng Chern. On the computational complexity of reliability redundancy allocation in a series system. *Operations research letters*, 11(5):309–315, 1992.

[22] Way Kuo and Rui Wan. Recent advances in optimal reliability allocation. *IEEE Transactions on Systems, Man, and Cybernetics-Part A: Systems and Humans*, 37(2):143–156, 2007.

[23] Way Kuo and V Rajendra Prasad. An annotated overview of system-reliability optimization. *IEEE Transactions on reliability*, 49(2):176–187, 2000.

[24] KB Misra. On optimal reliability design: a review. *IFAC Proceedings Volumes*, 8(1):27–36, 1975.

[25] Sadan Kulturel-Konak, Alice E Smith, and David W Coit. Efficiently solving the redundancy allocation problem using tabu search. *IIE transactions*, 35(6):515–526, 2003.

[26] Yun-Chia Liang and Alice E Smith. An ant colony optimization algorithm for the redundancy allocation problem (rap). *IEEE Transactions on reliability*, 53(3):417–423, 2004.

[27] Harish Garg and SP Sharma. Multi-objective reliability-redundancy allocation problem using particle swarm optimization. *Computers & Industrial Engineering*, 64(1):247–255, 2013.

[28] Abdullah Konak, David W Coit, and Alice E Smith. Multi-objective optimization using genetic algorithms: A tutorial. *Reliability Engineering & System Safety*, 91(9):992–1007, 2006.

[29] David W Coit and Alice E Smith. Reliability optimization of series-parallel systems using a genetic algorithm. *IEEE Transactions on reliability*, 45(2):254–260, 1996.

[30] Isis Didier Lins and Enrique López Droguett. Redundancy allocation problems considering systems with imperfect repairs using multi-objective genetic algorithms and discrete event simulation. *Simulation Modelling Practice and Theory*, 19(1):362–381, 2011.

[31] P Giuggioli Busacca, Marzio Marseguerra, and Enrico Zio. Multiobjective optimization by genetic algorithms: application to safety systems. *Reliability Engineering & System Safety*, 72(1):59–74, 2001.

[32] David W Coit and Jia Chen Liu. System reliability optimization with k-out-of-n subsystems. *International Journal of Reliability, Quality and Safety Engineering*, 7(02):129–142, 2000.

[33] David W Coit. Cold-standby redundancy optimization for nonrepairable systems. *Iie Transactions*, 33(6):471–478, 2001.

[34] David W Coit. Maximization of system reliability with a choice of redundancy strategies. *IIE transactions*, 35(6):535–543, 2003.

[35] Liudong Xing and Joanne Bechta Dugan. Analysis of generalized phased-mission system reliability, performance, and sensitivity. *IEEE Transactions on Reliability*, 51(2):199–211, 2002.

[36] Arun K Somani and Kishor S Trivedi. Phased-mission system analysis using boolean algebraic methods. In *Proceedings of the 1994 ACM SIGMETRICS conference on Measurement and modeling of computer systems*, pages 98–107, 1994.

[37] Xinyu Zang, Nairong Sun, and Kishor S Trivedi. A bdd-based algorithm for reliability analysis of phased-mission systems. *IEEE Transactions on Reliability*, 48(1):50–60, 1999.

[38] Mansoor Alam and Ubaid M Al-Saggaf. Quantitative reliability evaluation of repairable phased-mission systems using markov approach. *IEEE Transactions on Reliability*, 35(5):498–503, 1986.

[39] Yong Ou and Joanne Bechta Dugan. Modular solution of dynamic multi-phase systems. *IEEE Transactions on Reliability*, 53(4):499–508, 2004.

[40] Yuanshun Dai, Gregory Levitin, and Liudong Xing. Structure optimization of nonrepairable phased mission systems. *IEEE Transactions on Systems, Man, and Cybernetics: Systems*, 44(1):121–129, 2013.

[41] Xiang-Yu Li, Yan-Feng Li, and Hong-Zhong Huang. Redundancy allocation problem of phased-mission system with non-exponential components and mixed redundancy strategy. *Reliability Engineering & System Safety*, page 106903, 2020.

[42] Mehmet Nefes, Selman Demirel, Hasan H Ertok, and Cenk Sen. Reliability and cost focused optimization approach for a communication satellite payload redundancy allocation problem. *International Journal of Electronics and Communication Engineering*, 12(5):361–366, 2018.

[43] A Boudjemai, MH Bouanane, L Merad, and AM Si Mohammed. Small satellite structural optimisation using genetic algorithm approach. In *2007 3rd International Conference on Recent Advances in Space Technologies*, pages 398–406. IEEE, 2007.

[44] Ali Ravanbakhsh and Sebastian Franchini. Multiobjective optimization applied to structural sizing of low cost university-class microsatellite projects. *Acta Astronautica*, 79:212–220, 2012.

[45] Roberto L Galski, Fabiano L De Sousa, Fernando M Ramos, and Issamu Muraoka. Spacecraft thermal design with the generalized extremal optimization algorithm. *Inverse Problems in Science and Engineering*, 15(1):61–75, 2007.

[46] Saurabh Jain and Dan Simon. Genetic algorithm based charge optimization of lithium-ion batteries in small satellites. 2005.

[47] David J Richie, Vaios J Lappas, and Phil L Palmer. Sizing/optimization of a small satellite energy storage and attitude control system. *Journal of Spacecraft and Rockets*, 44(4):940–952, 2007.

[48] Lucien A Schmit. Structural design by systematic synthesis. In *Proceedings of the Second National Conference on Electronic Computation, ASCE, Sept., 1960*, 1960.

[49] Lucien A Schmit. Structural synthesis-its genesis and development. *AIAA Journal*, 19(10):1249–1263, 1981.

[50] LA Schmit. Structural synthesis: precursor and catalyst. 1984.

[51] Raphael T Haftka. Automated procedure for design of wing structures to satisfy strength and flutter requirements. *Work*, 50:8592, 1973.

[52] Raphael T Haftka. Optimization of flexible wing structures subject to strength and induced drag constraints. *AIAA Journal*, 15(8):1101–1106, 1977.

[53] Raphael T Haftka and Charles P Shore. Approximation methods for combined thermal/structural design. *NASA Technical Paper*, 1428, 1979.

[54] Ilan Kroo, Steve Altus, Robert Braun, Peter Gage, and Ian Sobieski. Multidisciplinary optimization methods for aircraft preliminary design. In *5th symposium on multidisciplinary analysis and optimization*, page 4325, 1994.

[55] Ian Sobieski and Ilan Kroo. Aircraft design using collaborative optimization. In *34th Aerospace Sciences Meeting and Exhibit*, page 715, 1996.

[56] Ravindra V Tappeta, Somanath Nagendra, and John E Renaud. A multidisciplinary design optimization approach for high temperature aircraft engine components. *Structural optimization*, 18(2-3):134–145, 1999.

[57] Ryan P Henderson, Joaquim RRA Martins, and Ruben E Perez. Aircraft conceptual design for optimal environmental performance. *The Aeronautical Journal*, 116(1175):1–22, 2012.

[58] Kazuhisa Chiba, Shigeru Obayashi, Kazuhiro Nakahashi, and Hiroyuki Morino. High-fidelity multidisciplinary design optimization of aerostructural wing shape for regional jet. In *23rd AIAA Applied Aerodynamics Conference*, page 5080, 2005.

[59] Kazuhisa Chiba, Akira Oyama, Shigeru Obayashi, Kazuhiro Nakahashi, and Hiroyuki Morino. Multidisciplinary design optimization and data mining for transonic regional-jet wing. *Journal of Aircraft*, 44(4):1100–1112, 2007.

[60] Brian Douglas Roth. *Aircraft family design using enhanced collaborative optimization*. Stanford University, 2008.

[61] Nicolas Bons and Joaquim RRA Martins. Aerostructural wing design exploration with multidisciplinary design optimization. In *AIAA Scitech 2020 Forum*, page 0544, 2020.

[62] Alessandro Sgueglia, Peter Schmollgruber, Nathalie Bartoli, Emmanuel Benard, Joseph Morlier, John Jasa, Joaquim RRA Martins, John T Hwang, and Justin S Gray. Multidisciplinary design optimization framework with coupled derivative computation for hybrid aircraft. *Journal of Aircraft*, 57(4):715–729, 2020.

[63] Charles D McAllister and Timothy W Simpson. Multidisciplinary robust design optimization of an internal combustion engine. *J. Mech. Des.*, 125(1):124–130, 2003.

[64] Philipp Geyer. Component-oriented decomposition for multidisciplinary design optimization in building design. *Advanced Engineering Informatics*, 23(1):12–31, 2009.

[65] Fan Yang and Dino Bouchlaghem. Genetic algorithm-based multiobjective optimization for building design. *Architectural Engineering and Design Management*, 6(1):68–82, 2010.

[66] Yuping He and John Mcphee. Multidisciplinary optimization of multibody systems with application to the design of rail vehicles. *Multibody System Dynamics*, 14(2):111–135, 2005.

[67] Junchen Yan, Osvaldo A Broesicke, Xin Tong, Dong Wang, Duo Li, and John C Crittenden. Multidisciplinary design optimization of distributed energy generation systems: The trade-offs between life cycle environmental and economic impacts. *Applied Energy*, 284:116197, 2021.

[68] Christian Pavese, Carlo Tibaldi, Frederik Zahle, and Taeseong Kim. Aeroelastic multidisciplinary design optimization of a swept wind turbine blade. *Wind Energy*, 20(12):1941–1953, 2017.

[69] Debiao Meng, Miao Liu, Shunqi Yang, Hua Zhang, and Ran Ding. A fluid–structure analysis approach and its application in the uncertainty-based multidisciplinary design and optimization for blades. *Advances in Mechanical Engineering*, 10(6):1687814018783410, 2018.

[70] BR Miao, YX Luo, QM Peng, YZ Qiu, H Chen, and ZK Yang. Multidisciplinary design optimization of lightweight carbody for fatigue assessment. *Materials & design*, 194:108910, 2020.

[71] Xiaobang Wang, Mao Li, Yuanzhi Liu, Wei Sun, Xueguan Song, and Jie Zhang. Surrogate based multidisciplinary design optimization of lithium-ion battery thermal management system in electric vehicles. *Structural and Multidisciplinary Optimization*, 56(6):1555–1570, 2017.

[72] Michael Kokkolaras, L Louca, G Delagrammatikas, N Michelena, Z Filipi, P Papalambros, J Stein, and D Assanis. Simulation-based optimal design of heavy trucks by model-based decomposition: An extensive analytical target cascading case study. *International Journal of Heavy Vehicle Systems*, 11(3-4):403–433, 2004.

[73] Majid Hosseini, Mehran Nosratollahi, and Hossein Sadati. Multidisciplinary design optimization of uav under uncertainty. *Journal of Aerospace Technology and Management*, 9:169–178, 2017.

[74] Maria Luiza Cassão Gatelli, Carlos Eduardo de Souza, and Marcos Daniel de Freitas Awruch. A study for a mdo process applied to conceptual design of a remotely piloted aircraft. In *FT2019. Proceedings of the 10th Aerospace Technology Congress, October 8-9, 2019, Stockholm, Sweden*, number 162, pages 45–55. Linköping University Electronic Press, 2019.

[75] Loic Brevault, Mathieu Balesdent, and Ali Hebbal. Multi-objective multidisciplinary design optimization approach for partially reusable launch vehicle design. *Journal of Spacecraft and Rockets*, 57(2):373–390, 2020.

[76] Kai Dresia, Simon Jentzsch, Günther Waxenegger-Wilfing, Robson Dos Santos Hahn, Jan Deeken, Michael Oschwald, and Fabio Mota. Multidisciplinary design optimization of reusable launch vehicles for different propellants and objectives. *Journal of Spacecraft and Rockets*, pages 1–13, 2021.

[77] John T Hwang, Dae Young Lee, James W Cutler, and Joaquim RRA Martins. Large-scale multidisciplinary optimization of a small satellite's design and operation. *Journal of Spacecraft and Rockets*, 51(5):1648–1663, 2014.

[78] David A Barnhart, Tatiana Kichkaylo, and Lucy Hoag. Spidr: Integrated systems engineering design-to-simulation software for satellite build. In *Conference on Systems Engineering Research*, 2009.

[79] Todd Mosher. Spacecraft design using a genetic algorithm optimization approach. In *1998 IEEE Aerospace Conference Proceedings (Cat. No. 98TH8339)*, volume 3, pages 123–134. IEEE, 1998.

[80] A Jafarsalehi, P Mohammad Zadeh, and M Mirshams. Collaborative optimization of remote sensing small satellite mission using genetic algorithms. *Transactions of Mechanical Engineering*, 36(M2):117, 2012.

[81] Todd Mosher. Applicability of selected multidisciplinary design optimization methods to conceptual spacecraft design. In *6th Symposium on Multidisciplinary Analysis and Optimization*, page 4052, 1996.

[82] E Riddle Taylor. Evaluation of multidisciplinary design optimization techniques as applied to spacecraft design. In *2000 IEEE Aerospace Conference. Proceedings (Cat. No. 00TH8484)*, volume 1, pages 371–384. IEEE, 2000.

[83] Wenrui Wu, Hai Huang, Shenyan Chen, and Beibei Wu. Satellite multidisciplinary design optimization with a high-fidelity model. *Journal of Spacecraft and Rockets*, 50(2):463–466, 2013.

[84] Alex S Fukunaga, Steve Chien, Darren Mutz, Robert L Sherwood, and Andre D Stechert. Automating the process of optimization in spacecraft design. In *1997 IEEE Aerospace Conference*, volume 4, pages 411–427. IEEE, 1997.

[85] Julia George, John Peterson, and Samuel Southard. Multidisciplinary integrated design assistant for spacecraft (midas). In *36th Structures, Structural Dynamics and Materials Conference*, page 1372, 1995.

[86] Melvin Ferebee, Jr, Patrick Troutman, Donald Monell, Patrick Troutman, Donald Monell, and Melvin Ferebee, Jr. Satellite systems design/simulation environment-a systems approach to pre-phase a design. In *35th Aerospace Sciences Meeting and Exhibit*, page 231, 1997.

[87] M Wilke, O Quirmbach, M Schiffner, and E Igenbergs. Mussat–a tool for satellite design in concept design centers. In *Proceedings of the 2nd European Systems Engineering Conference*. Citeseer, 2000.

[88] Jian Guo, Zheng You, and Dahai Ren. A distributed multidisciplinary design optimazation architecture for spacecraft design. In *9th AIAA/ISSMO Symposium on Multidisciplinary Analysis and Optimization*, page 5481, 2002.

[89] Yong Zhao, Xiaoqian Chen, and Zhenguo Wang. Side: A tool for integrated multidisciplinary design optimization of spacecraft. In *11th AIAA/ISSMO multidisciplinary analysis and optimization conference*, page 7119, 2006.

[90] Renhe Shi, Li Liu, Teng Long, Yufei Wu, and G Gary Wang. Multidisciplinary modeling and surrogate assisted optimization for satellite constellation systems. *Structural and Multidisciplinary Optimization*, 58(5):2173–2188, 2018.

[91] Brian W Chell, Steven Hoffenson, and Mark R Blackburn. A comparison of multidisciplinary design optimization architectures with an aircraft case study. In *AIAA Scitech 2019 Forum*, page 0700, 2019.

[92] Joaquim RRA Martins and Andrew B Lambe. Multidisciplinary design optimization: a survey of architectures. *AIAA journal*, 51(9):2049–2075, 2013.

[93] Nichols F Brown and John R Olds. Evaluation of multidisciplinary optimization techniques applied to a reusable launch vehicle. *Journal of Spacecraft and Rockets*, 43(6):1289–1300, 2006.

[94] Justin Gray, Kenneth T Moore, Tristan A Hearn, and Bret A Naylor. Standard platform for benchmarking multidisciplinary design analysis and optimization architectures. *AIAA journal*, 51(10):2380–2394, 2013.

[95] KF Hulme and CL Bloebaum. A simulation-based comparison of multidisciplinary design optimization solution strategies using cascade. *Structural and Multidisciplinary Optimization*, 19(1):17–35, 2000.

[96] Srinivas Kodiyalam. Evaluation of methods for multidisciplinary design optimization, phase 1. *NASA CR-1998-208716*, 1998.

[97] Srinivas Kodiyalam, Charles Yuan, and Jaroslaw Sobieski. Evaluation of methods for multidisciplinary design optimization, part 2. *NASA CR-2000-210313*, 2000.

[98] Ruben Perez, Hugh Liu, and Kamran Behdinan. Evaluation of multidisciplinary optimization approaches for aircraft conceptual design. In *10th AIAA/ISSMO multidisciplinary analysis and optimization conference*, page 4537, 2004.

[99] Nathan P Tedford and Joaquim RRA Martins. Benchmarking multidisciplinary design optimization algorithms. *Optimization and Engineering*, 11(1):159–183, 2010.

[100] Sang-Il Yi, Jung-Kyu Shin, and GJ Park. Comparison of mdo methods with mathematical examples. *Structural and Multidisciplinary Optimization*, 35(5):391–402, 2008.

[101] Christopher Marriage and Joaquim Martins. Reconfigurable semi-analytic sensitivity methods and mdo architectures within the pimdo framework. In *12th AIAA/ISSMO Multidisciplinary Analysis and Optimization Conference*, page 5956, 2008.

[102] Anukal Chiralaksanakul and Sankaran Mahadevan. First-order approximation methods in reliability-based design optimization. 2005.

[103] I Enevoldsen and John Dalsgaard Sørensen. Reliability-based optimization in structural engineering. *Structural safety*, 15(3):169–196, 1994.

[104] Markus Gasser and Gerhart Iwo Schuëller. Reliability-based optimization of structural systems. *Mathematical Methods of Operations Research*, 46(3):287–307, 1997.

[105] Manolis Papadrakakis and Nikos D Lagaros. Reliability-based structural optimization using neural networks and monte carlo simulation. *Computer methods in applied mechanics and engineering*, 191(32):3491–3507, 2002.

[106] JO Royset, A Der Kiureghian, and E Polak. Reliability-based optimal design of series structural systems. *Journal of Engineering Mechanics*, 127(6):607–614, 2001.

[107] Li Weiji and Yang Li. An effective optimization procedure based on structural reliability. *Computers & structures*, 52(5):1061–1067, 1994.

[108] Dan M Frangopol. Interactive reliability-based structural optimization. *Computers & structures*, 19(4):559–563, 1984.

[109] CK Prasad Varma Thampan and CS Krishnamoorthy. System reliability-based configuration optimization of trusses. *Journal of structural Engineering*, 127(8):947–956, 2001.

[110] Samer Hendawi and Dan M Frangopol. Design of composite hybrid plate girder bridges based on reliability and optimization. *Structural safety*, 15(1-2):149–165, 1994.

[111] Natalia M Alexandrov, JE Dennis, Robert Michael Lewis, and Virginia Torczon. A trust-region framework for managing the use of approximation models in optimization. *Structural optimization*, 15(1):16–23, 1998.

[112] Jianye Ching and Yi-Hung Hsieh. Local estimation of failure probability function and its confidence interval with maximum entropy principle. *Probabilistic Engineering Mechanics*, 22(1):39–49, 2007.

[113] Hector A Jensen and Michel A Catalan. On the effects of non-linear elements in the reliability-based optimal design of stochastic dynamical systems. *International Journal of Non-Linear Mechanics*, 42(5):802–816, 2007.

[114] Harold Kushner and G George Yin. *Stochastic approximation and recursive algorithms and applications*, volume 35. Springer Science & Business Media, 2003.

[115] AA Taflanidis and JL Beck. Stochastic subset optimization for optimal reliability problems. *Probabilistic Engineering Mechanics*, 23(2-3):324–338, 2008.

[116] Kalyanmoy Deb, Shubham Gupta, David Daum, Jürgen Branke, Abhishek Kumar Mall, and Dhanesh Padmanabhan. Reliability-based optimization using evolutionary algorithms. *IEEE Transactions on Evolutionary Computation*, 13(5):1054–1074, 2009.

[117] I-Tung Yang and Yi-Hung Hsieh. Reliability-based design optimization with discrete design variables and non-smooth performance functions: Ab-pso algorithm. *Automation in construction*, 20(5):610–619, 2011.

[118] Naser Safaeian Hamzehkolaei, Mahmoud Miri, and Mohsen Rashki. An enhanced simulation-based design method coupled with meta-heuristic search algorithm for accurate reliability-based design optimization. *Engineering with Computers*, 32(3):477–495, 2016.

[119] Asma Chakri, Xin-She Yang, Rabia Khelif, and Mohamed Benouaret. Reliability-based design optimization using the directional bat algorithm. *Neural Computing and Applications*, 30(8):2381–2402, 2018.

[120] Zeng Meng, Gang Li, Xuan Wang, Sadiq M Sait, and Ali Rıza Yıldız. A comparative study of metaheuristic algorithms for reliability-based design optimization problems. *Archives of Computational Methods in Engineering*, 28:1853–1869, 2021.

[121] Jafar Roshanian and Masoud Ebrahimi. Latin hypercube sampling applied to reliability-based multidisciplinary design optimization of a launch vehicle. *Aerospace Science and Technology*, 28(1):297–304, 2013.

[122] Xiongqing Yu and Xiaoping Du. Reliability-based multidisciplinary optimization for aircraft wing design. *Structures and Infrastructure Engineering*, 2(3-4):277–289, 2006.

[123] Xingzhi Hu, Xiaoqian Chen, Geoffrey T Parks, and Wen Yao. Review of improved monte carlo methods in uncertainty-based design optimization for aerospace vehicles. *Progress in Aerospace Sciences*, 86:20–27, 2016.

[124] Matthew Allen and Kurt Maute. Reliability-based design optimization of aeroelastic structures. *Structural and Multidisciplinary Optimization*, 27(4):228–242, 2004.

[125] Ricardo M Paiva, Curran Crawford, and Afzal Suleman. Robust and reliability-based design optimization framework for wing design. *AIAA journal*, 52(4):711–724, 2014.

[126] Ricardo Miguel Paiva. *A robust and reliability-based optimization framework for conceptual aircraft wing design*. PhD thesis, 2010.

[127] Debiao Meng, Yan-Feng Li, Hong-Zhong Huang, Zhonglai Wang, and Yu Liu. Reliability-based multidisciplinary design optimization using subset simulation analysis and its application in the hydraulic transmission mechanism design. *Journal of Mechanical Design*, 137(5):051402, 2015.

[128] Xiaoning Fan, Pingfeng Wang, and FangFang Hao. Reliability-based design optimization of crane bridges using kriging-based surrogate models. *Structural and Multidisciplinary Optimization*, 59(3):993–1005, 2019.

[129] Lei Li, Huan Wan, Wenjing Gao, Fujuan Tong, and Honglin Li. Reliability based multidisciplinary design optimization of cooling turbine blade considering uncertainty data statistics. *Structural and multidisciplinary optimization*, 59(2):659–673, 2019.

[130] Cheng Lu, Cheng-Wei Fei, Hao-Tian Liu, Huan Li, and Li-Qiang An. Moving extremum surrogate modeling strategy for dynamic reliability estimation of turbine blisk with multi-physics fields. *Aerospace Science and Technology*, 106:106112, 2020.

[131] Melike Nikbay and Muhammet N Kuru. Reliability based multidisciplinary optimization of aeroelastic systems with structural and aerodynamic uncertainties. *Journal of aircraft*, 50(3):708–715, 2013.

[132] ZL Huang, YS Zhou, C Jiang, J Zheng, and X Han. Reliability-based multidisciplinary design optimization using incremental shifting vector strategy and its application in electronic product design. *Acta Mechanica Sinica*, 34(2):285–302, 2018.

[133] Fan Hui and Li Weiji. An efficient method for reliability-based multidisciplinary design optimization. *Chinese Journal of Aeronautics*, 21(4):335–340, 2008.

[134] J Ahn and Jang-Hyuk Kwon. An efficient strategy for reliability-based multidisciplinary design optimization using bliss. *Structural and Multidisciplinary Optimization*, 31(5):363–372, 2006.

[135] Zhenzhong Chen, Haobo Qiu, Liang Gao, Xiaoke Li, and Peigen Li. A local adaptive sampling method for reliability-based design optimization using kriging model. *Structural and Multidisciplinary Optimization*, 49(3):401–416, 2014.

[136] Xiaoke Li, Haobo Qiu, Zhenzhong Chen, Liang Gao, and Xinyu Shao. A local kriging approximation method using mpp for reliability-based design optimization. *Computers & Structures*, 162:102–115, 2016.

[137] Satadru Roy, William A Crossley, Kenneth T Moore, Justin S Gray, and Joaquim RRA Martins. Next generation aircraft design considering airline operations and economics. In *2018 AIAA/ASCE/AHS/ASC Structures, Structural Dynamics, and Materials Conference*, page 1647, 2018.

[138] Satadru Roy, William A Crossley, Kenneth T Moore, Justin S Gray, and Joaquim RRA Martins. Monolithic approach for next-generation aircraft design considering airline operations and economics. *Journal of aircraft*, 56(4):1565–1576, 2019.

[139] Satadru Roy, William A Crossley, Bret Stanford, Kenneth T Moore, and Justin S Gray. A mixed integer efficient global optimization algorithm with multiple infill strategy-applied to a wing topology optimization problem. In *AIAA Scitech 2019 Forum*, page 2356, 2019.

[140] Samuel P Pullen and Bradford W Parkinson. System design under uncertainty: Evolutionary optimization of the gravity probe-b spacecraft. In *International Conference on Parallel Problem Solving from Nature*, pages 598–607. Springer, 1994.

[141] Todd Mosher. Conceptual spacecraft design using a genetic algorithm trade selection process. *Journal of Aircraft*, 36(1):200–208, 1999.

[142] Rania Hassan and William Crossley. Spacecraft reliability-based design optimization under uncertainty including discrete variables. *Journal of Spacecraft and Rockets*, 45(2):394–405, 2008.

[143] Jeffrey L Smith. Concurrent engineering in the jet propulsion laboratory project design center. *SAE transactions*, pages 1106–1118, 1998.

[144] Jairus Hihn, Gabriel Karpati, Debarati Chattopadhyay, Melissa McGuire, Chester Borden, John Panek, and Keith Warfield. Aerospace concurrent engineering design teams: current state, next steps and a vision for the future. In *AIAA Space 2011 Conference & Exposition*, page 7238, 2011.

[145] M Bandecchi, B Melton, and F Ongaro. Concurrent engineering applied to space mission assessment and design. *ESA bulletin*, 99(Journal Article), 1999.

[146] Andrew J Gerber and John P Crawford. Gajat a rapid prototyping mission architecture tool with embedded costing. 2004.

[147] Joseph A Aguilar, Andrew B Dawdy, and Glenn W Law. The aerospace corporation's concept design center. In *INCOSE International Symposium*, volume 8, pages 776–782. Wiley Online Library, 1998.

[148] James P Chase, Rebecca L Carter, and Jeffrey L Smith. System, cost, and risk analysis for access to space. 2004.

[149] Andre Girerd and Robert Shishko. Project trades model for complex space missions. In *AIAA Space 2003 Conference & Exposition*, page 6325, 2003.

[150] Inki Min, Eric Mahr, Ryan Vaughan, and Ivan Kellogg. Rapid space architecture development and analysis using an integrated toolset. In *2004 IEEE Aerospace Conference Proceedings (IEEE Cat. No. 04TH8720)*, volume 6, pages 3896–3906. IEEE, 2004.

[151] Elizabeth Morse, Tracy Leavens, Babak Cohanim, Corey Harmon, Eric Mahr, and Brian Lewis. Next-generation concurrent engineering: Developing models to complement point designs. In *2006 IEEE Aerospace Conference*, pages 15–pp. IEEE, 2006.

[152] Brian Lewis, Jeff Lang, and Richa Jolly. Modular concurrent engineering models: enabling alternative models in conceptual satellite design. In *2007 IEEE Aerospace Conference*, pages 1–8. IEEE, 2007.

[153] Allan McInnes, Daniel Harps, Jeffrey Lang, and Charles Swenson. A systems engineering tool for small satellite design. 2001.

[154] Guido Ridolfi, Erwin Mooij, and Sabrina Corpino. A system engineering tool for the design of satellite subsystems. In *AIAA modeling and simulation technologies conference*, page 6037, 2009.

[155] Young-Keun Chang, Ki-Lyong Hwang, and Suk-Jin Kang. Sedt (system engineering design tool) development and its application to small satellite conceptual design. *Acta Astronautica*, 61(7-8):676–690, 2007.

[156] Seradata SpaceTrak. https://www.seradata.com/products/spacetrak/, [Accessed] January 2021.

[157] Satellite Missions Database. https://directory.eoportal.org/web/eoportal/satellite-missions, [Accessed] January 2021.

[158] Edward L Kaplan and Paul Meier. Nonparametric estimation from incomplete observations. *Journal of the American statistical association*, 53(282):457–481, 1958.

[159] William Q Meeker and Luis A Escobar. *Statistical methods for reliability data*. John Wiley & Sons, 2014.

[160] Jerald F Lawless. *Statistical models and methods for lifetime data*, volume 362. John Wiley & Sons, 2011.

[161] Ronald T Anderson. Reliability design handbook. Technical report, RELIABILITY ANALYSIS CENTER GRIFFISS AFB NY, 1976.

[162] Kailash C Kapur and Michael Pecht. *Reliability Engineering*. John Wiley & Sons, Inc., 2014.

[163] Logan Beal, Daniel Hill, R Martin, and John Hedengren. Gekko optimization suite. *Processes*, 6(8):106, 2018.

[164] TAKEHISA Kohda, Ernest J Henley, and Koichi Inoue. Finding modules in fault trees. *IEEE Transactions on Reliability*, 38(2):165–176, 1989.

[165] JD Andrews and Rasa Remenyte. Fault tree conversion to binary decision diagrams. In *Proceedings of the 23rd ISSC*, 2005.

[166] Yunli Deng, He Wang, and Biao Guo. Bdd algorithms based on modularization for fault tree analysis. *Progress in Nuclear Energy*, 85:192–199, 2015.

[167] Aleksa Vukotic, Nicki Watt, Tareq Abedrabbo, Dominic Fox, and Jonas Partner. *Neo4j in action*. Manning Publications Co., 2014.

[168] Justin Gray. Mathematical foundations of systems analysis and optimization.

[169] Justin S Gray, John T Hwang, Joaquim RRA Martins, Kenneth T Moore, and Bret A Naylor. Openmdao: An open-source framework for multidisciplinary design, analysis, and optimization. *Structural and Multidisciplinary Optimization*, 59(4):1075–1104, 2019.

[170] John T Hwang and Joaquim RRA Martins. A computational architecture for coupling heterogeneous numerical models and computing coupled derivatives. *ACM Transactions on Mathematical Software (TOMS)*, 44(4):1–39, 2018.

[171] Joaquim RRA Martins and John T Hwang. Review and unification of methods for computing derivatives of multidisciplinary computational models. *AIAA journal*, 51(11):2582–2599, 2013.

[172] Jonathan R Behrens and Bhavya Lal. Exploring trends in the global small satellite ecosystem. *New Space*, 7(3):126–136, 2019.

[173] Tyler GR Reid, Andrew M Neish, Todd F Walter, and Per K Enge. Leveraging commercial broadband leo constellations for navigation. In *Proceedings of the ION GNSS*, pages 2300–2314, 2016.

[174] WILLIAM A CROSSLEY and Edwin A Williams. Simulated annealing and genetic algorithm approaches for discontinuous coverage satellite constellation design. *Engineering Optimization+ A35*, 32(3):353–371, 2000.

[175] Eric Frayssinhes. Investigating new satellite constellation geometries with genetic algorithms. In *Astrodynamics Conference*, page 3636, 1996.

[176] Quan He and Chao Han. Satellite constellation design with adaptively continuous ant system algorithm. *Chinese Journal of Aeronautics*, 20(4):297–303, 2007.

[177] Tania Savitri, Youngjoo Kim, Sujang Jo, and Hyochoong Bang. Satellite constellation orbit design optimization with combined genetic algorithm and semianalytical approach. *International Journal of Aerospace Engineering*, 2017, 2017.

[178] Peter Berlin. *Satellite platform design*. Kiruna Space and Environment Campus [Kiruna rymd-och miljöcampus], 2004.

[179] James R Wertz, David F Everett, and Jeffery J Puschell. *Space mission engineering: the new SMAD*. Microcosm Press, 2011.

[180] John G Walker. Satellite constellations. *Journal of the British Interplanetary Society*, 37:559–572, 1984.

[181] James Richard Wertz. *Mission Geometry: Orbit and Constellation Design and Management*. Springer, 2001.

[182] Leon Blitzer. Handbook of orbital perturbations. *University of Arizona*, 1970.

[183] Yoshihide Kozai. The motion of a close earth satellite. *The Astronomical Journal*, 64:367, 1959.

[184] David A Vallado. *Fundamentals of astrodynamics and applications*, volume 12. Springer Science & Business Media, 2001.

[185] Elmer Franklin Bruhn. *Analysis and design of flight vehicle structures*. Tri-State Offset Co., 1965.

[186] Thomas P Sarafin and Wiley J Larson. *Spacecraft structures and mechanisms–from concept to launch*. Springer, 1995.

[187] D Kraft. A software package for sequential quadratic programming. *DLR German Aerospace Research Center Institute for Flight Mechanics TR, Koln, Germany*, 1998.

[188] Andrew B Lambe and Joaquim RRA Martins. Extensions to the design structure matrix for the description of multidisciplinary design, analysis, and optimization processes. *Structural and Multidisciplinary Optimization*, 46(2):273–284, 2012.

[189] Mohamed Amine Bouhlel, Nathalie Bartoli, Abdelkader Otsmane, and Joseph Morlier. Improving kriging surrogates of high-dimensional design models by partial least squares dimension reduction. *Structural and Multidisciplinary Optimization*, 53(5):935–952, 2016.

[190] Philip E. Gill, Walter Murray, Michael A. Saunders, and Elizabeth Wong. User's guide for SNOPT 7.7: Software for large-scale nonlinear programming. Center for Computational Mathematics Report CCoM 18-1, Department of Mathematics, University of California, San Diego, La Jolla, CA, 2018.

[191] Philip E. Gill, Walter Murray, and Michael A. Saunders. SNOPT: An SQP algorithm for large-scale constrained optimization. *SIAM Rev.*, 47:99–131, 2005.

[192] Adamantios Mettas. Reliability allocation and optimization for complex systems. In *Annual Reliability and Maintainability Symposium. 2000 Proceedings. International Symposium on Product Quality and Integrity (Cat. No. 00CH37055)*, pages 216–221. IEEE, 2000.

[193] Graeme J Kennedy and Joaquim RRA Martins. A parallel finite-element framework for large-scale gradient-based design optimization of high-performance structures. *Finite Elements in Analysis and Design*, 87:56–73, 2014.

A
Acronyms

ADC Attitude Determination and Control Subsystem

AIC Akaike Information Criterion

AMIEGO-MIMOS A Mixed Integer Efficient Global Optimization algorithm - Multiple Infill via a Multi-Objective Strategy

ANT Antenna (switches)

APOPT Advanced Process OPTimizer

BAT Battery

BDD Binary Decision Diagram

COMM Communication Subsystem

CPU Central Processing Unit

DPY Deployment

DSS Distributed Space Systems

DSU Rad Hard Memory

EAT Equal Apportionment Technique

EPS Power Subsystem

ES Earth Sensor

F/V Failure rate over Value

FOO Feasibility of Objectives

GM Graphical Method

IDF Individual Discipline Feasible

ILP Integer Linear Programming problem

IMU Intertial Measurement Unit

KOH Jeong and Koh Method

LEO Low Earth Orbit

MDA Multidisciplinary Analysis

MDF Multidisciplinary Feasible

MDO Multidisciplinary Design Optimization

MINLP Mixed Integer Non-Linear Programming problem

MLE Maximum Likelihood Estimate

NLBGS Nonlinear Block Gauss-Seidel iterative solver

NLP Non-Linear Programming problem

OBC Onboard Computer

PCU Power Conditioning Module

PDU Power Distribution Module

PMS Phased Mission System

PROP Propulsion Subsystem

PT Propellant Tanks (valves)

RAD Radiator

RAP Redundancy Allocation Problem

RBMDO Reliability-Based Multidisciplinary Design Optimization

RCR Receiver

RRAP Reliability - Redundancy Allocation Problem

RW Reaction Wheel

SADM Solar Array Drive Motor

SAND Simultaneous ANalysis and Design

SLSQP Sequential Least SQuares Programming algorithm

SNOPT Sparse Nonlinear OPTimizer

SP Solar Panel Sections

SPMS Single Phase Mission System

STR Structure Subsystem

StS Star Sensor

TCS Thermal Subsystem

ThR Thrusters

TSR Transmitter

XDSM extended Design Structure Matrix

B
Glossary

Akaike Information Criterion An estimator of prediction error and thereby relative quality of statistical models for a given set of data (lower value is preferred)

Burn-in Process by which components of a system are tested before being placed in service to check for early failures

Censoring A form of missing data problem in which time to event is not observed

Coefficient of Determination An estimator to describe how well a distribution fits a set of observations (1 indicates perfect fit)

Conceptual Design Phase Initial system design phase where the functional requirements are translated to the design parameters

Fault Tree Shows the logical relationships between the events and the causes leading to failure events

ILP Optimization problems with integer design variables and linear functions in the objective function and the constraints.

Infant Mortality Initial operational period of a system with decreasing failure rate, also known as early failures

Kaplan-Meier Estimator A non-parametric statistic used to estimate the survival function from lifetime data

Large Satellite Satellite with mass greater than 500 kg

Maximum Likelihood Estimation A method for estimating distribution parameters from sample data such that the probability (likelihood) of obtaining the observed data is maximized

Microsatellite Satellite with mass between 10 - 100 kg

MINLP Optimization problems with continuous and integer design variables and nonlinear functions in the objective function and/or the constraints.

Monte Carlo A broad class of computational algorithms that rely on repeated random sampling to obtain numerical results

NLP Optimization problems with continuous design variables and nonlinear functions in the objective function and/or the constraints.

NP-hard The complexity class of problems that are intrinsically harder than those that can be solved by a nondeterministic Turing machine in polynomial time

Reliability An indicator that conveys how well the system performs during a given operational period without any failure or a need for repair work

Reliability Growth Improvement in the reliability of the system by changing its design and/or manufacturing process

Small Satellite Satellite of low mass and size, usually under 500 kg

Space grade components Electronic components that are hardened to survive the harsh space environment

Survival Analysis A branch of statistics for analyzing the expected duration of time until one event occurs, such as failure

System An orderly grouping of interdependent elements linked together according to a plan to achieve a specific goal

C

DESIRA: Graphical User-Interface

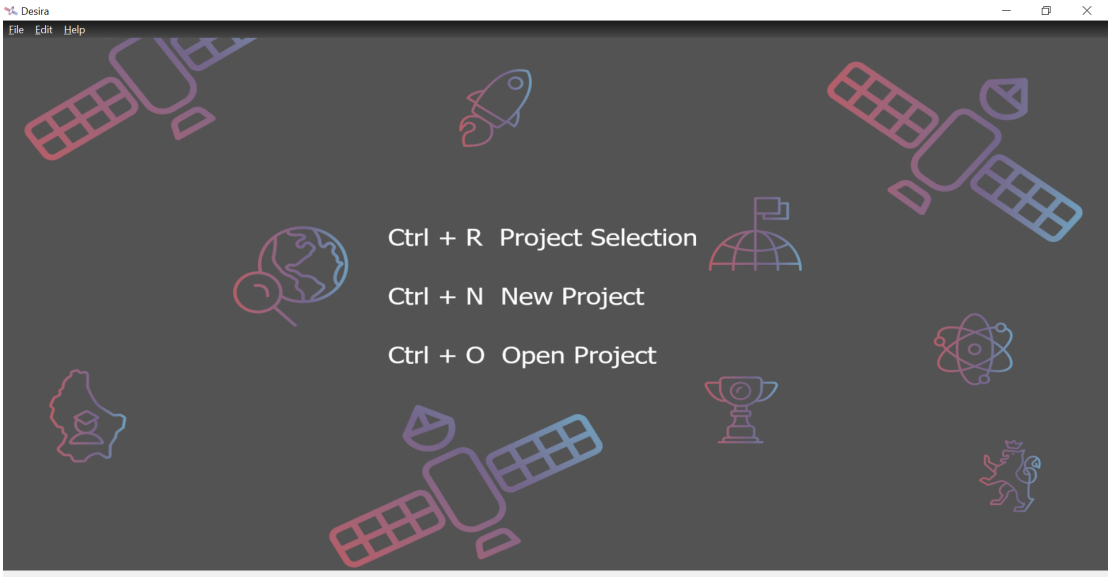
Desira
File Edit Help
Ctrl + R Project Selection
Ctrl + N New Project
Ctrl + O Open Project

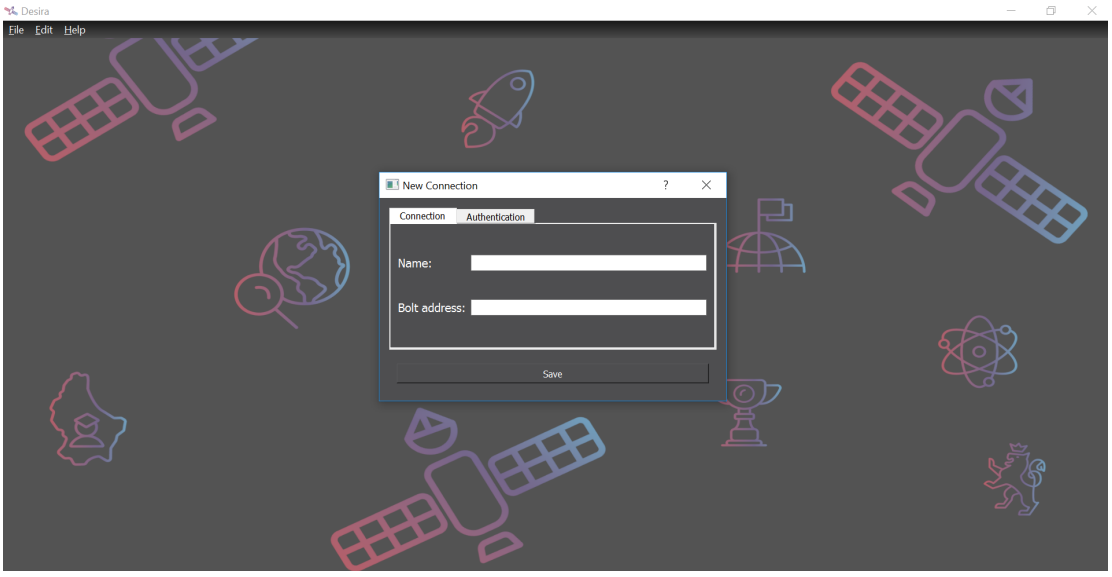
Desira
File Edit Help
New Connection
Connection
Authentication
Name:
Bolt address:
Save

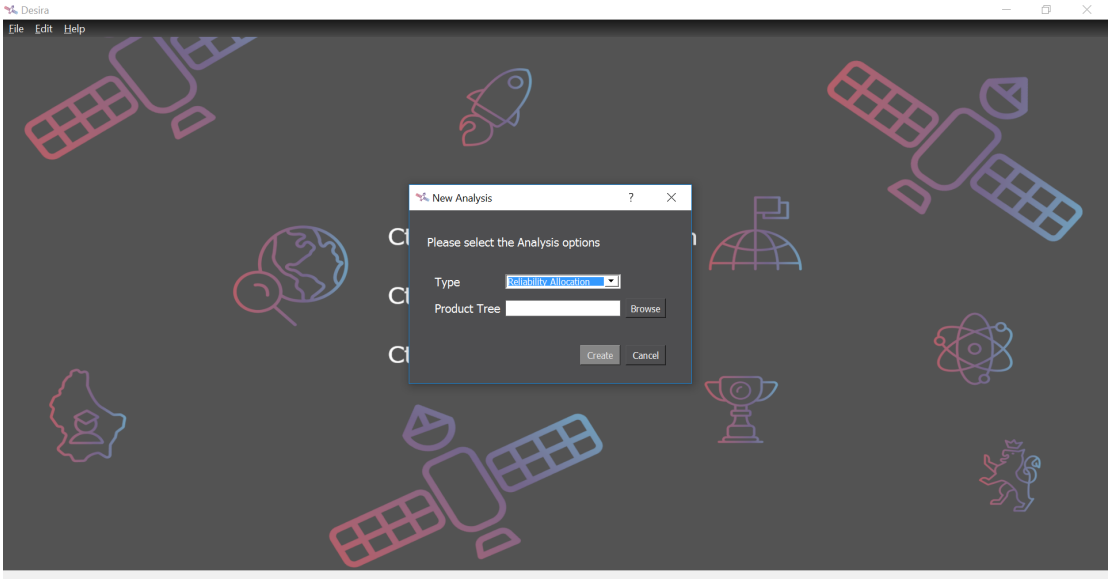
Desira
File Edit Help
New Analysis
Please select the Analysis options
Type
Reliability Allocation
Product Tree
Browse
Create
Cancel


Project
Add user Allocation
Level
Select
Element
Select
User Inputs
C:/System Engineering/
Browse
Plot
Reliability Parameters
Initial System Reliability
0.649
Life Time (years)
4
Run
Reliability Growth
Target System Reliability
0.75
Run
Reliability Optimization
Cost Estimate
C:/System Engineering/Dissertation
Browse
Optimize
Export

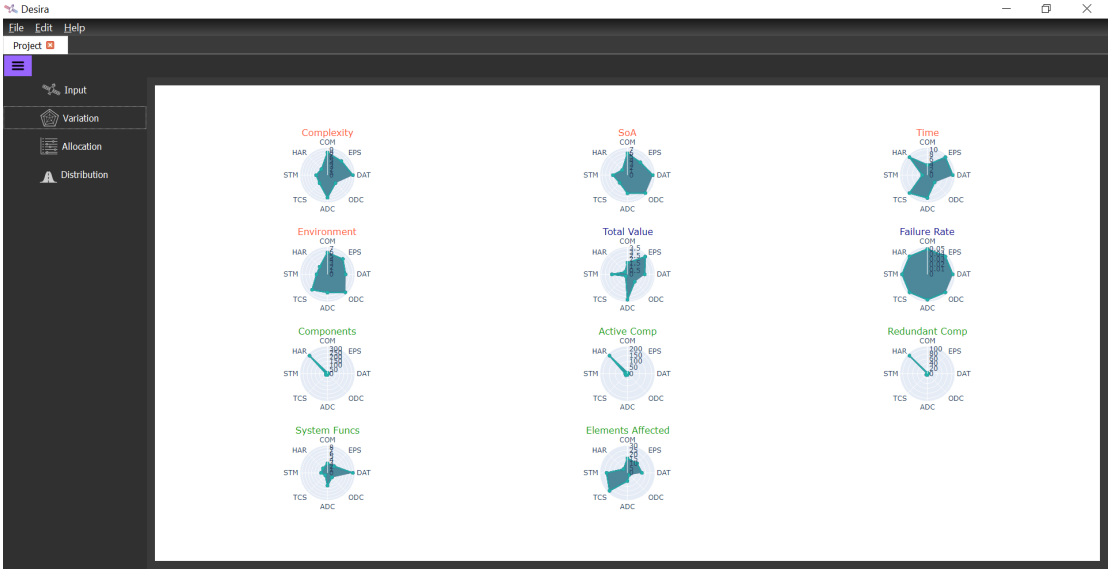
Desira
File Edit Help
Project
Input
Variation
Allocation
Distribution
Complexity
SoA
Time
Environment
Total Value
Failure Rate
Components
Active Comp
Redundant Comp
System Funcs
Elements Affected
COM EPS DAT ODC ADC TCS STM HAR


Desira
File Edit Help
Project
All Results
Final Result
Variation of Reliability
Reliability
Variation of FIT
FIT
DAT EPS COM HAR STM TCS ADC ODC

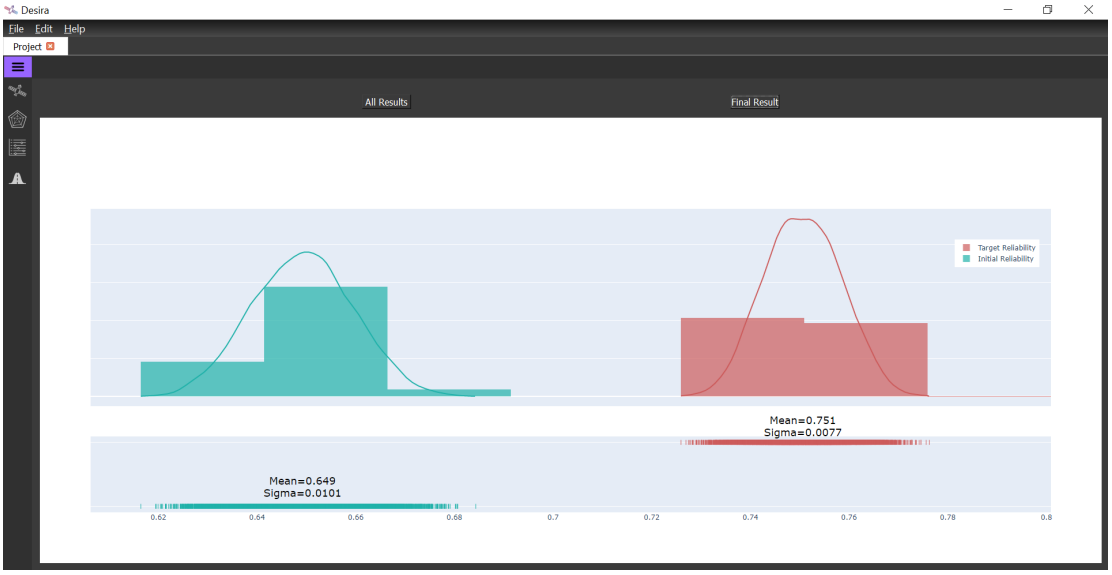
Desira
File Edit Help
Project
All Results
Final Result
Target Reliability
Initial Reliability
Mean=0.751
Sigma=0.0077
Mean=0.649
Sigma=0.0101
0.62
0.64
0.66
0.68
0.7
0.72
0.74
0.76
0.78
0.8

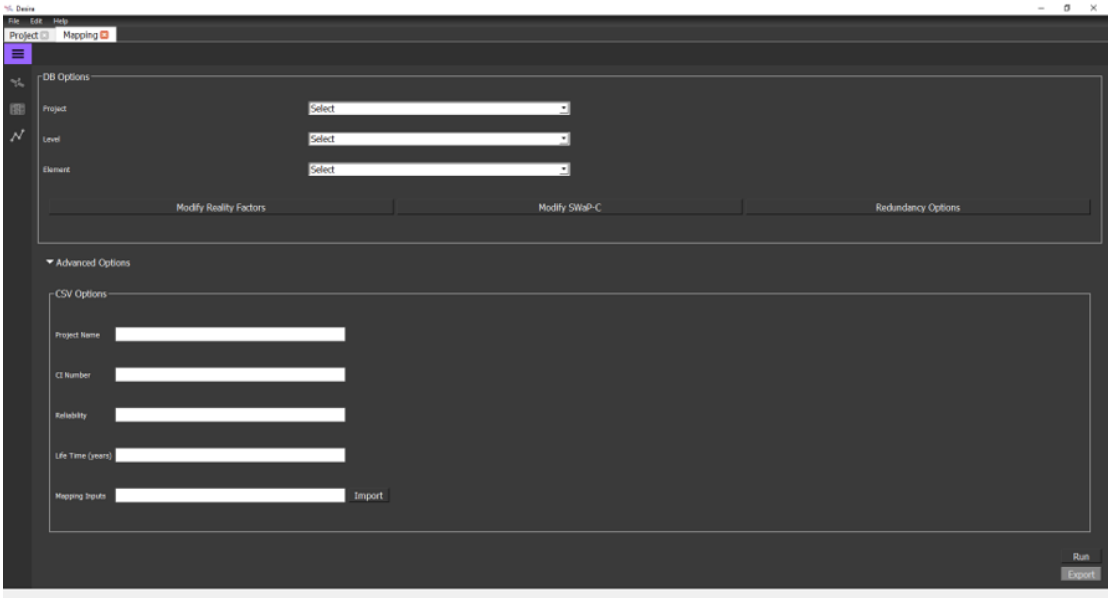
Project
Mapping
DB Options
Project
Level
Element
Select
Modify Reality Factors
Modify SWaP-C
Redundancy Options
Advanced Options
CSV Options
Project Name
CI Number
Reliability
Life Time (years)
Mapping Inputs
Import
Run
Export

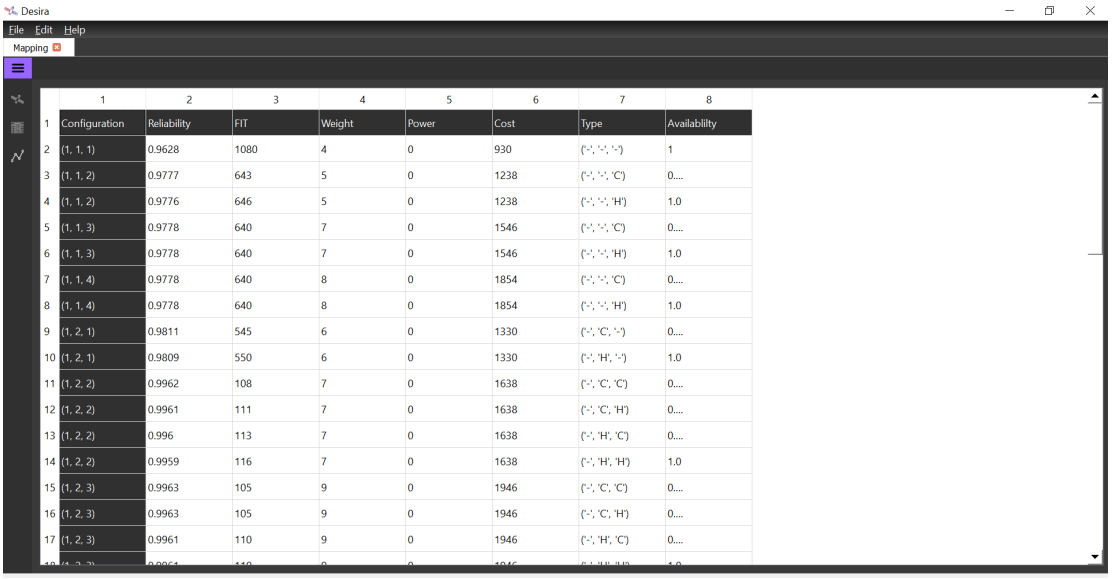

	1	2	3	4	5	6	7	8
1	Configuration	Reliability	FIT	Weight	Power	Cost	Type	Availablilty
2	(1, 1, 1)	0.9628	1080	4	0	930	('-', '-', '-')	1
3	(1, 1, 2)	0.9777	643	5	0	1238	('-', '-', 'C')	0....
4	(1, 1, 2)	0.9776	646	5	0	1238	('-', '-', 'H')	1.0
5	(1, 1, 3)	0.9778	640	7	0	1546	('-', '-', 'C')	0....
6	(1, 1, 3)	0.9778	640	7	0	1546	('-', '-', 'H')	1.0
7	(1, 1, 4)	0.9778	640	8	0	1854	('-', '-', 'C')	0....
8	(1, 1, 4)	0.9778	640	8	0	1854	('-', '-', 'H')	1.0
9	(1, 2, 1)	0.9811	545	6	0	1330	('-', 'C', '-')	0....
10	(1, 2, 1)	0.9809	550	6	0	1330	('-', 'H', '-')	1.0
11	(1, 2, 2)	0.9962	108	7	0	1638	('-', 'C', 'C')	0....
12	(1, 2, 2)	0.9961	111	7	0	1638	('-', 'C', 'H')	0....
13	(1, 2, 2)	0.996	113	7	0	1638	('-', 'H', 'C')	0....
14	(1, 2, 2)	0.9959	116	7	0	1638	('-', 'H', 'H')	1.0
15	(1, 2, 3)	0.9963	105	9	0	1946	('-', 'C', 'C')	0....
16	(1, 2, 3)	0.9963	105	9	0	1946	('-', 'C', 'H')	0....
17	(1, 2, 3)	0.9961	110	9	0	1946	('-', 'H', 'C')	0....